The Palomar Testbed Interferometer Calibrator Catalog

G. T. van Belle

Michelson Science Center, California Institute of Technology, Pasadena, CA 91125

gerard@ipac.caltech.edu

G. van Belle

Department of Biostatistics, University of Washington, Seattle, WA 98195-7232

vanbelle@u.washington.edu

M. J. Creech-Eakman

New Mexico Tech

mce@kestrel.nmt.edu

J. Coyne

University of Cambridge

jc466@cam.ac.uk

A. F. Boden, R. L. Akeson, D. R. Ciardi, K. M. Rykoski, R. R. Thompson

Michelson Science Center, California Institute of Technology, Pasadena, CA 91125

bode, akeson, ciardi, kmr, thompson@ipac.caltech.edu

B. F. Lane

Massachusetts Institute of Technology

blane@MIT.EDU

and

The PTI Collaboration

Jet Propulsion Laboratory & Michelson Science Center

ABSTRACT

The Palomar Testbed Interferometer (PTI) archive of observations between 1998 and 2005 is examined for objects appropriate for calibration of optical long-baseline interferometer observations - stars that are predictably point-like and single. Approximately 1,400 nights of data on 1,800 objects were examined for this investigation. We compare those observations to an intensively studied object that is a suitable calibrator, HD217014, and statistically compare each candidate calibrator to that object by computing both a Mahalanobis distance and a Principal Component Analysis. Our hypothesis is that the frequency distribution of visibility data associated with calibrator stars differs from non-calibrator stars such as binary stars. Spectroscopic binaries resolved by PTI, objects known to be unsuitable for calibrator use, are similarly tested to establish detection limits of this approach. From this investigation, we find more than 350 observed stars suitable for use as calibrators (with an additional ≈ 140 being rejected), corresponding to $\gtrsim 95\%$ sky coverage for PTI. This approach is noteworthy in that it rigorously establishes calibration sources through a traceable, empirical methodology, leveraging the predictions of spectral energy distribution modeling but also verifying it with the rich body of PTI's on-sky observations.

Subject headings: instrumentation: interferometers, instrumentation: high angular resolution, techniques: high angular resolution, techniques: interferometric, catalogs, stars: fundamental parameters stars: imaging, binaries: general, infrared: stars

1. Introduction

Visible and near-infrared interferometers are powerful tools for measuring the minute angular sizes of nearby stars. However, establishing absolute system responses in the presence of atmospheric turbulence and instrument imperfections is a challenging proposition that requires careful attention to detail when constructing an observational approach. Use of objects predicted to be point-like calibration sources is routinely employed in astronomical interferometry in the optical (Mozurkewich et al. 1991; Boden et al. 1998a; Bordé et al. 2002; van Belle & van Belle 2005). However, given the incomplete nature of our knowledge of these sources, it is not enough to merely predict the expected fringe visibility from these objects - calibration sources need to be rigorously evaluated for their actual observed interferometric visibility, and its appropriateness for use in calibrating the instrument. Herein we

examine the body of calibration data taken upon the sky from near-infrared, long-baseline interferometric measurements taken with the Palomar Testbed Interferometer (PTI). Similar efforts have begun for the Very Large Telescope Interferometer (VLTI) (Richichi & Percheron 2005).

PTI is an 85 to 110 m H- and K-band (1.6 μm and 2.2 μm) interferometer located at Palomar Observatory and is described in detail in Colavita et al. (1999). It has three 40-cm apertures used in pairwise combination for measurement of stellar fringe visibility on sources that range in angular size from 0.05 to 5.0 milliarcseconds, being able to resolve individual sources $\theta \gtrsim 1.0$ mas in size. PTI has been in nightly operation since 1997, with minimum downtime for throughout the intervening years. The data from PTI considered herein covers the range from the beginning of 1998 (when the standardized data pipeline went into place) until the end of 2005 (when the analysis of this manuscript was begun). Over the 8 years of operation discussed in this study, PTI was on the sky in its single-star visibility mode 1,390 nights[1], producing over 83,000 125 second stellar 'scans' on 1,818 individual objects. PTI has a minimum K-band fringe spacing of ≈ 4.3 mas at the sky position of the calibration objects, making many of these stars readily resolvable.

As is standard practice in optical interferometry, a typical set of observations with PTI involves observation of target objects of scientific interest, bracketed by calibration objects. The calibration objects serve the purpose of characterizing the point-response, or system visibility (V_{sys}^2), of the interferometer in conjunction with the atmosphere, and as such, the interleaved calibrator-target-calibrator observations are done on timescales expected to be shorter than the seeing evolution time of the atmosphere (typically less than 15 minutes). By measuring V_{sys}^2, a properly normalized measurement of the target star's visibility may be obtained for meaningful astrophysical interpretation (van Belle & van Belle 2005). These calibration objects are selected *a priori* to be as close to point-like as is possible, having visibilities measured by PTI to be very nearly unity. The primary limitation on selection of truly point-like calibrators is the sensitivity of the instrument, coupled with considerations of dynamic range. Towards the end of having nearly point-like calibrators, calibrator lists are vetted for binary systems, which are excluded due to the sub-unity system response measured from such systems. The decrease of the measured visibility from the desired characterization of V_{sys}^2 is due to the interferometer's ability to resolve out even milli-arcsecond separation binaries.

Unfortunately, incomplete knowledge of the true physical nature of the calibration objects can result in binary systems not being properly excluded during the vetting process

---

[1]The remaining nights were spent on other instrument modes or were lost to maintenance or weather.

that selects potential calibrators. Given this reality of calibrator selection, a number of additional steps are taken to ensure rigorously defensible characterization of V_{sys}^2. First, given the uncertain nature of possible calibrators, employing multiple calibrators for any given target star observation is also standard operating procedure for PTI observations. Second, these clusters of calibrators are observed on multiple nights, since chance geometry may make a binary system readily apparent on one night but not on another. Finally, these objects may be compared to known 'good' calibrators for appropriateness as calibration objects, which this study will examine in detail.

2. Approach

To establish a properly normalize the squared visibility[2] for a science target in the expected [0:1] range, the system response is used to account for the effect of instrumental and atmospheric imperfections and normalize the visibility measured for that target, V_{meas}^2:

$$V_{\mathrm{norm}}^2(\text{target}) = \frac{V_{\mathrm{meas}}^2(\text{target})}{V_{\mathrm{sys}}^2} \tag{1}$$

The system visibility, V_{sys}^2, is established from measurements of point-like calibration sources. However, due to the extreme resolution of interferometric instruments, event nominally 'unresolved' objects need to have their measured V_{meas}^2 corrected for partial resolution:

$$V_{\mathrm{sys}}^2 = \frac{V_{\mathrm{meas}}^2(\text{calibrator})}{V_{\mathrm{pred}}^2(\text{calibrator})} \tag{2}$$

Interleaved observations of targets and calibrators are done on a time scale expected to be less than the atmospheric seeing evolution time, which at the Palomar site is typically 30 minutes or longer. PTI's automated star queue duty cycle is 4 to 8 minutes per star, so calibrator-target-calibrator interleaving is comfortably accomplished with sufficient cadence to satisfy this requirement.

Assuming that a uniform disk brightness profile appropriately characterizes the stellar disk of the calibration source, the predicted visibility V_{pred}^2 may be derived from some expectation of the star's angular size, θ, and the known system configuration parameters of baseline B and wavelength, λ:

$$V_{\mathrm{pred}}^2 = \left[\frac{2J_1(\pi\theta B/\lambda)}{\pi\theta B/\lambda} \right]^2 \tag{3}$$

[2]Squared visibility is referred to herein as simply, 'visibility', which is consistent with other articles in the literature.

In estimating V_{pred}^2, and by extension V_{sys}^2, it is important to properly quantify errors in B, λ, and θ, and propagate them through the Bessel function. The need for 'point-like' calibrators is prompted by potential unknown biases present in the *a priori* estimation of the calibrator angular size, θ, and to avoid non-linear effects found in the Bessel function. Proper error propagation is observed throughout all of these steps, including propagation of uncertainties in angular size estimate, σ_θ, into V_{pred}^2 and measurement error, σ_{V^2}, for both V_{meas}^2(target) and V_{meas}^2(calibrator). The particulars and implications of this requirement are examined in much greater detail in van Belle & van Belle (2005). In practice, for calibrators previously uncharacterized by PTI, 2 or more calibration sources are used in tandem to all for cross-calibration and elimination of bad calibrators.

For this study, the full list of stars observed by PTI from 1998 to 2005 was collected from the PTI archive[3]. A set of calibrator selection criteria was established (§3), and for each of the objects in the archive that qualified as a potential calibrator, a spectral energy distribution (SED) fit was used to refine its predicted angular size (§4). Objects which were small enough for use as calibrators were kept as possible calibrators. The predicted angular size could then be used to account for the partial resolution by the interferometer of the object's angular size in attempting to normalize the object's raw interferometer data (§5). The data obtained from the normalization step were then examined with Mahalanobis distance and Principal Component Analysis tests for departures from point-source response and evidence of hidden binarity (§6). Finally, we will examine the likelihood that stars observed by PTI that appear to be solid calibrators are actually undetected binaries (§7).

3. Calibrator Selection Criteria

In order to maximize the likelihood that any random star observable by PTI is appropriate for use as a calibrator, a number of criteria have been developed over the years of operation of the instrument. Since each principal investigator selected his or her own calibration sources for their projects, it is unclear the exact criteria that went into the selection of both targets and calibrators found in the complete PTI archive. However, since we are evaluating the sources after the fact, we may vet the observed list of potential calibrators using a single homogenous set of criteria:

- Potential calibration sources must be bright enough to be tracked by PTI in the appropriate available dynamic range. This translates roughly to a V band magnitude of

---

[3]Online at the Michelson Science Center, http://msc.caltech.edu.

~ 10.0 or brighter (for tip-tilt tracking), and a K band magnitude of ~ 5.0 or brighter (for fringe tracking).

- These sources need to be appropriately 'point-like' in size, which conservatively for PTI is less than $\lesssim 1.0$ mas in size, as discussed extensively in van Belle & van Belle (2005), with final predicted size from detailed SED fitting (see §4). This corresponds to a measured visibility $V^2 \gtrsim 0.90$ that serves well to characterize the system visibility (interferometer plus atmosphere) and is statistically tolerant to errors and even biases in the *a priori* estimation of the calibrator size.

- Finally, for system visibility characterization, these stars must be expected to exhibit constant measured visibilities. As such, they should not be known to be a binary system, or suspected to be one, according to the astrometric references in the Hipparcos database (Perryman et al. 1997). The Hipparcos H59 multiplicity flag is of particular utility here, not only calling out those objects for which a full astrometric solution has been obtained, but those which have unexplained degrees of astrometric variability.

The 499 potential sources in the PTI database which satisfy these criteria are found in Table 1, the contents of which will be discussed in the next section. The PTI data available for these sources will then be evaluated in §6 for evidence of binarity or departures in *a priori* size expectations that make them unsuitable for use as calibrators.

4. Spectral Energy Distribution Fitting

For each of the potential calibrator stars observed in this investigation, a spectral energy distribution (SED) fit was performed. This fit was accomplished using photometry available in the literature as the input values, with template spectra appropriate for the spectral types indicated for the stars in question. The template spectra, from Pickles (1998), were adjusted by the fitting routine to account for overall flux level, wavelength-dependent reddening, and expected angular size. Reddening corrections were based upon the empirical reddening determination described by Cardelli et al. (1989), which differs little from van de Hulst's theoretical reddening curve number 15 (Johnson 1968; Dyck et al. 1996). Both narrowband and wideband photometry in the 0.3 μm to 30 μm were used as available, including Johnson UBV (see, for example, Eggen (1963, 1972); Moreno (1971)), Stromgren $ubvy\beta$ (Piirola 1976), 2Mass JHK_s (Cutri et al. 2003), Geneva (Rufener 1976), Vilnius $UPXYZS$ (Zdanavicius et al. 1972), and $WBVR$ (Kornilov et al. 1991); flux calibrations were based upon the values given in Cox (2000). For each star, the primary references for the photometric data are given in Table 1.

Table 1.   Sources of photometry for stars tested as PTI calibrators.

HD	WBVR	Geneva	DDO	Vilnius	2MASS	IRAS	Johnson	Stromgren	JP11
71	Y	-	-	-	-	Y			
166	Y	Y	Y	-	Y	Y	90, 18, 19, 92, 243		270, 262, 230
167	Y	-	Y	-	Y	Y			
905	Y	Y	-	Y	-	Y	107		270, 87
1083	Y	-	-	-	Y	-			270, 146
1279	Y	Y	-	Y	Y	-	28		270, 146, 161
1404	Y	Y	-	-	Y	Y	90, 6, 18, 88, 90, 243	90	270, 129, 87, 246, 260
1406	Y	Y	Y	-	Y	Y			
1671	Y	Y	-	Y	Y	Y	107, 105, 69, 243		270, 87
2114	Y	-	Y	-	Y	Y	90, 58, 92		
2190	-	-	-	-	Y	Y			
2344	-	-	-	-	Y	Y			270, 262
2454	Y	-	-	Y	Y	Y	90, 107, 105, 174, 58, 243		270, 185, 258, 151, 252, 143, 124, 87
2507	Y	-	-	-	Y	Y	134		
2628	Y	-	-	Y	Y	Y	102, 69, 243		
2758	-	-	-	-	Y	-			
2942	Y	-	-	-	Y	-	233		
3268	Y	-	-	-	Y	Y	105, 243		270, 114, 87
4841	Y	-	-	-	Y	-	17		270, 232
4881	Y	-	-	-	Y	-			270, 146
6210	Y	-	-	-	-	Y	173, 68, 69		270, 87
6288	Y	-	-	-	-	-	90, 58		
6833	Y	-	Y	Y	-	Y	13, 92		270, 217, 130, 262, 267
6903	Y	-	Y	Y	-	Y	134		270, 145, 262, 266
6920	Y	Y	-	-	-	Y	25, 236		270, 252, 262, 87
7034	Y	-	-	Y	-	-	88, 236		270, 145, 230
7189	-	-	-	-	-	Y			270, 262
7299	Y	-	-	-	-	Y			
7476	Y	-	-	-	-	Y	90, 45, 243		270, 87, 185, 268, 258
7590	Y	-	-	-	-	Y			270, 114, 230
7804	Y	Y	-	-	-	Y	94, 90, 6, 18, 45, 90, 243	90	270, 87, 185
7964	Y	-	-	-	-	Y	90, 88, 90, 243	90	270, 87, 129
8335	Y	-	-	-	Y	-	90, 58		270, 230
8357	Y	-	-	-	-	Y			
8671	Y	-	-	-	-	Y	134, 164		270, 87

Table 1—Continued

HD	WBVR	Geneva	DDO	Vilnius	2MASS	IRAS	Johnson	Stromgren	JP11
8673	Y	-	-	-	-	Y	105, 164, 243		270, 87
8799	Y	Y	-	Y	-	-	90, 69, 90, 135, 243	90, 135	
9329	Y	-	-	-	-	Y			
9407	Y	-	-	Y	-	Y	13, 92		
10112	-	-	-	-	Y	Y			
10205	Y	-	-	-	Y	-	90, 88, 90, 243	90	
10874	Y	-	-	-	Y	Y	134, 164		270, 87
11007	-	-	-	-	Y	-	105, 243		270, 87, 262
11151	Y	-	-	-	Y	Y	105		270, 87
11946	Y	-	-	-	Y	-	88, 243		270, 127, 269, 146
11973	Y	-	-	-	Y	-	90, 102, 65, 69, 40, 90, 243	90	
12235	Y	Y	Y	Y	Y	-	90, 45, 243		270, 252, 262, 266, 87
12303	Y	Y	-	-	Y	-	90, 88, 90, 243	90	270, 225, 161
12573	Y	-	-	-	Y	-	90, 112, 71, 205		270, 87, 185, 258
13403	Y	-	-	-	Y	-	231, 33, 231, 243		270, 114, 230
13421	Y	-	-	Y	Y	Y	90, 58, 243		270, 254, 252, 247, 230, 186, 262, 266, 262, 87
13468	Y	-	Y	-	Y	Y	90, 58, 243		270, 230
13555	Y	Y	-	-	Y	-	105, 243		270, 266, 262, 150, 87
14055	Y	Y	-	-	Y	Y	90, 88, 90, 243, 211	90	270, 129, 146, 127
15257	Y	-	-	-	Y	Y	243		270, 200, 129, 87, 256
15335	Y	Y	Y	-	Y	Y	134, 243		270, 87, 266, 262
16220	Y	-	-	-	Y	Y	105, 164		270, 87
16234	Y	-	-	Y	Y	Y	105, 243		270, 262, 266, 263, 87
16327	Y	-	-	-	Y	-	105		
16399	Y	-	-	Y	Y	-	90, 45, 243		270, 258, 114, 87, 185
16647	Y	-	-	Y	Y	Y	90, 107, 105, 58, 243		270, 185, 258, 87
17093	Y	Y	-	-	-	Y	0	0	0
17228	Y	-	Y	-	Y	Y	134, 243		
17573	Y	Y	-	-	Y	-	90, 88, 90, 212, 243	90	
17616	Y	-	-	-	Y	Y	229		270, 262
18012	Y	-	-	-	Y	Y	243		270, 262
18404	Y	Y	-	Y	Y	Y	90, 105, 12, 90, 243	90	270, 87
18411	Y	-	-	-	Y	Y	90, 88, 90, 243	90	270, 87
18757	Y	Y	-	-	Y	-	101, 13		270, 114, 250, 230
18768	Y	-	-	-	Y	-	201		270, 114, 230

Table 1—Continued

HD	WBVR	Geneva	DDO	Vilnius	2MASS	IRAS	Johnson	Stromgren	JP11
19107	Y	Y	-	-	Y	Y	90, 58, 243		270, 247, 185, 87, 259
19994	Y	-	Y	-	Y	-	90, 105, 19, 58, 243		
20150	Y	-	-	-	Y	Y	90, 88, 90, 243	90	270, 127, 129, 146
20418	Y	Y	-	Y	Y	-	90, 138, 15, 88		270, 169, 138
20675	Y	-	-	-	Y	Y	134, 105, 243, 203, 105		270, 87
20677	Y	Y	-	-	Y	Y	90, 88, 90, 243	90	270, 87
21019	Y	-	-	-	Y	-	90, 49, 59, 243		
21686	Y	-	-	-	Y	Y	94, 88, 243		270, 127, 91, 146
21770	Y	Y	-	-	Y	-	90, 136, 105, 11, 25, 90, 243	90	270, 91, 87
22780	Y	Y	-	-	Y	-	138, 23		270, 225, 138
22879	Y	Y	-	-	Y	Y	101, 206, 208, 13, 241, 49, 109, 243	109	270, 150, 262, 231, 114, 230, 266, 250
23408	Y	Y	Y	Y	Y	Y	3, 90, 138, 22, 88, 90, 118	120, 90	270, 138, 188, 194, 91, 87
23630	Y	-	Y	Y	Y	-			270, 87, 129, 138, 91, 188, 194
23862	Y	Y	Y	Y	Y	-		90, 163, 120	
24357	Y	Y	-	-	Y	-	90, 102, 105, 12, 90	90	270, 200, 129, 85, 87, 262, 266, 269
24843	Y	-	Y	-	Y	Y	134, 221, 243		
25490	Y	Y	-	-	Y	Y	94, 90, 49, 88, 72, 90, 243	90	270, 146, 91, 87, 185, 127
25570	Y	-	-	-	Y	Y	90, 105, 45, 12, 90, 243	90	270, 185, 87
25621	Y	Y	-	-	Y	Y	90, 105, 45, 243		270, 145, 185, 143, 151
25680	Y	Y	Y	-	Y	Y	90, 18, 19, 243		270, 230, 262, 266
25867	Y	-	-	Y	Y	Y	100, 111, 105, 243		270, 269, 129, 87
25948	Y	-	-	-	Y	-			270, 87
25975	Y	-	Y	-	Y	Y	90, 13, 92, 243, 181		
26605	Y	-	Y	-	Y	Y			
26737	Y	Y	-	Y	Y	-	189, 12, 104	104	270, 230, 85, 266
26764	Y	-	-	Y	Y	Y	88		270, 269
27084	Y	Y	-	-	Y	Y	90, 39, 116		270, 87
27322	Y	-	-	-	Y	-	236		270, 87
27397	Y	Y	Y	Y	Y	Y	90, 105, 12, 90, 109	132, 109, 90	
27459	Y	Y	Y	Y	Y	Y	90, 105, 12, 90, 109	132, 109, 90	
27524	Y	-	Y	Y	Y	-	12, 104, 153	104	270, 260, 230, 262, 85, 114, 266
27777	Y	-	-	-	Y	-			270, 225, 161
27848	Y	Y	Y	Y	Y	-	12, 104, 153	104	270, 266, 230, 85, 262
27859	-	Y	Y	Y	Y	-	12, 104, 109	132, 109, 104	270, 231
27901	Y	Y	-	Y	Y	Y	90, 105, 12, 90	90	270, 85, 260, 87

Table 1—Continued

HD	WBVR	Geneva	DDO	Vilnius	2MASS	IRAS	Johnson	Stromgren	JP11
27946	Y	Y	-	Y	Y	Y	90, 100, 105, 12, 90, 243	90	270, 204, 260, 129, 85, 87, 258, 187
28024	Y	-	-	Y	Y	Y	90, 100, 102, 12, 88, 90, 243	90	
28355	Y	Y	-	Y	Y	Y	90, 12, 88, 90, 243, 211	90	270, 85, 247, 129, 87, 91, 260, 186, 230, 200
28556	Y	-	-	Y	Y	-	90, 105, 11, 12, 90, 243	90	270, 260, 247, 186, 230, 129, 85, 87, 200
28568	Y	Y	-	Y	Y	-	12, 104	104	270, 85, 266, 230, 262
28677	Y	Y	-	Y	Y	Y	90, 105, 12, 90	90	270, 247, 266, 87, 85, 262
28704	Y	-	-	-	Y	-	105, 243		270, 87
28978	Y	Y	-	-	Y	-	90, 6, 18, 45, 90	90	270, 185, 127, 146
29645	Y	-	Y	-	Y	Y	105, 164		270, 252, 87
29721	Y	-	-	-	Y	-	229		270, 161
30111	Y	-	-	-	Y	Y			
30562	Y	-	-	-	Y	-	90, 49, 81, 59, 72, 243		270, 262, 250, 185, 258, 266
30739	Y	Y	-	-	Y	Y	90, 117, 134, 69, 88, 59, 90	90	270, 127, 91, 146
30823	Y	-	-	-	Y	-	189, 33		270, 146, 225, 127
31295	Y	-	-	Y	Y	Y	90, 117, 134, 69, 88, 90, 243	90	270, 127, 146, 185, 91
31592	Y	-	-	-	Y	-	229		270, 161
31662	Y	-	-	-	Y	-	134		
32301	Y	Y	-	Y	Y	-	90, 12, 88, 90, 243	90	270, 262, 230, 262, 85, 260, 129, 87, 200
32630	Y	Y	Y	-	Y	-	3, 90, 138, 98, 168, 7, 54, 53, 63, 88, 26, 70, 76, 90	180, 90	270, 129, 138, 225, 87
32715	Y	-	-	-	Y	Y	229		270, 87
33167	Y	-	-	-	Y	Y	105, 243		270, 87
33256	Y	Y	Y	-	Y	Y	90, 11, 59, 243		270, 262, 247, 185, 87
33608	Y	-	-	-	Y	Y	90, 98, 59		270, 252, 185, 87
34053	Y	-	-	-	Y	-	173		270, 146
34137	-	-	-	-	Y	Y			
34503	Y	Y	-	Y	Y	-	90, 138, 1, 24, 49, 90	90	
34578	Y	Y	-	Y	Y	Y	3, 90, 54, 92, 88, 243		270, 91, 87
34658	Y	-	-	-	Y	Y	90, 11, 45, 243, 227		270, 185, 87, 253
36512	Y	Y	-	Y	Y	-	3, 90, 149, 138, 1, 7, 37, 24, 42, 49, 44, 26, 55, 237, 20, 49, 76, 90, 119, 131, 110, 205, 243	119, 103, 90, 110, 131	270, 200, 185, 138
37147	Y	-	-	Y	Y	Y	90, 12, 90, 104, 243	104, 90	270, 247, 230, 129, 87
37329	Y	-	Y	-	Y	Y	236		

Table 1—Continued

HD	WBVR	Geneva	DDO	Vilnius	2MASS	IRAS	Johnson	Stromgren	JP11
37394	Y	-	Y	-	Y	Y	90, 101, 18, 19, 92, 90, 243	90, 109	270, 262, 230
37594	Y	-	-	-	Y	-	90, 45		270, 87, 185
38558	Y	-	-	Y	Y	-	102, 105		270, 87
38858	Y	-	Y	-	Y	-	90, 98, 45, 243		270, 266, 262
41074	Y	-	-	-	Y	Y	105, 243		270, 230, 145
41117	Y	Y	-	-	Y	Y	3, 90, 138, 168, 1, 29, 43, 88, 70, 76, 90, 110	110, 90	270, 225, 129, 138
41330	Y	Y	Y	-	Y	Y	134, 243		270, 87, 262
41636	Y	-	Y	-	Y	Y	90, 13, 92, 243		
42807	Y	Y	Y	-	Y	Y	62, 19, 92, 243		
43042	Y	Y	-	-	Y	Y	90, 105, 11, 88, 243		270, 252, 247, 129, 87
43043	Y	-	-	-	Y	Y			270, 262
43318	Y	Y	-	-	Y	Y	90, 105, 13, 59, 49		270, 213, 87, 247, 186, 262, 230, 262, 266, 262
43386	Y	Y	-	-	Y	Y	90, 105, 173, 11, 88, 243		
43587	Y	-	Y	-	Y	Y	90, 47, 243		
45067	Y	-	Y	-	Y	Y	90, 192, 81, 59, 237, 49, 243		270, 247, 186, 262, 230, 266, 252, 87
45542	Y	-	-	-	Y	Y	90, 126, 138, 65, 23, 88, 90	90	
46300	Y	Y	Y	-	Y	Y	90, 168, 189, 47, 25, 88, 90, 233, 243, 211	163, 90	270, 185, 91, 146, 127, 86
47703	Y	-	-	-	Y	Y	134		270, 87
48682	Y	-	Y	-	Y	Y	142, 62, 19, 92, 243		
48805	Y	-	-	-	Y	Y			270, 262
50019	Y	Y	-	Y	Y	-	3, 90, 121, 54, 92, 88, 90, 243	90	270, 87
50692	Y	Y	-	-	Y	-	62, 5, 243		270, 266, 87, 262
51000	Y	Y	-	-	Y	Y	134		270, 87
51530	Y	-	-	-	Y	-	105, 243		270, 262, 266, 230, 87, 262
52711	Y	Y	-	-	Y	Y	101, 105, 62, 243		270, 87, 266, 230, 262
55575	Y	Y	Y	-	Y	Y	90, 13, 243		270, 87, 262
56537	Y	Y	-	-	Y	Y	3, 94, 90, 149, 223, 7, 6, 18, 92, 88, 20, 90, 243	90	
57006	Y	-	-	-	Y	Y	90, 45		270, 186, 230, 247, 87, 262, 266
58461	Y	-	-	-	-	Y	90, 243		270, 198, 185, 150, 151
58551	Y	-	-	-	-	-	93, 38		270, 262, 230, 266, 87, 262, 114
58715	Y	Y	-	-	-	Y	90, 24, 88, 59, 90, 243	175, 90	
58855	Y	Y	-	-	-	-	90, 105, 11, 243		270, 87
58946	Y	Y	-	Y	-	-	3, 90, 93, 168, 7, 69, 19, 10, 38, 92, 70, 90, 135, 243	135, 90	
59984	Y	-	-	-	-	-	90, 47, 73, 243		270, 87, 247, 186, 230, 262, 256, 262, 249, 266

Table 1—Continued

HD	WBVR	Geneva	DDO	Vilnius	2MASS	IRAS	Johnson	Stromgren	JP11
60111	Y	-	-	-	-	Y	90, 47		270, 258, 185, 268, 145, 87, 247
61110	Y	Y	-	-	-	Y	90, 105, 11, 69, 90, 243	90	270, 91, 129, 87, 200, 262, 230
64493	-	-	-	-	-	Y			
67006	Y	-	-	-	-	-	90, 88, 90, 243	90	270, 91, 262, 230, 129, 87
67228	Y	-	Y	-	-	-	90, 38, 243		270, 197, 230, 266, 247, 87, 262
69478	Y	-	Y	-	-	Y	90, 58, 92		
71030	Y	-	-	-	-	Y	105, 243		270, 195, 87
71148	Y	Y	Y	-	-	Y	134, 243		270, 87, 262
73262	Y	Y	Y	-	-	-	90, 49, 88, 237, 90, 243	90	270, 200, 186, 129, 146, 91, 151, 152, 127, 230, 86
73665	Y	-	Y	-	-	Y	90, 106, 93, 199, 2, 41, 38, 92, 20, 90, 226, 243, 181	90	270, 224, 115, 262
74198	Y	-	-	-	-	-	90, 69, 90, 243	90	270, 146, 127
75137	Y	Y	-	-	-	-	90, 47, 88, 90, 243	90	
75332	Y	-	-	-	-	Y	105		270, 87, 252
75596	-	-	-	-	-	-	97, 125, 49		270, 230
75732	Y	Y	-	-	-	-			
75927	-	-	-	-	-	-	189		
78366	Y	Y	Y	-	-	Y	134, 243		270, 252, 87, 262
78715	Y	Y	Y	-	-	Y	134		
79373	Y	-	-	-	-	Y	236		
79439	Y	Y	-	-	-	Y	90, 6, 18, 88, 90, 243	90	
79452	Y	Y	Y	-	-	-	90, 13, 56, 181		270, 87, 262, 86
79969	-	-	-	-	-	-	101, 56, 89, 243		
80715	Y	-	-	-	-	-	101, 92		
81192	Y	Y	Y	-	-	Y	13, 56, 243		270, 262, 86
82106	-	Y	-	-	-	Y	101, 56, 74, 19, 237, 61, 243		270, 265, 230, 262, 257
82443	Y	Y	-	-	-	Y	56, 148, 243	148	
82621	Y	Y	-	-	-	Y	90, 88, 90, 243	90	270, 146, 127
83287	Y	-	-	Y	-	-	88, 243		270, 87
83362	Y	-	-	-	-	Y			270, 262
84737	Y	Y	Y	-	-	Y	90, 140, 121, 171, 62, 19, 88, 78, 90, 243	109, 90	270, 246, 252, 129, 87
85795	Y	Y	-	-	-	Y	243		
86728	Y	Y	-	-	-	-	90, 101, 13, 62, 34, 243		270, 258, 246, 260, 162, 87, 252, 129, 266, 262, 265, 262
87696	Y	Y	Y	Y	-	Y	3, 90, 102, 7, 6, 18, 54, 69, 92, 90, 243	90	270, 200, 230, 262, 162, 252, 87, 127, 129, 246
87737	Y	Y	Y	Y	-	Y	94, 90, 25, 88, 90, 233, 243, 203, 94, 90, 25, 88	90	
87883	-	-	-	-	-	Y			

Table 1—Continued

HD	WBVR	Geneva	DDO	Vilnius	2MASS	IRAS	Johnson	Stromgren	JP11
88737	Y	-	-	-	-	Y	134, 243		270, 252, 87
88972	-	-	-	-	-	-			270, 230, 262
89125	Y	Y	-	-	-	-	90, 18, 19, 90, 243	109, 90	
89389	Y	-	-	-	-	Y	164		270, 87, 114
89744	Y	-	-	Y	-	Y	105		270, 87, 252
90277	Y	-	Y	-	-	Y	90, 102, 105, 11, 69, 90, 243	90	270, 230, 129, 87, 262, 246
90508	Y	Y	-	-	-	-	90, 101, 13, 11, 19, 243		
90839	Y	Y	-	-	-	Y	3, 90, 93, 4, 54, 69, 19, 38, 92, 90, 243, 211	90	
91262	-	-	-	-	-	-			
91752	Y	-	-	-	-	-	116, 105, 243		270, 87
92825	Y	Y	-	-	-	Y	88, 243		270, 87
93702	Y	-	-	-	-	-	229, 243		270, 127, 269, 178, 182, 146
95128	Y	Y	Y	Y	-	Y	90, 140, 121, 11, 18, 33, 19, 88, 243		270, 252, 246, 262, 129, 87
95241	Y	-	Y	Y	-	-	116, 105, 243		270, 87, 262
95934	Y	Y	-	-	-	-	116		
96738	Y	Y	-	-	-	-	116		
97334	Y	Y	Y	-	-	Y	116, 140, 154, 121, 62		270, 252, 87
97633	Y	Y	Y	-	-	-	90, 25, 88, 70, 90, 243, 211	90	270, 87, 124, 91, 146, 127
98058	Y	Y	-	Y	-	-	90, 168, 49, 90, 243	90	
98664	Y	Y	Y	-	-	Y	94, 90, 88, 60, 237, 90, 243	90	270, 91, 146, 127, 160
98824	Y	-	-	-	-	-	13, 56, 243		270, 262
99285	Y	-	-	Y	-	-	116, 105, 243		270, 166, 87
99984	Y	-	-	Y	-	Y	116, 105, 243		270, 87
100563	Y	-	-	Y	Y	Y	90, 105, 60		270, 185, 252, 87
100655	Y	-	Y	-	Y	Y	157, 236		
102124	Y	Y	-	Y	Y	Y	90, 58, 88, 243		270, 266, 113, 247, 262, 200, 186, 256, 129, 87, 252, 230, 246
103095	Y	-	-	-	Y	-	3, 90, 101, 93, 159, 190, 210, 208, 7, 54, 56, 69, 19, 92, 70, 90, 176, 205, 243, 211	90, 180, 170, 176, 109	
104556	Y	-	-	-	Y	-	101, 159, 13, 56		270, 250, 183, 262
105089	Y	-	Y	-	Y	Y	90, 58		270, 230
105475	Y	-	-	Y	Y	Y	159, 56, 92, 243		270, 264
107213	Y	-	-	Y	Y	-	116, 243		270, 191, 252, 87, 266, 264, 262
107904	Y	Y	-	-	Y	-	102, 116, 243		
108471	Y	Y	Y	-	Y	Y	90, 60, 243		
108722	Y	Y	-	Y	Y	Y	90, 105, 11, 243		270, 252, 262, 246, 230, 129, 87, 191, 228, 200, 91, 264

Table 1—Continued

HD	WBVR	Geneva	DDO	Vilnius	2MASS	IRAS	Johnson	Stromgren	JP11
108765	Y	-	-	Y	Y	-	116, 57, 243		270, 228, 87, 191
108806	-	-	-	-	Y	-	157		
109217	Y	-	Y	-	Y	Y	157, 243		
110296	-	Y	-	-	Y	Y	77		
110315	-	-	Y	Y	Y	Y	139, 243		
110392	-	-	-	-	Y	-	159, 157		
110411	Y	-	-	-	Y	Y	90, 88, 90, 243, 211	90	
110897	Y	Y	Y	Y	Y	Y	90, 105, 190, 13, 11, 19, 90, 243	90, 109	270, 130, 262, 191, 87, 230
111395	Y	Y	Y	Y	Y	Y	90, 11, 66, 25, 243		270, 262
111604	Y	-	-	-	Y	Y	77, 57, 35		270, 87, 228, 191
113095	Y	Y	Y	Y	Y	Y	116		
113337	Y	-	-	Y	Y	Y	105, 243		270, 87
113771	-	-	Y	-	Y	-	157		
114210	-	-	-	-	-	-			
114762	-	-	-	-	Y	-	101, 139, 210, 13, 243		270, 231, 191, 230, 266, 262, 250
115383	Y	Y	Y	Y	Y	Y	90, 140, 121, 11, 25, 19, 58, 88, 237, 235, 243		270, 91, 246, 258, 186, 252, 260, 266, 245, 230, 213, 247, 262, 129, 87, 262
116831	Y	-	-	-	Y	-	90, 123, 112, 165, 58		270, 185, 230, 87
118232	Y	Y	-	Y	Y	Y	90, 88, 90, 243, 211	90	270, 87
119288	Y	-	-	-	Y	Y	90, 105, 139, 60, 243		
119550	Y	-	-	-	Y	-	139		270, 266, 261, 230, 114
120048	Y	-	Y	Y	Y	Y	116		
120066	Y	-	Y	-	Y	Y	90, 101, 60, 243		
120509	-	-	-	-	Y	-			
120510	Y	-	-	-	Y	-			270, 230, 266, 114
121107	Y	Y	Y	-	Y	Y	116, 239		
121560	Y	-	-	-	Y	Y	116, 243		270, 87
122365	Y	-	-	Y	Y	-	90, 60		270, 185, 87
122408	Y	Y	Y	Y	Y	-	3, 94, 90, 164, 6, 18, 37, 24, 49, 74, 21, 88, 237, 20, 90, 243	90	
122563	Y	Y	Y	Y	Y	Y	90, 13, 64, 237, 109, 243, 181	109	270, 258, 257, 129, 186, 130, 245, 230, 162, 87, 247, 217, 262, 266, 246, 256, 260, 262, 91, 86
122676	Y	-	-	-	Y	-			270, 262
123033	Y	-	-	-	Y	-	243		
124102	-	-	-	-	Y	-	239		270, 262
124985	-	-	-	-	Y	-			270, 230
125161	Y	Y	-	Y	Y	Y	90, 88, 90, 211	90	
125162	Y	Y	-	Y	Y	-	90, 69, 90, 243	90	270, 91, 127, 146, 160

Table 1—Continued

HD	WBVR	Geneva	DDO	Vilnius	2MASS	IRAS	Johnson	Stromgren	JP11
125451	Y	Y	-	-	Y	-	94, 90, 6, 11, 18, 90, 243	90	270, 87
126248	Y	Y	-	Y	Y	-	74, 88, 243		270, 87, 222, 185
126512	-	Y	-	Y	Y	-	101, 243		270, 258, 266, 262, 230
127334	Y	-	Y	Y	Y	Y	243		270, 114, 87, 262
128167	Y	Y	Y	Y	Y	Y	90, 93, 171, 11, 18, 19, 38, 88, 90, 243, 211	90, 180, 170	270, 266, 230, 129, 262, 87, 200, 127, 246, 86
128332	Y	-	-	-	Y	Y	134, 243		270, 145, 87
129153	Y	Y	-	Y	Y	Y	116, 243		270, 247, 87
130109	Y	Y	Y	Y	Y	Y	3, 94, 90, 99, 149, 93, 190, 7, 37, 24, 49, 74, 67, 38, 88, 237, 20, 90, 243	90	270, 190, 262, 186, 213, 230, 214, 127, 124, 129, 146, 151, 91, 162, 113, 152, 200
130396	-	-	-	-	Y	-			270, 266, 230
130917	Y	Y	-	Y	Y	-	116		270, 87
130948	Y	Y	-	Y	Y	Y	116, 243		270, 214, 179, 230, 262
132052	Y	-	-	-	Y	Y	94, 90, 107, 105, 11, 49, 74, 90, 243, 211	90	270, 87
132145	Y	-	-	-	Y	-	116, 243		270, 146
132254	Y	-	-	Y	Y	Y	105, 243		270, 87
132772	Y	-	-	Y	Y	Y	116, 105		270, 87
133002	Y	-	-	Y	Y	-	134, 243		270, 230
133485	Y	-	Y	-	Y	Y	116		
134044	Y	-	-	-	Y	Y	134, 105, 203		270, 87
134047	Y	-	Y	-	Y	Y	90, 58, 237, 233		
134083	Y	Y	-	Y	Y	-	90, 190, 6, 11, 18, 69, 38, 90, 243, 211	90	270, 129, 87, 91, 246, 127, 262, 230, 222, 200, 190
134323	Y	Y	-	Y	Y	Y	112, 243		270, 262
135204	Y	-	-	-	Y	-	101, 13, 18, 19, 81, 49, 243		
135502	Y	Y	-	-	Y	Y	69, 243		270, 137, 146, 127
136118	Y	-	-	-	Y	-			270, 230, 114
136643	Y	-	Y	-	Y	Y	134		
137003	-	-	-	-	Y	Y	108, 155		
137510	Y	-	Y	-	Y	Y	134, 243		270, 87
138085	Y	-	-	Y	Y	Y	243		
138527	Y	-	-	-	Y	-	243		270, 161, 214
138803	Y	-	-	-	Y	-			270, 87
139074	Y	-	Y	Y	Y	Y	134		
139761	Y	-	-	Y	Y	Y	134		
140117	Y	-	Y	-	Y	Y	128		
140775	Y	Y	-	-	Y	Y	90, 6, 18, 74, 90, 243, 211	90	270, 152, 124, 185, 127, 269, 146
140812	-	-	-	-	Y	-	236		270, 230

Table 1—Continued

HD	WBVR	Geneva	DDO	Vilnius	2MASS	IRAS	Johnson	Stromgren	JP11
141003	Y	-	-	Y	Y	-	3, 94, 90, 99, 199, 7, 6, 18, 37, 4, 24, 88, 20, 90, 243	90	
141187	Y	-	-	-	Y	-	243		270, 152, 127, 146
141851	Y	-	-	-	Y	Y	90, 60		270, 185, 251, 152, 196, 263
142093	-	-	-	-	Y	-	209		270, 114, 266, 230
142908	Y	-	-	Y	Y	-	90, 105, 11, 243		270, 258, 262, 269, 246, 230, 260, 269, 190, 200, 252, 129, 87, 91
143687	Y	-	-	-	Y	Y	236		
143894	Y	-	-	-	Y	Y	90, 88, 90, 243, 211	90	270, 87
144579	Y	-	-	Y	Y	Y	101, 208, 18, 56, 19, 243		270, 262, 230
144622	-	-	-	-	Y	Y			
144874	Y	-	-	Y	Y	Y	94, 243		270, 230, 145, 269
145457	Y	-	-	-	Y	Y	243		
146233	Y	-	Y	Y	Y	-	90, 101, 140, 121, 18, 19, 58, 36, 48, 243		270, 197, 179, 230, 262, 266
146603	Y	-	Y	-	Y	Y	134, 243		
147025	Y	-	-	-	Y	Y	229		270, 262
147449	Y	-	Y	-	Y	Y	90, 107, 105, 49, 74, 88, 237, 90, 243, 211, 203, 49, 74, 84, 88	90	270, 247, 185, 87
147547	Y	Y	-	Y	Y	Y	3, 94, 90, 105, 54, 65, 69, 20, 90, 243, 203	90	
148048	Y	-	-	Y	Y	Y	105, 69, 40, 243		270, 230
148317	Y	-	-	-	Y	Y			270, 266, 230, 114
149630	Y	Y	-	-	Y	Y	90, 88, 90, 243	90	270, 127, 146
149661	Y	-	Y	Y	Y	-	90, 101, 140, 112, 207, 18, 19, 58, 237, 90, 243	109, 90	
149681	Y	-	-	Y	Y	Y	243		
150177	Y	-	-	-	Y	Y	105, 74, 203		270, 145, 185, 249, 248, 262, 266, 230
151044	Y	Y	-	-	Y	Y	6, 18, 104	104	270, 114, 230
151627	Y	-	Y	-	Y	Y	134		
152308	Y	-	-	-	Y	-	229, 243		
152598	Y	-	-	Y	Y	-	105, 243		270, 107, 230, 269
152614	Y	-	-	-	Y	Y	90, 88, 90, 243	90	270, 91, 161, 230
152792	Y	Y	Y	-	Y	Y	13, 243		270, 114, 262, 230
152863	Y	Y	Y	Y	Y	-	90, 6, 18, 90, 243, 203, 6	90	
153226	Y	-	Y	-	Y	Y	56, 243		270, 262
153287	Y	-	Y	-	Y	Y	221		
154345	Y	-	-	-	Y	-	101, 18, 19, 92, 243		270, 114, 230, 262
154417	Y	-	Y	Y	Y	-	90, 60, 243		
154633	Y	Y	Y	-	Y	Y	134, 243		
156826	Y	-	Y	Y	Y	Y	90, 58, 95, 48, 243		270, 262

Table 1—Continued

HD	WBVR	Geneva	DDO	Vilnius	2MASS	IRAS	Johnson	Stromgren	JP11
157214	Y	Y	-	-	Y	-	3, 90, 101, 105, 210, 208, 54, 69, 19, 43, 80, 92, 243		270, 258, 250, 190, 265, 230, 262, 129, 87
157935	Y	-	-	-	Y	-			270, 266, 230
158063	Y	-	-	-	Y	-			270, 230
158633	Y	-	-	Y	Y	-	90, 101, 18, 19		270, 230, 262
159222	Y	Y	Y	Y	Y	Y	140, 62, 92, 243		270, 230, 262
159332	Y	-	-	-	Y	Y	94, 105, 243		270, 87, 252
159410	-	-	-	-	Y	Y			
160507	Y	-	-	-	Y	Y			
161149	Y	-	-	-	Y	Y	147, 107, 105, 233, 243		270, 253, 87
161868	Y	-	Y	Y	Y	-	3, 94, 90, 99, 149, 177, 190, 7, 37, 24, 49, 74, 27, 80, 88, 237, 20, 90, 135, 176, 205, 243	90, 176, 135	270, 256, 270, 213, 113, 152, 186, 230, 91, 151, 214, 124, 127, 162, 129, 146, 86
163641	Y	-	-	-	Y	-	90, 58		270, 152, 185, 146
164259	Y	-	Y	Y	Y	Y	3, 94, 90, 97, 105, 37, 49, 74, 43, 237, 240, 20, 90, 243	90	270, 185, 87, 86
164353	Y	-	Y	Y	Y	-	90, 138, 167, 184, 49, 65, 83, 52, 88, 90, 233, 243, 203, 90, 138, 167, 49, 65, 83, 52, 88	90	
164595	Y	-	-	-	Y	Y	154, 243		270, 262
166014	Y	-	-	-	Y	Y	90, 88, 90, 243	90	
166205	Y	-	-	Y	Y	Y	90, 88, 90, 243	90	270, 146
166435	Y	-	-	-	Y	Y	243		270, 230, 114
166620	Y	Y	Y	Y	Y	-	3, 90, 101, 62, 56, 69, 19, 92, 30, 90, 243	109, 90	270, 230, 262, 130
167768	Y	-	Y	Y	Y	Y	90, 13, 60, 243, 181		
168009	Y	Y	Y	-	Y	Y	134, 243		270, 87, 262
168151	Y	Y	-	Y	Y	-	105, 69, 40, 243		270, 87
168914	Y	-	-	Y	Y	-	88, 243		270, 87
169702	Y	-	-	Y	Y	Y	88, 243		270, 87
170920	Y	-	-	-	Y	-	90, 58, 205		270, 230, 87, 185
171834	Y	-	-	Y	Y	-	90, 105, 58, 243, 203, 58		270, 185, 263, 87
173093	Y	-	-	-	Y	-	90, 133, 58		270, 185, 145, 152
173417	Y	-	-	Y	Y	Y	105		270, 87
173920	Y	-	-	Y	Y	Y	134		
174160	Y	Y	-	-	Y	Y	134, 233		270, 107, 230
174368	-	-	-	-	Y	-			
175545	-	-	Y	-	Y	Y	243		270, 230, 262
175679	Y	-	-	Y	Y	-	90, 112, 60, 243		
176303	Y	Y	-	-	Y	Y	90, 6, 18, 69, 32, 90, 243, 203, 6, 69, 32, 88	90	
176437	Y	-	Y	Y	Y	-	3, 90, 168, 190, 229, 7, 54, 69, 234, 239, 242, 90, 243	90	270, 129, 146, 162, 190, 127, 91, 260
176707	Y	-	-	Y	Y	Y	134		

Table 1—Continued

HD	WBVR	Geneva	DDO	Vilnius	2MASS	IRAS	Johnson	Stromgren	JP11
176896	Y	-	-	Y	Y	Y	134		
177196	Y	Y	-	Y	Y	Y	90, 6, 18, 88, 90, 243	90	270, 87
177756	Y	Y	-	Y	Y	Y	90, 37, 24, 49, 74, 90, 243	90	270, 129, 161, 91
178187	Y	Y	-	Y	Y	-			270, 87
178539	Y	-	-	-	Y	Y			
178798	Y	-	-	-	Y	Y			
180242	Y	-	-	-	Y	Y	69		
180777	Y	Y	-	Y	Y	Y	90, 6, 18, 88, 90, 243	90	270, 230
181440	Y	-	-	Y	Y	-	90, 58, 243		270, 185, 161, 230
181655	-	Y	Y	Y	Y	Y	56, 243		270, 262
182488	Y	Y	Y	Y	Y	Y	140, 107, 62, 56, 19		270, 262, 230
182564	Y	-	-	-	Y	Y	90, 88, 90, 243	90	
182807	Y	Y	-	-	Y	-	90, 101, 105, 13, 243, 203, 13		270, 87, 263, 250
182900	Y	-	-	-	Y	-	105, 69, 233, 243		270, 87
184385	Y	-	-	-	Y	-	33		270, 262
184499	Y	Y	-	-	Y	-	101, 210, 208, 13, 243		270, 262, 250, 197, 114, 230
184606	Y	Y	-	-	Y	-	90, 168, 33, 69, 90, 211, 203, 90, 168, 33, 69	90	
184663	Y	-	-	-	Y	-	83		270, 185, 87
184930	Y	-	Y	Y	Y	-	90, 138, 49, 74, 237, 240, 90	90	270, 127, 190, 162, 245, 91, 262, 200, 129, 138, 230, 213, 186
184960	Y	Y	-	Y	Y	Y	90, 105, 6, 18, 90, 243	90	270, 87
185018	Y	-	-	-	Y	-	134		270, 253
185395	Y	Y	-	Y	Y	-	90, 18, 69, 19, 90, 243, 203, 90, 18, 69, 19	90	
185423	Y	-	-	-	Y	-	138, 83		270, 138, 185
185872	Y	-	-	Y	Y	-	229, 243		270, 161
186547	Y	-	-	-	Y	-			270, 161, 91
186568	Y	Y	-	-	Y	-	233, 243, 96		
186760	Y	Y	-	Y	Y	Y	105		270, 262, 87
187013	Y	Y	-	Y	Y	-	3, 90, 105, 4, 65, 69, 19, 92, 243, 203, 3, 8, 4, 50, 65, 75, 69, 19, 92, 88, 79		270, 91, 258, 262, 230, 252, 260, 262, 129, 87
187638	Y	-	-	-	Y	-	134		
187691	Y	Y	-	Y	Y	-	88, 243, 203		
187923	Y	Y	Y	Y	Y	-	34, 243, 203		270, 266, 262, 87
190771	Y	-	Y	Y	Y	Y	69, 243, 203, 69		
192425	Y	Y	-	-	Y	-	90, 88, 90, 243, 211	90	270, 91, 146, 127
192640	Y	Y	-	Y	Y	Y	90, 98, 69, 31, 90, 243, 211	90	
192985	Y	-	-	-	Y	Y	105, 69, 243		270, 87

Table 1—Continued

HD	WBVR	Geneva	DDO	Vilnius	2MASS	IRAS	Johnson	Stromgren	JP11
193556	Y	-	-	-	Y	Y	112, 193, 233	193	
193621	Y	Y	-	-	Y	-	189, 51, 69		270, 91, 146
193664	Y	-	Y	Y	Y	-	90, 101, 18, 19, 243		270, 262, 230
194012	Y	-	-	-	Y	Y	154, 105, 62, 193, 233	193	270, 252, 230, 87
194279	Y	Y	-	Y	Y	-			
194688	Y	-	-	Y	Y	Y	134		
194953	Y	-	Y	-	Y	Y	74		
195019	Y	-	-	-	Y	Y	243		
195050	Y	Y	-	Y	Y	-	98, 69, 40, 31, 243		270, 146, 127
195194	Y	-	-	-	Y	-	141, 98		270, 262
195564	Y	-	Y	Y	Y	-	90, 49, 82, 243, 203, 90, 49		
196134	Y	-	-	-	Y	Y	107		
196360	Y	-	-	-	Y	Y	98		
196850	Y	Y	-	-	Y	-	98, 243		270, 230, 114
197076	Y	Y	Y	Y	Y	-	208, 62, 92, 243		
198390	Y	-	-	Y	Y	-	105, 243		270, 87
198478	Y	-	Y	Y	Y	-			
198976	Y	-	-	Y	Y	Y	134		
199763	Y	-	-	-	Y	Y			
199960	Y	-	Y	Y	Y	Y	74, 243		270, 262, 266, 87
200031	Y	-	-	-	Y	Y	98, 221, 227, 203		270, 262
200253	Y	-	-	Y	Y	-	134		
200577	Y	-	Y	Y	Y	Y	134, 207		
200723	Y	-	-	-	Y	-	243, 50		
201078	Y	Y	-	-	Y	Y	134, 202, 236, 216, 203		
202240	Y	Y	-	-	Y	-	98, 202, 122, 220		270, 87
202314	Y	Y	Y	-	Y	Y	112, 233, 216, 203		270, 253
202575	-	-	Y	-	Y	Y	14, 243, 203		270, 262, 230, 265
203245	Y	-	-	Y	Y	-	138, 215, 69		270, 138
204153	Y	-	-	Y	Y	Y	105, 189, 69, 31		270, 87
204403	Y	-	-	-	Y	-	138, 88, 243		270, 138
204642	Y	-	Y	-	Y	-	108, 243		
206043	Y	-	-	Y	Y	Y	105, 243		270, 87
206646	Y	-	-	-	Y	-			
206660	Y	-	-	-	Y	Y			270, 262

Table 1—Continued

HD	WBVR	Geneva	DDO	Vilnius	2MASS	IRAS	Johnson	Stromgren	JP11
206774	Y	-	-	-	Y	-	243		
206860	Y	-	Y	Y	Y	-	134, 207, 243		
207088	Y	-	Y	-	Y	Y	243		
207978	Y	Y	-	-	Y	-	105, 243		270, 230, 262, 266, 87
208667	-	-	-	-	Y	-			
209166	Y	-	-	-	Y	-	105, 243		270, 87
210074	Y	-	-	Y	Y	-			270, 87
210129	Y	Y	-	-	Y	-	90, 13		270, 91, 158, 146, 161
210264	Y	-	-	-	Y	-			270, 262
210373	-	-	-	-	Y	-			
210460	Y	-	Y	Y	Y	-	134, 243		270, 262, 266, 230, 265, 262, 263, 87
210855	Y	Y	-	-	Y	Y	105, 156, 144, 33, 243		270, 87
211096	Y	-	-	Y	Y	-	219		270, 146, 127
211211	Y	-	-	Y	Y	-	229		270, 146, 127
211432	Y	-	-	Y	Y	Y	134		
211976	Y	-	-	-	Y	-	90, 105, 58, 243		270, 258, 185, 87, 268
212593	Y	Y	-	Y	Y	Y	90, 25, 88, 90, 243	180, 170, 90	270, 161
213025	Y	-	-	-	Y	Y			
213323	Y	-	-	-	Y	-	229		270, 263, 146, 127
213558	Y	Y	-	Y	Y	-	90, 88, 90, 243	90	270, 129, 146, 200, 113, 91, 127, 190
213619	Y	-	-	-	Y	-	243		270, 266, 230
213660	Y	-	-	Y	Y	-	229		270, 87
214023	-	-	-	-	Y	-	108		
214680	Y	Y	Y	Y	Y	-	3, 90, 98, 184, 229, 1, 7, 16, 54, 69, 9, 43, 30, 234, 238, 239, 242, 70, 76, 90, 135, 176, 205, 243, 203	90, 176, 135	
214734	Y	-	-	Y	Y	Y	88, 243, 203		270, 87
214923	Y	Y	-	Y	Y	-	94, 90, 24, 88, 90, 135, 243	135, 90	270, 91, 200, 129, 161
215510	Y	-	Y	Y	Y	-	134		
215549	Y	-	Y	-	Y	Y	13, 92, 243		
216502	-	-	-	-	Y	Y			
216538	Y	-	-	-	Y	-			270, 161
216735	Y	-	-	-	Y	Y	3, 94, 90, 97, 37, 24, 49, 92, 88, 30, 237, 90, 243, 211	90	270, 185, 127, 146, 129
216831	Y	Y	-	-	Y	-			
217014	Y	Y	Y	Y	Y	-	3, 19, 70, 78, 90, 92, 94, 97, 140, 211, 233, 243	86, 87, 129, 186, 200, 230, 246, 252, 254, 262, 266, 270	90, 109

Table 1—Continued

HD	WBVR	Geneva	DDO	Vilnius	2MASS	IRAS	Johnson	Stromgren	JP11
218235	Y	-	-	-	Y	-	105, 243		270, 87, 152
218261	Y	-	-	Y	Y	-	134, 243, 203		270, 114, 87
218396	Y	-	-	Y	Y	-	107, 243		270, 266, 230, 262, 87, 244, 255
218470	Y	-	-	-	Y	Y	134, 105, 167, 243		270, 87, 262
218687	Y	-	-	-	Y	-			270, 266, 230
219080	Y	Y	-	-	Y	-			270, 129, 87, 262, 91, 230, 262, 107
219446	Y	-	-	-	Y	Y			
219623	Y	-	-	Y	Y	-	105, 243		270, 262, 87
221293	Y	-	-	Y	Y	Y	134		
221354	Y	Y	-	-	Y	-	101, 13, 25, 243		270, 250, 172
222173	Y	Y	-	Y	Y	Y	90, 25, 88, 90, 243	90	270, 129, 161
222439	Y	-	Y	Y	Y	-	3, 90, 218, 88, 90, 243	90	270, 129, 146, 127
222603	Y	Y	-	Y	Y	Y	90, 121, 6, 18, 37, 49, 92, 88, 90, 243	90	270, 87, 91, 185
223346	Y	-	-	-	Y	-	90, 105, 58		270, 268, 185, 258, 87
223421	Y	-	-	Y	Y	-	105, 69, 243		270, 87
224995	Y	-	-	Y	Y	-	90, 58		270, 258, 185, 268, 87

References. — 2MASS - Cutri et al. (2003), DDO - McClure (1976), Geneva - Rufener (1976), IRAS - Beichman et al. (1988), Vilnius - Zdanavicius et al. (1972), WBVR - Kornilov et al. (1991), (1) - Sharpless (1952), (2) - Johnson (1952), (3) - Johnson & Morgan (1953), (4) - Johnson (1953), (5) - Giclas (1954), (6) - Miczaika (1954), (7) - Johnson & Harris (1954), (8) - Johnson (1955), (9) - Harris (1955), (10) - Fitch (1955), (11) - Naur (1955), (12) - Johnson & Knuckles (1955), (13) - Roman (1955), (14) - Mumford (1956), (15) - Harris (1956), (16) - Hiltner & Johnson (1956), (17) - Hiltner (1956), (18) - Johnson & Knuckles (1957), (19) - Niconov et al. (1957), (20) - Arp (1958), (21) - Hardie (1958), (22) - Johnson & Mitchell (1958), (23) - Mendoza V. (1958), (24) - Hogg (1958), (25) - Bouigue (1959), (26) - Grant (1959), (27) - de Vaucouleurs (1959), (28) - Koch (1960), (29) - Hardie et al. (1960), (30) - Oosterhoff (1960), (31) - Malmquist K.G. & Ljunggren B. And Oja T. (1960), (32) - Bronkalla & Notni (1961), (33) - Bouigue et al. (1961), (34) - Wallerstein & Helfer (1961), (35) - Slettebak et al. (1961), (36) - Irwin (1961), (38) - Serkowski (1961), (39) - Hoag et al. (1961), (40) - Ljunggren & Oja (1961), (41) - Gehrels & Owings (1962), (42) - Sharpless (1962), (43) - Nikrasova et al. (1962), (44) - Gascoigne (1962), (45) - Cousins (1962), (46) - Lake (1962), (47) - Cousins (1962), (48) - Lake (1962), (49) - Cousins & Stoy (1962), (50) - Eggen (1963), (51) - Bouigue et al. (1963), (52) - Wallerstein et al. (1963), (53) - Crawford (1963), (54) - Oja (1963), (55) - Tifft (1963), (56) - Argue (1963), (57) - Westerlund (1963), (58) - Cousins (1963), (59) - Cousins (1963), (60) - Cousins (1963), (61) - Stoy (1963), (62) - Marlborough (1964), (63) - Shao (1964), (64) - Sandage (1964), (65) - Tolbert (1964), (66) - Harris & Upgren (1964), (67) - Oke (1964), (68) - Sjögren (1964), (69) - Ljunggren & Oja (1965), (70) - Johnson (1964), (71) - Cousins (1964), (72) - Lake (1964), (73) - Lake (1964), (74) - Cousins (1964), (75) - Eggen (1965), (76) - Johnson (1965), (77) - Ljunggren (1966), (78) - Johnson (1965), (79) - Nekrasova & Nikonov (1965), (80) - Alcaino (1965), (81) - Przybylski & Kennedy (1965), (82) - Lake (1965), (83) - Cousins (1965), (84) - Iriarte et al. (1965), (85) - Crawford & Perry (1966), (86) - Williams (1966), (87) - Crawford et al. (1967), (88) - Häggkvist & Oja (1966), (89) - Häggkvist (1966), (90) - Johnson et al. (1966), (91) - Cameron (1966),

(92) - Argue (1966), (93) - Jerzykiewicz & Serkowski (1966), (94) - Gutierrez-Moreno & et al. (1966), (95) - Evans (1966), (96) - Eggen (1966), (97) - Pfleiderer et al. (1966), (98) - Appenzeller (1966), (99) - van den Bergh (1967), (100) - Landolt (1967), (101) - Cowley et al. (1967), (102) - Danziger & Dickens (1967), (103) - Mendoza (1967), (104) - Mendoza (1967), (106) - Dickens et al. (1968), (107) - Breger (1968), (108) - Bakos (1968), (109) - Johnson et al. (1968), (110) - Lee (1968), (111) - Jones (1969), (112) - Rybka (1969), (113) - Perry (1969), (114) - Perry (1969), (115) - Crawford & Barnes (1969), (116) - Häggkvist & Oja (1969), (117) - Häggkvist & Oja (1969), (118) - Erro (1969), (119) - Mendoza (1969), (120) - Iriarte (1969), (121) - Fernie (1969), (122) - Millis (1969), (123) - Shobbrook et al. (1969), (124) - Barry (1969), (125) - Haug & Walter (1970), (126) - Haug (1970), (127) - Johansen & Gyldenkerne (1970), (128) - McClure (1970), (129) - Crawford & Barnes (1970), (130) - Bond (1970), (131) - Mendoza (1970), (132) - Iriarte (1970), (133) - Stobie (1970), (134) - Haggkvist & Oja (1970), (135) - Moreno (1971), (136) - Jerzykiewicz (1971), (137) - Wolff & Wolff (1971), (138) - Crawford et al. (1971), (139) - Giclas et al. (1971), (140) - Fernie et al. (1971), (141) - Walker (1971), (142) - Lutz (1971), (143) - Eggen (1971), (144) - Kubinec (1973), (145) - Danziger & Faber (1972), (146) - Crawford et al. (1972), (147) - Zissell (1972), (148) - Sturch & Helfer (1972), (149) - Bok et al. (1972), (150) - Eggen (1972), (151) - Stokes (1972), (152) - Stokes (1972), (153) - Sturch (1972), (154) - Epps (1972), (155) - Ardeberg et al. (1973), (156) - Wramdemark (1973), (157) - Haggkvist & Oja (1973), (158) - Kubiak (1973), (159) - Schild (1973), (160) - Warren (1973), (161) - Crawford et al. (1973), (162) - Philip & Philip (1973), (163) - Allen (1973), (164) - Penston (1973), (165) - Cousins (1973), (166) - Eggen (1973), (167) - Haupt & Schroll (1974), (168) - Neckel (1974), (169) - Crawford & Barnes (1974), (170) - Veeder (1974), (171) - Elliott (1974), (172) - Olson (1974), (173) - Breger (1974), (174) - Lucke (1974), (175) - Glass (1974), (176) - Mendoza & Gonzalez (1974), (177) - Celis S. (1975), (178) - Heck & Manfroid (1975), (179) - Crawford (1975), (180) - Glass (1975), (181) - Jennens & Helfer (1975), (182) - Wolf & Morrison (1975), (183) - Blaauw et al. (1976), (184) - Burnichon & Garnier (1976), (185) - Gronbech & Olsen (1976), (186) - Gronbech et al. (1976), (187) - Mechler (1976), (188) - Crawford & Perry (1976), (189) - Deutschman et al. (1976), (190) - Piirola (1976), (191) - Hilditch et al. (1976), (192) - Wickramasinghe & Warren (1976), (193) - Fernie (1976), (194) - McNamara (1976), (195) - McMillan et al. (1976), (196) - Garmany & Ianna (1977), (197) - Olsen (1977), (198) - Knude (1977), (199) - Lutz & Lutz (1977), (200) - Warren & Hesser (1977), (201) - Markkanen (1977), (202) - Szabados L. (1977), (203) - Nicolet (1978), (204) - Oblak (1978), (205) - Mendoza et al. (1978), (206) - Carney (1978), (207) - Blanco et al. (1979), (208) - Carney & Aaronson (1979), (209) - Nakagiri & Yamashita (1979), (210) - Carney (1979), (211) - Moffett & Barnes (1979), (212) - Echevarria et al. (1979), (213) - Loden et al. (1980), (214) - Heck & Manfroid (1980), (215) - Lindgren & Bern (1980), (216) - Moffett & Barnes (1980), (217) - Bond (1980), (218) - Harmanec et al. (1980), (219) - Wesselink et al. (1980), (220) - Henden (1980), (221) - Guetter (1980), (222) - Knude (1981), (223) - Szabados (1981), (224) - Olsen (1982), (225) - Westin (1982), (226) - Coleman (1982), (227) - Parsons & Montemayor (1982), (228) - Hill & Barnes (1982), (229) - Oja (1983), (230) - Olsen (1983), (231) - Carney (1983), (232) - Zhang (1983), (233) - Fernie (1983), (234) - Oja (1984), (235) - Kilkenny & Malcolm (1984), (236) - Guetter & Hewitt (1984), (237) - Cousins (1984), (238) - Oja (1985), (239) - Oja (1985), (240) - Kozok (1985), (241) - Norris et al. (1985), (242) - Oja (1986), (243) - Mermilliod (1986), (244) - Schuster & Nissen (1986), (245) - Kilkenny & Menzies (1986), (246) - Reglero et al. (1987), (247) - Manfroid & Sterken (1987), (248) - Kilkenny (1987), (249) - Cousins (1987), (250) - Schuster & Nissen (1988), (251) - Franco (1989), (252) - Fabregat & Reglero (1990), (253) - Arellano Ferro et al. (1990), (254) - Oblak (1990), (255) - Mendoza et al. (1990), (256) - Gray & Olsen (1991), (257) - Reglero & Fabregat (1991), (258) - Stetson (1991), (259) - Penprase (1992), (260) - Taylor & Joner (1992), (261) - Schuster et al. (1993), (262) - Olsen (1993), (263) - Sowell & Wilson (1993), (264) - Pena et al. (1993), (265) - Olsen (1994), (266) - Olsen (1994), (267) - Anthony-Twarog & Twarog (1994), (268) - Joner et al. (1995), (269) - Jordi et al. (1996), (270) - Hauck & Mermilliod (1998),

Starting with a reference spectral type and luminosity class as cited by SIMBAD, template spectra were fit to the photometric data. Templates in adjacent locations in spectral type and luminosity class were also tested for best fit, with the fit with best χ^2 being selected in the end for use in this study. For example, a star indicated by SIMBAD to be a G2IV would have its photometry fit to the 9 templates of spectral type G1, G2 and G3, and for luminosity classes V, IV, and III. From the best SED fit, estimates were obtained for each star for their bolometric flux (F_{BOL}), angular size (θ_{EST}), and reddening (A_V); effective temperature was fixed for each of the Pickles (1998) library spectra. The results of the fitting are given in Table 2, and an example SED fitting plot is given in Figure 1.

Also given in Table 2 are estimates of luminosity for each of these stars. The first estimate was derived from the bolometric flux from the fitting, combined with a Hipparcos distance (Perryman et al. 1997); a small number of these objects ($N = 11$) did not have such data available and a distance was estimated from comparison of the apparent visible brightness m_V to the visible M_V brightness expected from the best-fit spectral type (Cox 2000), and the SED fit reddening. The second estimate was established from the luminosity expected from the best-fit spectral type. The agreement between these two disparate estimates provided us with additional confidence in our fits, particularly from the standpoint of selection of proper luminosity class for the SED fit.

Table 2. Summary of spectral energy distribution fits for potential PTI calibrator stars, including total number of photometric points used, N_{PHOT}, reduced chi-squared χ^2_ν, reddening A_V, bolometric flux at the source F_{BOL}, luminosity estimate from bolometric flux L_{FBOL} and from spectral type L_{SP}, and estimated angular size θ_{EST}.

HD	Spectral Type	N_{PHOT}	χ^2_ν	A_V (mag)	F_{BOL} (10^8 erg cm^{-2} s^{-1})	$\log L_{FBOL}$ ($L_\odot$)	$\log L_{SP}$ ($L_\odot$)	θ_{EST} (mas)
71	K1III	3	4.39	0.38 ± 0.07	7.45 ± 0.17	2.11 ± 0.11	1.88 ± 0.50	0.690 ± 0.036
166	G8V	41	0.35	0.02 ± 0.02	10.46 ± 0.08	-0.21 ± 0.04	-0.14 ± 0.25	0.626 ± 0.013
167	G8III	8	0.76	0.13 ± 0.03	7.34 ± 0.09	1.94 ± 0.50	1.74 ± 0.50	0.594 ± 0.036
905	F0V	42	0.85	0.09 ± 0.01	14.40 ± 0.13	0.74 ± 0.02	0.85 ± 0.25	0.400 ± 0.010
1083	A0IV	16	0.44	0.03 ± 0.02	8.54 ± 0.14	1.63 ± 0.34	2.46 ± 0.33	0.167 ± 0.010
1279	B5III	37	0.95	0.30 ± 0.01	34.98 ± 0.25	2.97 ± 0.62	3.86 ± 0.50	0.153 ± 0.025
1404	A2V	55	1.00	0.08 ± 0.03	44.12 ± 0.33	1.41 ± 0.10	1.46 ± 0.25	0.465 ± 0.023
1406	K2III	15	1.30	0.23 ± 0.02	6.87 ± 0.08	1.74 ± 0.46	1.94 ± 0.50	0.728 ± 0.037
1671	F5IV	41	0.33	0.12 ± 0.02	26.75 ± 0.23	1.30 ± 0.12	1.55 ± 0.33	0.626 ± 0.030
2114	G5III	17	0.72	0.00 ± 0.05	16.21 ± 0.20	2.22 ± 0.61	1.67 ± 0.50	0.805 ± 0.054
2190	K5III	4	0.07	0.03 ± 0.19	6.03 ± 0.39	2.95 ± 2.17	2.38 ± 0.50	0.831 ± 0.071
2344	G5III	12	2.03	0.14 ± 0.03	7.25 ± 0.08	2.04 ± 0.70	1.67 ± 0.50	0.445 ± 0.028
2454	F5V	60	1.11	0.00 ± 0.01	9.62 ± 0.08	0.60 ± 0.02	0.55 ± 0.25	0.398 ± 0.009
2507	G5III	10	1.68	0.07 ± 0.03	9.69 ± 0.14	1.79 ± 0.40	1.67 ± 0.50	0.646 ± 0.041
2628	A7V	75	0.45	0.20 ± 0.02	24.94 ± 0.67	1.40 ± 0.03	1.05 ± 0.25	0.422 ± 0.012
2758	G0V	4	1.56	0.00 ± 0.10	0.39 ± 0.01	0.15 ± 1.63^a	0.21 ± 0.25	0.102 ± 0.002
2942	G8III	21	0.83	0.12 ± 0.03	10.90 ± 0.37	1.85 ± 0.09	1.74 ± 0.50	0.720 ± 0.045
3268	F5V	26	0.59	0.22 ± 0.02	8.80 ± 0.07	0.59 ± 0.11	0.55 ± 0.25	0.383 ± 0.009
4841	B5I	19	1.24	1.99 ± 0.02	63.51 ± 0.59	5.03 ± 1.63^a	4.76 ± 0.50	0.232 ± 0.009
4881	A0V	16	0.29	0.22 ± 0.02	11.58 ± 0.19	2.65 ± 0.79	1.76 ± 0.25	0.207 ± 0.013
6210	F8IV	36	0.39	0.06 ± 0.01	12.80 ± 0.16	1.41 ± 0.03	1.40 ± 0.33	0.518 ± 0.017
6288	A7V	50	0.41	0.10 ± 0.02	9.98 ± 0.07	1.00 ± 0.13	1.05 ± 0.25	0.267 ± 0.007
6833	G8III	41	0.95	0.78 ± 0.04	13.90 ± 0.12	2.36 ± 0.58	1.74 ± 0.50	0.788 ± 0.050
6903	G0IV	33	0.53	0.33 ± 0.04	23.06 ± 0.23	2.04 ± 0.27	1.29 ± 0.33	0.715 ± 0.026
6920	F8IV	36	0.37	0.13 ± 0.04	17.06 ± 0.18	1.17 ± 0.12	1.40 ± 0.33	0.575 ± 0.023
7034	A7III	32	1.25	0.31 ± 0.02	27.91 ± 0.84	2.41 ± 0.44	2.81 ± 0.50	0.446 ± 0.034
7189	G8III	12	0.67	0.15 ± 0.03	5.51 ± 0.07	1.81 ± 0.52	1.74 ± 0.50	0.505 ± 0.031
7299	K0III	8	1.25	0.04 ± 0.03	6.92 ± 0.08	1.57 ± 0.37	1.82 ± 0.50	0.613 ± 0.033
7476	F2V	37	1.40	0.33 ± 0.02	14.28 ± 0.14	0.93 ± 0.12	0.50 ± 0.25	0.518 ± 0.014
7590	G0V	20	0.51	0.04 ± 0.02	6.27 ± 0.05	0.04 ± 0.06	0.21 ± 0.25	0.411 ± 0.008
7804	A2V	51	1.04	0.26 ± 0.02	28.75 ± 0.22	1.61 ± 0.19	1.46 ± 0.25	0.384 ± 0.018
7964	A0IV	35	1.71	0.22 ± 0.02	44.18 ± 1.16	2.10 ± 0.25	2.46 ± 0.33	0.385 ± 0.024
8335	K1III	22	1.30	0.09 ± 0.03	9.50 ± 0.11	1.92 ± 0.47	1.88 ± 0.50	0.773 ± 0.041
8357	G2V	36	2.41	0.72 ± 0.01	6.49 ± 0.15	0.62 ± 0.03	0.10 ± 0.25	0.439 ± 0.009
8671	F6V	21	0.30	0.10 ± 0.02	11.66 ± 0.11	0.79 ± 0.10	0.49 ± 0.25	0.474 ± 0.011
8673	F6V	25	0.69	0.01 ± 0.01	7.55 ± 0.06	0.54 ± 0.10	0.49 ± 0.25	0.382 ± 0.009
8799	F5V	52	0.40	0.00 ± 0.03	30.58 ± 0.22	0.88 ± 0.08	0.55 ± 0.25	0.704 ± 0.019
9329	K0III	8	1.35	0.70 ± 0.04	9.83 ± 0.17	1.93 ± 0.45	1.82 ± 0.50	0.695 ± 0.039
9407	G2V	21	1.08	0.09 ± 0.01	7.16 ± 0.05	-0.01 ± 0.04	0.10 ± 0.25	0.460 ± 0.009
10112	M2III	4	2.84	0.00 ± 0.12	4.33 ± 0.06	2.68 ± 1.63^a	2.78 ± 0.50	0.830 ± 0.043
10205	B6IV	47	1.47	0.12 ± 0.01	63.14 ± 0.44	2.93 ± 0.50	3.24 ± 0.33	0.277 ± 0.013
10874	F5IV	21	0.46	0.06 ± 0.02	7.79 ± 0.07	0.92 ± 0.15	1.55 ± 0.33	0.356 ± 0.016
11007	F8V	22	0.36	0.12 ± 0.02	13.15 ± 0.15	0.49 ± 0.07	0.36 ± 0.25	0.578 ± 0.011
11151	F5V	24	1.56	0.00 ± 0.01	10.22 ± 0.06	0.80 ± 0.02	0.55 ± 0.25	0.411 ± 0.009
11946	A0V	40	0.42	0.01 ± 0.01	24.06 ± 0.16	1.67 ± 0.03	1.76 ± 0.25	0.295 ± 0.019

Table 2—Continued

HD	Spectral Type	N_{PHOT}	χ^2_ν	A_V (mag)	F_{BOL} (10^8 erg cm^{-2} s^{-1})	$\log L_{FBOL}$ ($L_\odot$)	$\log L_{SP}$ ($L_\odot$)	θ_{EST} (mas)
11973	A7V	43	0.35	0.19 ± 0.03	36.56 ± 1.71	1.28 ± 0.03	1.05 ± 0.25	0.511 ± 0.017
12235	G0V	79	0.48	0.09 ± 0.01	12.39 ± 0.09	0.57 ± 0.02	0.21 ± 0.25	0.572 ± 0.010
12303	B6IV	42	1.74	0.26 ± 0.01	57.01 ± 0.49	2.96 ± 0.46	3.24 ± 0.33	0.287 ± 0.014
12573	A2V	62	1.52	0.53 ± 0.01	31.04 ± 0.43	1.88 ± 0.05	1.46 ± 0.25	0.384 ± 0.018
13403	G2V	31	0.30	0.06 ± 0.02	4.53 ± 0.05	0.38 ± 0.11	0.10 ± 0.25	0.373 ± 0.007
13421	F8IV	59	0.33	0.02 ± 0.01	14.48 ± 0.07	0.91 ± 0.02	1.40 ± 0.33	0.551 ± 0.018
13468	G8III	25	0.57	0.12 ± 0.04	14.66 ± 0.16	1.73 ± 0.29	1.74 ± 0.50	0.845 ± 0.055
13555	F6V	41	0.42	0.01 ± 0.02	21.36 ± 0.21	0.78 ± 0.09	0.49 ± 0.25	0.639 ± 0.017
14055	A0V	68	0.76	0.01 ± 0.02	75.39 ± 1.32	1.49 ± 0.02	1.76 ± 0.25	0.522 ± 0.033
15257	A7V	51	0.46	0.19 ± 0.01	21.95 ± 0.12	1.19 ± 0.02	1.05 ± 0.25	0.396 ± 0.010
15335	F8V	36	0.32	0.14 ± 0.02	12.60 ± 0.13	0.57 ± 0.09	0.36 ± 0.25	0.545 ± 0.010
16220	F6V	22	0.21	0.10 ± 0.02	9.22 ± 0.09	0.94 ± 0.14	0.49 ± 0.25	0.422 ± 0.010
16234	F5V	41	0.52	0.21 ± 0.01	16.84 ± 0.13	0.81 ± 0.10	0.55 ± 0.25	0.530 ± 0.012
16327	F5IV	19	0.50	0.16 ± 0.02	9.75 ± 0.08	1.32 ± 0.24	1.55 ± 0.33	0.393 ± 0.018
16399	F5IV	44	0.22	0.06 ± 0.02	7.46 ± 0.06	1.20 ± 0.25	1.55 ± 0.33	0.348 ± 0.016
16647	F0V	68	1.31	0.24 ± 0.01	10.09 ± 0.10	0.69 ± 0.03	0.85 ± 0.25	0.335 ± 0.009
17093	A7V	67	0.10	0.10 ± 0.04	23.11 ± 1.25	1.02 ± 0.03	1.05 ± 0.25	0.406 ± 0.015
17228	G8III	13	0.72	0.04 ± 0.03	10.35 ± 0.14	1.71 ± 0.33	1.74 ± 0.50	0.700 ± 0.043
17573	B57V	44	1.90	0.11 ± 0.02	240.80 ± 6.46	2.26 ± 0.03	2.96 ± 0.25	0.426 ± 0.091
17616	K1IV	19	0.30	0.28 ± 0.02	7.25 ± 0.10	1.55 ± 0.72	0.73 ± 0.33	0.672 ± 0.026
18012	G8IV	19	1.19	0.57 ± 0.02	6.89 ± 0.10	1.47 ± 0.42	0.80 ± 0.33	0.633 ± 0.019
18404	F2V	38	1.47	0.28 ± 0.01	16.16 ± 0.25	0.71 ± 0.02	0.50 ± 0.25	0.480 ± 0.012
18411	A2V	31	1.94	0.32 ± 0.02	43.42 ± 0.41	2.13 ± 0.35	1.46 ± 0.25	0.488 ± 0.023
18757	G2V	37	0.38	0.01 ± 0.01	6.16 ± 0.06	0.00 ± 0.07	0.10 ± 0.25	0.428 ± 0.008
18768	G0V	23	0.92	0.15 ± 0.02	5.77 ± 0.05	0.59 ± 0.13	0.21 ± 0.25	0.411 ± 0.008
19107	A5V	46	0.44	0.11 ± 0.02	21.29 ± 0.17	1.09 ± 0.11	1.18 ± 0.25	0.351 ± 0.010
19994	G0V	46	0.43	0.02 ± 0.04	25.53 ± 0.22	0.60 ± 0.06	0.21 ± 0.25	0.815 ± 0.023
20150	B8V	53	5.29	0.35 ± 0.01	63.02 ± 1.00	2.33 ± 0.07	2.32 ± 0.25	0.315 ± 0.054
20418	B57V	33	1.07	0.15 ± 0.02	71.18 ± 1.05	2.69 ± 0.06	2.96 ± 0.25	0.232 ± 0.049
20675	F2V	25	0.73	0.31 ± 0.02	14.86 ± 0.42	0.99 ± 0.02	0.50 ± 0.25	0.460 ± 0.013
20677	A2V	38	1.55	0.20 ± 0.01	35.21 ± 0.24	1.40 ± 0.10	1.46 ± 0.25	0.409 ± 0.019
21019	G2V	63	0.48	0.13 ± 0.01	11.22 ± 0.09	0.68 ± 0.10	0.10 ± 0.25	0.555 ± 0.011
21686	A0IV	32	1.35	0.01 ± 0.02	25.78 ± 0.23	2.12 ± 0.37	2.46 ± 0.33	0.294 ± 0.018
21770	F2V	81	0.76	0.16 ± 0.02	22.36 ± 0.50	0.97 ± 0.02	0.50 ± 0.25	0.564 ± 0.015
22780	B6IV	33	1.43	0.16 ± 0.02	39.51 ± 0.31	2.88 ± 0.65	3.24 ± 0.33	0.214 ± 0.010
22879	F6V	73	1.27	0.24 ± 0.01	6.82 ± 0.04	0.10 ± 0.07	0.49 ± 0.25	0.369 ± 0.009
23408	B6IV	86	1.13	0.13 ± 0.01	168.10 ± 0.88	2.81 ± 0.37	3.24 ± 0.33	0.454 ± 0.022
23630	B6IV	50	0.45	0.12 ± 0.03	411.30 ± 3.40	3.21 ± 0.36	3.24 ± 0.33	0.708 ± 0.037
23862	B6IV	61	3.34	0.28 ± 0.02	67.28 ± 1.13	2.47 ± 0.33	3.24 ± 0.33	0.284 ± 0.014
24357	F0V	62	0.24	0.12 ± 0.01	11.55 ± 0.12	0.79 ± 0.02	0.85 ± 0.25	0.358 ± 0.009
24843	K1III	16	1.47	0.07 ± 0.03	10.57 ± 0.13	1.73 ± 0.33	1.88 ± 0.50	0.831 ± 0.045
25490	A2V	62	0.73	0.06 ± 0.03	76.84 ± 0.55	1.58 ± 0.11	1.46 ± 0.25	0.614 ± 0.030
25570	F0V	38	0.24	0.18 ± 0.01	19.65 ± 0.19	0.90 ± 0.02	0.85 ± 0.25	0.467 ± 0.012
25621	F02IV	73	0.76	0.45 ± 0.01	27.04 ± 0.63	1.01 ± 0.02	1.77 ± 0.33	0.576 ± 0.034
25680	G2V	42	1.15	0.01 ± 0.02	12.12 ± 0.10	0.03 ± 0.05	0.10 ± 0.25	0.600 ± 0.013

Table 2—Continued

HD	Spectral Type	N_{PHOT}	χ^2_ν	A_V (mag)	F_{BOL} (10^8 erg cm^{-2} s^{-1})	$\log L_{FBOL}$ ($L_\odot$)	$\log L_{SP}$ ($L_\odot$)	θ_{EST} (mas)
25867	F0V	69	1.25	0.16 ± 0.01	23.56 ± 0.38	0.75 ± 0.02	0.85 ± 0.25	0.511 ± 0.013
25948	F5V	17	1.42	0.00 ± 0.01	7.94 ± 0.04	0.75 ± 0.02	0.55 ± 0.25	0.362 ± 0.008
25975	K1IV	23	0.24	0.00 ± 0.04	12.63 ± 0.13	0.89 ± 0.10	0.73 ± 0.33	0.828 ± 0.037
26605	G8III	8	1.61	0.36 ± 0.07	11.79 ± 0.25	1.73 ± 0.45	1.74 ± 0.50	0.731 ± 0.050
26737	F5V	40	1.17	0.00 ± 0.01	3.76 ± 0.03	0.55 ± 0.03	0.55 ± 0.25	0.249 ± 0.005
26764	A0V	25	0.75	0.24 ± 0.02	29.99 ± 0.23	2.04 ± 0.26	1.76 ± 0.25	0.334 ± 0.021
27084	A7V	31	0.66	0.17 ± 0.02	20.16 ± 0.21	1.60 ± 0.22	1.05 ± 0.25	0.372 ± 0.010
27322	A0V	24	0.52	0.33 ± 0.01	17.72 ± 0.24	1.70 ± 0.04	1.76 ± 0.25	0.253 ± 0.016
27397	F0V	67	1.47	0.02 ± 0.01	14.38 ± 0.08	0.96 ± 0.13	0.85 ± 0.25	0.400 ± 0.010
27459	A7V	67	1.32	0.01 ± 0.01	19.37 ± 0.12	1.13 ± 0.15	1.05 ± 0.25	0.371 ± 0.010
27524	F5V	45	1.39	0.00 ± 0.01	4.70 ± 0.03	0.59 ± 0.03	0.55 ± 0.25	0.278 ± 0.006
27777	B6IV	20	1.15	0.26 ± 0.02	28.93 ± 0.43	2.50 ± 0.51	3.24 ± 0.33	0.205 ± 0.010
27848	F6V	55	1.40	0.00 ± 0.01	4.15 ± 0.02	0.57 ± 0.20	0.49 ± 0.25	0.283 ± 0.007
27859	G0V	69	0.47	0.12 ± 0.01	2.23 ± 0.01	0.21 ± 0.20	0.21 ± 0.25	0.244 ± 0.004
27901	F0V	43	0.67	0.24 ± 0.01	12.86 ± 0.09	0.99 ± 0.02	0.85 ± 0.25	0.378 ± 0.010
27946	A7V	76	0.72	0.11 ± 0.01	21.24 ± 0.14	1.11 ± 0.12	1.05 ± 0.25	0.391 ± 0.010
28024	A7V	51	0.54	0.26 ± 0.03	57.85 ± 0.41	1.61 ± 0.12	1.05 ± 0.25	0.666 ± 0.021
28355	A5V	82	0.98	0.15 ± 0.02	29.45 ± 0.19	1.35 ± 0.14	1.18 ± 0.25	0.401 ± 0.012
28556	A7V	80	0.73	0.12 ± 0.01	18.50 ± 0.10	1.08 ± 0.13	1.05 ± 0.25	0.368 ± 0.010
28568	F5V	52	0.26	0.02 ± 0.01	6.34 ± 0.05	0.53 ± 0.11	0.55 ± 0.25	0.327 ± 0.007
28677	F0V	52	0.54	0.12 ± 0.01	11.00 ± 0.05	0.84 ± 0.03	0.85 ± 0.25	0.349 ± 0.009
28704	F02IV	22	0.38	0.24 ± 0.02	10.99 ± 0.14	1.16 ± 0.19	1.77 ± 0.33	0.376 ± 0.022
28978	A2V	49	1.45	0.23 ± 0.02	17.74 ± 0.14	1.94 ± 0.44	1.46 ± 0.25	0.296 ± 0.013
29645	F8V	26	0.20	0.14 ± 0.02	12.91 ± 0.15	0.60 ± 0.10	0.36 ± 0.25	0.520 ± 0.009
29721	B6IV	19	1.76	0.57 ± 0.02	34.49 ± 0.48	2.62 ± 0.50	3.24 ± 0.33	0.224 ± 0.011
30111	G8III	16	0.20	0.26 ± 0.02	6.16 ± 0.07	1.90 ± 0.64	1.74 ± 0.50	0.550 ± 0.033
30562	G0V	48	0.38	0.21 ± 0.03	15.49 ± 0.13	0.53 ± 0.08	0.21 ± 0.25	0.641 ± 0.015
30739	A2V	52	1.90	0.19 ± 0.01	50.66 ± 0.39	1.75 ± 0.25	1.46 ± 0.25	0.544 ± 0.025
30823	A5III	29	2.04	0.06 ± 0.02	13.32 ± 0.10	2.02 ± 0.42	2.88 ± 0.50	0.280 ± 0.027
31295	A2V	56	1.07	0.23 ± 0.02	45.07 ± 0.32	1.29 ± 0.11	1.46 ± 0.25	0.470 ± 0.022
31592	A0V	19	0.75	0.01 ± 0.02	14.25 ± 0.12	1.57 ± 0.27	1.76 ± 0.25	0.227 ± 0.014
31662	F5V	18	1.08	0.01 ± 0.02	9.60 ± 0.10	0.61 ± 0.10	0.55 ± 0.25	0.398 ± 0.009
32301	A5V	76	1.18	0.02 ± 0.02	34.60 ± 0.22	1.43 ± 0.15	1.18 ± 0.25	0.448 ± 0.013
32630	B3V	83	1.59	0.11 ± 0.02	605.20 ± 3.42	2.93 ± 0.16	3.53 ± 0.25	0.374 ± 0.079
32715	F5V	19	0.55	0.01 ± 0.02	7.09 ± 0.07	0.54 ± 0.09	0.55 ± 0.25	0.342 ± 0.008
33167	F2V	22	0.94	0.35 ± 0.02	16.02 ± 0.20	1.03 ± 0.13	0.50 ± 0.25	0.523 ± 0.013
33256	F5V	47	0.13	0.04 ± 0.04	23.75 ± 0.21	0.67 ± 0.06	0.55 ± 0.25	0.630 ± 0.020
33608	F2V	56	0.33	0.28 ± 0.02	14.38 ± 0.55	0.82 ± 0.03	0.50 ± 0.25	0.452 ± 0.014
34053	A2V	19	1.50	0.42 ± 0.02	9.98 ± 0.14	2.10 ± 0.63	1.46 ± 0.25	0.248 ± 0.011
34137	K2III	4	0.41	0.41 ± 0.13	7.90 ± 0.24	2.36 ± 0.94	1.94 ± 0.50	0.775 ± 0.044
34503	B5III	57	1.36	0.13 ± 0.02	286.40 ± 2.00	3.41 ± 0.43	3.86 ± 0.50	0.404 ± 0.066
34578	F0II	50	1.30	0.50 ± 0.02	40.16 ± 0.30	4.05 ± 2.37	3.62 ± 0.50	0.598 ± 0.081
34658	F02IV	65	0.52	0.24 ± 0.01	22.47 ± 0.28	1.41 ± 0.05	1.77 ± 0.33	0.525 ± 0.030
36512	B0V	121	2.57	0.04 ± 0.01	326.70 ± 4.29	4.36 ± 1.14	4.76 ± 0.25	0.125 ± 0.022
37147	A7V	65	1.00	0.07 ± 0.01	15.91 ± 0.09	1.16 ± 0.15	1.05 ± 0.25	0.340 ± 0.009

Table 2—Continued

HD	Spectral Type	N_{PHOT}	χ^2_ν	A_V (mag)	F_{BOL} (10^8 erg cm^{-2} s^{-1})	$\log L_{FBOL}$ ($L_\odot$)	$\log L_{SP}$ ($L_\odot$)	θ_{EST} (mas)
37329	G8III	11	0.62	0.16 ± 0.03	10.11 ± 0.15	1.73 ± 0.43	1.74 ± 0.50	0.679 ± 0.042
37394	K0V	47	1.49	0.12 ± 0.01	10.07 ± 0.07	-0.33 ± 0.04	-0.34 ± 0.25	0.652 ± 0.013
37594	F0V	26	0.45	0.01 ± 0.02	10.21 ± 0.12	0.74 ± 0.10	0.85 ± 0.25	0.336 ± 0.009
38558	A7III	29	1.05	0.58 ± 0.02	22.53 ± 0.23	3.03 ± 1.20	2.81 ± 0.50	0.442 ± 0.033
38858	G0V	32	0.75	0.21 ± 0.01	13.29 ± 0.11	0.00 ± 0.06	0.21 ± 0.25	0.594 ± 0.011
41074	F0V	32	0.34	0.11 ± 0.01	12.26 ± 0.13	1.01 ± 0.03	0.85 ± 0.25	0.369 ± 0.009
41117	B3I	75	0.96	1.09 ± 0.02	237.80 ± 1.41	5.02 ± 1.63^a	4.98 ± 0.50	0.343 ± 0.130
41330	F8V	32	0.58	0.19 ± 0.02	10.22 ± 0.11	0.35 ± 0.08	0.36 ± 0.25	0.505 ± 0.009
41636	K0III	20	1.26	0.18 ± 0.03	11.25 ± 0.12	1.69 ± 0.30	1.82 ± 0.50	0.768 ± 0.043
42807	G2V	46	0.92	0.00 ± 0.01	7.67 ± 0.07	-0.10 ± 0.06	0.10 ± 0.25	0.461 ± 0.009
43042	F6V	49	0.51	0.01 ± 0.02	22.43 ± 0.19	0.50 ± 0.06	0.49 ± 0.25	0.655 ± 0.017
43043	G8III	16	0.19	0.03 ± 0.02	7.34 ± 0.08	1.78 ± 0.53	1.74 ± 0.50	0.587 ± 0.035
43318	F6V	69	0.41	0.13 ± 0.03	15.84 ± 0.12	0.80 ± 0.09	0.49 ± 0.25	0.563 ± 0.016
43386	F5V	52	0.31	0.00 ± 0.03	25.30 ± 0.20	0.48 ± 0.06	0.55 ± 0.25	0.643 ± 0.019
43587	F8V	89	0.17	0.19 ± 0.02	16.62 ± 0.12	0.29 ± 0.05	0.36 ± 0.25	0.609 ± 0.013
45067	F8V	60	0.18	0.09 ± 0.02	13.02 ± 0.10	0.65 ± 0.10	0.36 ± 0.25	0.537 ± 0.010
45542	B5III	32	1.90	0.14 ± 0.02	154.60 ± 1.15	3.06 ± 0.53	3.86 ± 0.50	0.317 ± 0.052
46300	A0I	71	2.99	0.01 ± 0.01	52.28 ± 0.32	3.54 ± 1.30	4.58 ± 0.50	0.375 ± 0.019
47703	F5IV	22	0.55	0.31 ± 0.01	8.90 ± 0.07	1.24 ± 0.04	1.55 ± 0.33	0.379 ± 0.017
48682	F8V	46	0.18	0.06 ± 0.04	23.34 ± 0.20	0.30 ± 0.04	0.36 ± 0.25	0.709 ± 0.019
48805	G0III	25	0.97	0.51 ± 0.03	11.13 ± 0.55	2.55 ± 0.19	2.36 ± 0.50	0.581 ± 0.040
50019	A47IV	87	0.99	0.12 ± 0.02	102.80 ± 2.63	2.07 ± 0.03	2.10 ± 0.33	0.880 ± 0.057
50692	F8V	39	0.48	0.13 ± 0.03	14.57 ± 0.14	0.13 ± 0.06	0.36 ± 0.25	0.585 ± 0.013
51000	G5III	25	0.31	0.02 ± 0.05	14.09 ± 0.18	1.79 ± 0.35	1.67 ± 0.50	0.758 ± 0.051
51530	F5V	38	0.66	0.27 ± 0.01	10.25 ± 0.10	0.86 ± 0.14	0.55 ± 0.25	0.429 ± 0.010
52711	G0V	47	0.40	0.01 ± 0.03	11.35 ± 0.10	0.11 ± 0.06	0.21 ± 0.25	0.546 ± 0.014
55575	F8V	36	0.97	0.15 ± 0.02	16.12 ± 0.16	0.16 ± 0.04	0.36 ± 0.25	0.641 ± 0.012
56537	A2V	79	0.70	0.28 ± 0.03	121.40 ± 0.72	1.50 ± 0.09	1.46 ± 0.25	0.798 ± 0.039
57006	F5IV	67	0.38	0.28 ± 0.01	13.99 ± 0.27	1.19 ± 0.03	1.55 ± 0.33	0.476 ± 0.022
58461	F2V	35	1.15	0.30 ± 0.02	13.32 ± 0.14	0.70 ± 0.09	0.50 ± 0.25	0.490 ± 0.013
58551	F5V	40	0.32	0.13 ± 0.02	6.39 ± 0.06	0.28 ± 0.09	0.55 ± 0.25	0.344 ± 0.008
58715	B8V	65	0.96	0.01 ± 0.02	304.70 ± 2.10	2.41 ± 0.15	2.32 ± 0.25	0.693 ± 0.120
58855	F5V	35	0.32	0.07 ± 0.02	19.50 ± 0.16	0.38 ± 0.06	0.55 ± 0.25	0.571 ± 0.013
58946	F0V	93	0.87	0.01 ± 0.02	53.91 ± 0.29	0.76 ± 0.06	0.85 ± 0.25	0.773 ± 0.021
59984	F5V	59	0.61	0.30 ± 0.01	13.30 ± 0.11	0.57 ± 0.09	0.55 ± 0.25	0.498 ± 0.011
60111	F0V	42	0.75	0.03 ± 0.02	17.65 ± 0.17	1.00 ± 0.11	0.85 ± 0.25	0.400 ± 0.010
61110	F02IV	64	0.20	0.31 ± 0.02	40.89 ± 0.29	1.48 ± 0.15	1.77 ± 0.33	0.668 ± 0.039
64493	K3III	4	0.14	0.11 ± 0.20	6.22 ± 0.42	2.03 ± 0.74	2.09 ± 0.50	0.719 ± 0.066
67006	A2V	47	1.38	0.18 ± 0.01	7.33 ± 0.08	1.01 ± 0.15	1.46 ± 0.25	0.437 ± 0.020
67228	G0V	76	0.37	0.26 ± 0.03	25.44 ± 1.01	0.64 ± 0.02	0.21 ± 0.25	0.819 ± 0.022
69478	G8III	17	1.68	0.07 ± 0.02	9.82 ± 0.11	2.51 ± 0.99	1.74 ± 0.50	0.689 ± 0.042
71030	F5V	42	0.30	0.02 ± 0.01	9.44 ± 0.06	0.78 ± 0.03	0.55 ± 0.25	0.395 ± 0.009
71148	G0V	36	0.31	0.16 ± 0.01	9.09 ± 0.08	0.13 ± 0.01	0.21 ± 0.25	0.490 ± 0.009
73262	A2V	80	1.82	0.06 ± 0.02	60.76 ± 0.41	1.76 ± 0.16	1.46 ± 0.25	0.556 ± 0.026
73665	K0III	65	1.13	0.00 ± 0.02	9.46 ± 0.06	1.98 ± 0.52	1.82 ± 0.50	0.698 ± 0.038

Table 2—Continued

HD	Spectral Type	N_{PHOT}	χ_ν^2	A_V (mag)	F_{BOL} (10^8 erg cm^{-2} s^{-1})	$\log L_{FBOL}$ ($L_\odot$)	$\log L_{SP}$ ($L_\odot$)	θ_{EST} (mas)
74198	A0V	35	1.23	0.01 ± 0.02	40.68 ± 0.34	1.48 ± 0.14	1.76 ± 0.25	0.381 ± 0.024
75137	A0IV	49	1.26	0.01 ± 0.02	53.30 ± 0.40	2.25 ± 0.34	2.46 ± 0.33	0.423 ± 0.026
75332	F5V	23	0.30	0.20 ± 0.02	9.80 ± 0.09	0.40 ± 0.08	0.55 ± 0.25	0.402 ± 0.009
75596	F6V	20	0.43	0.05 ± 0.02	0.96 ± 0.01	0.22 ± 0.28	0.49 ± 0.25	0.138 ± 0.003
75732	K0V	68	2.90	0.25 ± 0.02	14.50 ± 0.38	-0.15 ± 0.01	-0.34 ± 0.25	0.775 ± 0.018
75927	A0IV	7	0.03	0.12 ± 0.03	0.65 ± 0.01	1.88 ± 1.63^a	2.46 ± 0.33	0.047 ± 0.003
78366	F8V	52	0.42	0.12 ± 0.04	12.32 ± 0.61	0.15 ± 0.02	0.36 ± 0.25	0.527 ± 0.016
78715	G5III	21	1.20	0.00 ± 0.03	11.60 ± 0.32	1.78 ± 0.07	1.67 ± 0.50	0.700 ± 0.044
79373	K2III	16	9.18	0.36 ± 0.02	8.04 ± 0.20	1.94 ± 0.11	1.94 ± 0.50	0.782 ± 0.040
79439	A5V	47	0.42	0.11 ± 0.02	32.49 ± 0.26	1.13 ± 0.10	1.18 ± 0.25	0.434 ± 0.013
79452	G0III	69	0.82	0.65 ± 0.03	21.06 ± 1.62	2.11 ± 0.08	2.36 ± 0.50	0.799 ± 0.060
79969	K3V	27	1.00	0.07 ± 0.02	5.68 ± 0.06	-0.26 ± 0.07	-0.58 ± 0.25	0.598 ± 0.014
80715	K3V	26	1.77	0.11 ± 0.02	3.39 ± 0.03	-0.20 ± 0.09	-0.58 ± 0.25	0.500 ± 0.012
81192	G5III	57	0.96	0.33 ± 0.02	10.42 ± 0.33	1.69 ± 0.09	1.67 ± 0.50	0.663 ± 0.042
82106	K3V	50	1.06	0.09 ± 0.02	5.61 ± 0.05	-0.55 ± 0.05	-0.58 ± 0.25	0.598 ± 0.014
82443	G8V	28	0.42	0.09 ± 0.01	4.98 ± 0.04	-0.31 ± 0.05	-0.14 ± 0.25	0.429 ± 0.008
82621	A2V	42	1.37	0.10 ± 0.02	43.89 ± 0.38	1.96 ± 0.19	1.46 ± 0.25	0.482 ± 0.022
83287	A7V	28	1.09	0.01 ± 0.02	19.03 ± 0.16	0.94 ± 0.10	1.05 ± 0.25	0.369 ± 0.010
83362	G5III	16	1.78	0.04 ± 0.02	6.34 ± 0.07	2.26 ± 1.12	1.67 ± 0.50	0.516 ± 0.032
84737	G0V	72	0.67	0.11 ± 0.01	24.81 ± 0.16	0.42 ± 0.05	0.21 ± 0.25	0.839 ± 0.016
85795	A2V	43	0.58	0.25 ± 0.02	27.30 ± 0.54	1.60 ± 0.03	1.46 ± 0.25	0.360 ± 0.017
86728	G2V	81	0.88	0.10 ± 0.02	23.81 ± 0.16	0.22 ± 0.04	0.10 ± 0.25	0.790 ± 0.016
87696	A7V	96	0.65	0.01 ± 0.02	41.01 ± 0.23	1.00 ± 0.08	1.05 ± 0.25	0.539 ± 0.014
87737	A0I	76	2.51	0.01 ± 0.02	136.10 ± 0.81	4.26 ± 1.64	4.58 ± 0.50	0.602 ± 0.031
87883	G8V	3	0.41	0.56 ± 0.05	4.42 ± 0.07	-0.35 ± 0.01	-0.14 ± 0.25	0.405 ± 0.008
88737	F8IV	37	0.87	0.03 ± 0.01	10.11 ± 0.05	0.93 ± 0.03	1.40 ± 0.33	0.460 ± 0.015
88972	F0V	23	0.95	0.22 ± 0.02	2.05 ± 0.03	0.77 ± 0.07	0.85 ± 0.25	0.151 ± 0.004
89125	F6V	45	0.44	0.09 ± 0.01	13.73 ± 0.10	0.35 ± 0.06	0.49 ± 0.25	0.513 ± 0.012
89389	F8V	23	0.29	0.13 ± 0.02	7.55 ± 0.10	0.34 ± 0.08	0.36 ± 0.25	0.421 ± 0.007
89744	F8V	30	0.32	0.01 ± 0.02	13.24 ± 0.14	0.80 ± 0.09	0.36 ± 0.25	0.546 ± 0.010
90277	A7V	56	0.72	0.24 ± 0.01	38.05 ± 0.28	1.68 ± 0.17	1.05 ± 0.25	0.532 ± 0.014
90508	F8V	52	0.42	0.27 ± 0.01	8.49 ± 0.07	0.17 ± 0.06	0.36 ± 0.25	0.455 ± 0.008
90839	F6V	69	0.53	0.16 ± 0.03	37.32 ± 0.24	0.29 ± 0.03	0.49 ± 0.25	0.830 ± 0.023
91262	G0V	4	0.11	0.02 ± 0.10	0.62 ± 0.01	0.16 ± 1.63^a	0.21 ± 0.25	0.128 ± 0.003
91752	F5V	38	0.71	0.00 ± 0.01	7.90 ± 0.10	0.72 ± 0.02	0.55 ± 0.25	0.361 ± 0.008
92825	A2V	28	1.10	0.23 ± 0.02	27.85 ± 0.32	1.55 ± 0.18	1.46 ± 0.25	0.392 ± 0.018
93702	A0IV	38	1.22	0.21 ± 0.01	25.81 ± 0.20	1.93 ± 0.32	2.46 ± 0.33	0.295 ± 0.018
95128	G0V	70	0.41	0.13 ± 0.03	27.40 ± 0.18	0.23 ± 0.03	0.21 ± 0.25	0.863 ± 0.022
95241	F8V	35	0.61	0.17 ± 0.02	11.22 ± 0.10	0.86 ± 0.11	0.36 ± 0.25	0.524 ± 0.010
95934	A5V	33	0.55	0.01 ± 0.01	9.91 ± 0.10	1.30 ± 0.04	1.18 ± 0.25	0.239 ± 0.007
96738	A0IV	25	1.72	0.31 ± 0.02	19.12 ± 0.15	1.97 ± 0.31	2.46 ± 0.33	0.258 ± 0.015
97334	G0V	41	0.20	0.11 ± 0.01	7.91 ± 0.07	0.07 ± 0.07	0.21 ± 0.25	0.460 ± 0.008
97633	A2V	63	1.22	0.01 ± 0.02	129.30 ± 0.91	2.08 ± 0.14	1.46 ± 0.25	0.784 ± 0.037
98058	A7V	52	0.91	0.12 ± 0.03	46.02 ± 0.34	1.71 ± 0.17	1.05 ± 0.25	0.574 ± 0.018
98664	B9V	59	1.85	0.05 ± 0.02	91.93 ± 0.66	2.09 ± 0.17	2.04 ± 0.25	0.443 ± 0.066

Table 2—Continued

HD	Spectral Type	N_{PHOT}	χ^2_ν	A_V (mag)	F_{BOL} (10^8 erg cm^{-2} s^{-1})	$\log L_{FBOL}$ ($L_\odot$)	$\log L_{SP}$ ($L_\odot$)	θ_{EST} (mas)
98824	K1III	25	1.06	0.03 ± 0.02	6.86 ± 0.08	2.08 ± 0.83	1.88 ± 0.50	0.592 ± 0.031
99285	F0V	46	0.81	0.21 ± 0.01	17.82 ± 0.10	1.10 ± 0.02	0.85 ± 0.25	0.445 ± 0.011
99984	F5V	31	0.30	0.25 ± 0.01	12.89 ± 0.12	1.10 ± 0.13	0.55 ± 0.25	0.474 ± 0.011
100563	F5V	40	0.60	0.03 ± 0.02	12.96 ± 0.11	0.46 ± 0.08	0.55 ± 0.25	0.461 ± 0.011
100655	K0III	13	1.58	0.09 ± 0.02	9.29 ± 0.11	1.76 ± 0.39	1.82 ± 0.50	0.705 ± 0.039
102124	A5V	89	0.39	0.03 ± 0.02	30.27 ± 0.20	1.10 ± 0.10	1.18 ± 0.25	0.412 ± 0.013
103095	G8V	117	3.01	0.11 ± 0.01	9.02 ± 0.12	-0.63 ± 0.04	-0.14 ± 0.25	0.579 ± 0.012
104556	G8IV	63	2.00	0.31 ± 0.01	9.29 ± 0.11	0.95 ± 0.03	0.80 ± 0.33	0.592 ± 0.017
105089	K0III	22	0.65	0.02 ± 0.03	9.74 ± 0.11	1.85 ± 0.46	1.82 ± 0.50	0.714 ± 0.040
105475	K0III	23	0.91	0.15 ± 0.01	6.11 ± 0.06	1.91 ± 0.10	1.82 ± 0.50	0.575 ± 0.031
107213	F8V	48	0.85	0.01 ± 0.01	7.52 ± 0.06	0.76 ± 0.13	0.36 ± 0.25	0.412 ± 0.008
107904	F02IV	41	1.36	0.17 ± 0.02	10.97 ± 0.20	1.56 ± 0.04	1.77 ± 0.33	0.367 ± 0.021
108471	G8III	24	1.79	0.05 ± 0.02	9.14 ± 0.08	2.14 ± 0.65	1.74 ± 0.50	0.660 ± 0.040
108722	F02IV	70	0.18	0.28 ± 0.02	20.19 ± 0.74	1.44 ± 0.04	1.77 ± 0.33	0.498 ± 0.030
108765	A2V	39	0.82	0.31 ± 0.02	17.24 ± 0.15	1.51 ± 0.20	1.46 ± 0.25	0.305 ± 0.014
108806	K1III	6	2.81	0.90 ± 0.04	2.85 ± 0.03	2.40 ± 2.34	1.88 ± 0.50	0.432 ± 0.023
109217	G8III	13	0.87	0.09 ± 0.06	12.03 ± 0.18	1.90 ± 0.40	1.74 ± 0.50	0.708 ± 0.047
110296	K3IV	13	1.95	1.71 ± 0.08	2.26 ± 0.05	1.70 ± 0.80	0.75 ± 0.33	0.968 ± 0.270
110315	K4V	31	2.35	0.25 ± 0.01	3.28 ± 0.03	-0.68 ± 0.01	-0.67 ± 0.25	0.525 ± 0.014
110392	G8III	9	0.32	0.03 ± 0.02	2.97 ± 0.03	1.55 ± 0.55	1.74 ± 0.50	0.375 ± 0.023
110411	A0V	56	1.66	0.12 ± 0.01	36.60 ± 0.36	1.19 ± 0.02	1.76 ± 0.25	0.363 ± 0.023
110897	F8V	98	1.50	0.01 ± 0.01	11.20 ± 0.06	0.02 ± 0.04	0.36 ± 0.25	0.504 ± 0.009
111395	G5V	51	0.78	0.10 ± 0.02	9.16 ± 0.06	-0.07 ± 0.06	-0.06 ± 0.25	0.530 ± 0.010
111604	A5V	32	0.51	0.16 ± 0.02	13.50 ± 0.11	1.77 ± 0.28	1.18 ± 0.25	0.274 ± 0.008
113095	G8III	24	0.81	0.08 ± 0.04	14.49 ± 0.16	1.84 ± 0.31	1.74 ± 0.50	0.822 ± 0.053
113337	F5V	34	2.55	0.00 ± 0.01	9.47 ± 0.06	0.62 ± 0.01	0.55 ± 0.25	0.395 ± 0.009
113771	G8III	7	0.26	0.05 ± 0.03	3.39 ± 0.04	1.77 ± 0.78	1.74 ± 0.50	0.402 ± 0.024
114210	A0IV	4	0.66	0.00 ± 0.09	0.54 ± 0.01	2.09 ± 1.63^a	2.46 ± 0.33	0.042 ± 0.003
114762	F6V	47	0.80	0.25 ± 0.01	3.17 ± 0.03	0.21 ± 0.19	0.49 ± 0.25	0.283 ± 0.007
115383	F8V	116	0.39	0.16 ± 0.02	26.44 ± 0.14	0.43 ± 0.05	0.36 ± 0.25	0.753 ± 0.016
116831	A5V	61	1.40	0.03 ± 0.01	10.30 ± 0.07	1.26 ± 0.04	1.18 ± 0.25	0.244 ± 0.007
118232	A2V	67	1.58	0.37 ± 0.01	52.34 ± 0.92	1.75 ± 0.02	1.46 ± 0.25	0.499 ± 0.023
119288	F0V	83	1.59	0.26 ± 0.01	11.19 ± 0.14	0.65 ± 0.02	0.85 ± 0.25	0.352 ± 0.009
119550	G2V	31	0.22	0.01 ± 0.02	4.95 ± 0.06	0.75 ± 0.18	0.10 ± 0.25	0.373 ± 0.007
120048	G8III	17	0.50	0.07 ± 0.05	14.04 ± 0.17	1.83 ± 0.26	1.74 ± 0.50	0.827 ± 0.054
120066	G0V	72	0.29	0.14 ± 0.01	8.78 ± 0.11	0.41 ± 0.02	0.21 ± 0.25	0.481 ± 0.009
120509	F6V	4	0.50	0.09 ± 0.09	1.05 ± 0.01	0.69 ± 0.42	0.49 ± 0.25	0.143 ± 0.004
120510	F6V	24	0.15	0.00 ± 0.02	5.53 ± 0.05	0.75 ± 0.16	0.49 ± 0.25	0.326 ± 0.008
121107	G5III	30	0.62	0.00 ± 0.04	16.53 ± 0.80	2.36 ± 0.10	1.67 ± 0.50	0.835 ± 0.056
121560	F5V	21	0.59	0.20 ± 0.02	9.66 ± 0.12	0.25 ± 0.07	0.55 ± 0.25	0.422 ± 0.010
122365	A2V	33	1.79	0.31 ± 0.02	13.19 ± 0.13	1.51 ± 0.22	1.46 ± 0.25	0.267 ± 0.012
122408	A2V	78	0.93	0.33 ± 0.03	64.53 ± 0.36	1.96 ± 0.19	1.46 ± 0.25	0.596 ± 0.029
122563	G0IV	144	0.96	1.10 ± 0.02	8.67 ± 0.04	2.28 ± 0.62	1.29 ± 0.33	0.774 ± 0.031
122676	G2V	25	0.94	0.31 ± 0.01	5.17 ± 0.04	0.04 ± 0.01	0.10 ± 0.25	0.392 ± 0.007
123033	F5V	23	0.44	0.07 ± 0.02	4.67 ± 0.06	0.44 ± 0.13	0.55 ± 0.25	0.273 ± 0.006

Table 2—Continued

HD	Spectral Type	N_{PHOT}	χ_ν^2	A_V (mag)	F_{BOL} (10^8 erg cm^{-2} s^{-1})	$\log L_{FBOL}$ ($L_\odot$)	$\log L_{SP}$ ($L_\odot$)	θ_{EST} (mas)
124102	G2IV	15	1.86	0.05 ± 0.02	1.11 ± 0.01	0.57 ± 0.36	1.20 ± 0.33	0.178 ± 0.006
124985	F6V	15	0.69	0.34 ± 0.02	1.27 ± 0.02	0.80 ± 0.09	0.49 ± 0.25	0.157 ± 0.004
125161	A5V	35	1.17	0.06 ± 0.02	32.47 ± 0.26	0.96 ± 0.06	1.18 ± 0.25	0.435 ± 0.013
125162	A2V	64	1.38	0.21 ± 0.02	55.38 ± 0.38	1.19 ± 0.06	1.46 ± 0.25	0.582 ± 0.028
125451	F2V	74	1.67	0.22 ± 0.01	22.49 ± 0.30	0.68 ± 0.01	0.50 ± 0.25	0.566 ± 0.014
126248	A3V	46	1.43	0.30 ± 0.01	29.59 ± 0.20	1.30 ± 0.14	1.36 ± 0.25	0.401 ± 0.014
126512	F8V	44	1.16	0.17 ± 0.02	3.24 ± 0.03	0.35 ± 0.13	0.36 ± 0.25	0.298 ± 0.006
127334	G5V	34	0.59	0.10 ± 0.01	8.34 ± 0.08	0.16 ± 0.05	-0.06 ± 0.25	0.508 ± 0.010
128167	F0V	103	1.29	0.18 ± 0.01	49.21 ± 0.70	0.57 ± 0.01	0.85 ± 0.25	0.739 ± 0.019
128332	F5V	25	0.17	0.21 ± 0.02	8.03 ± 0.06	0.33 ± 0.05	0.55 ± 0.25	0.365 ± 0.008
129153	A7V	39	0.70	0.03 ± 0.01	10.84 ± 0.07	0.98 ± 0.15	1.05 ± 0.25	0.278 ± 0.007
130109	A0V	135	0.48	0.00 ± 0.02	97.97 ± 2.33	1.68 ± 0.02	1.76 ± 0.25	0.595 ± 0.038
130396	F6V	16	0.14	0.08 ± 0.02	2.94 ± 0.03	0.34 ± 0.13	0.49 ± 0.25	0.237 ± 0.006
130917	A3V	32	1.80	0.23 ± 0.01	15.53 ± 0.11	1.60 ± 0.19	1.36 ± 0.25	0.283 ± 0.010
130948	F8V	47	0.52	0.12 ± 0.02	13.06 ± 0.10	0.12 ± 0.05	0.36 ± 0.25	0.548 ± 0.010
132052	F0V	49	0.41	0.08 ± 0.03	44.38 ± 0.31	1.03 ± 0.08	0.85 ± 0.25	0.692 ± 0.021
132145	A2V	21	1.32	0.11 ± 0.02	6.98 ± 0.09	1.61 ± 0.36	1.46 ± 0.25	0.193 ± 0.009
132254	F6V	29	0.47	0.06 ± 0.02	15.06 ± 0.12	0.46 ± 0.05	0.49 ± 0.25	0.542 ± 0.013
132772	F0V	16	1.09	0.14 ± 0.02	15.99 ± 0.13	1.10 ± 0.02	0.85 ± 0.25	0.421 ± 0.011
133002	F8IV	32	0.57	0.42 ± 0.01	21.61 ± 0.08	1.10 ± 0.01	1.40 ± 0.33	0.673 ± 0.022
133485	K0III	10	0.89	0.15 ± 0.03	8.63 ± 0.13	1.79 ± 0.34	1.82 ± 0.50	0.689 ± 0.038
134044	F8V	24	0.19	0.00 ± 0.02	7.58 ± 0.10	0.31 ± 0.07	0.36 ± 0.25	0.414 ± 0.007
134047	G8III	34	0.42	0.06 ± 0.02	11.54 ± 0.32	1.99 ± 0.08	1.74 ± 0.50	0.741 ± 0.046
134083	F2V	98	0.67	0.17 ± 0.02	29.03 ± 0.16	0.55 ± 0.05	0.50 ± 0.25	0.670 ± 0.018
134323	G8III	48	0.51	0.05 ± 0.03	11.72 ± 0.50	2.07 ± 0.10	1.74 ± 0.50	0.747 ± 0.048
135204	G8V	39	0.45	0.04 ± 0.02	6.88 ± 0.05	-0.19 ± 0.05	-0.14 ± 0.25	0.503 ± 0.010
135502	A2V	36	0.85	0.23 ± 0.01	22.98 ± 0.24	1.54 ± 0.15	1.46 ± 0.25	0.356 ± 0.016
136118	F8V	20	0.46	0.02 ± 0.02	4.47 ± 0.05	0.58 ± 0.15	0.36 ± 0.25	0.319 ± 0.006
136643	K1III	7	0.16	0.54 ± 0.13	7.99 ± 0.15	1.86 ± 0.44	1.88 ± 0.50	1.050 ± 0.110
137003	G8IV	9	1.58	0.54 ± 0.02	7.34 ± 0.14	1.85 ± 0.55	0.80 ± 0.33	0.445 ± 0.013
137510	G0V	21	0.75	0.14 ± 0.02	8.89 ± 0.08	0.69 ± 0.13	0.21 ± 0.25	0.489 ± 0.009
138085	G5III	18	0.71	0.31 ± 0.03	11.09 ± 0.12	1.91 ± 0.51	1.67 ± 0.50	0.697 ± 0.044
138527	B9V	23	0.85	0.10 ± 0.02	11.36 ± 0.15	1.79 ± 0.35	2.04 ± 0.25	0.168 ± 0.025
138803	F0V	24	0.97	0.07 ± 0.01	6.84 ± 0.04	0.93 ± 0.03	0.85 ± 0.25	0.275 ± 0.007
139074	G8III	17	0.64	0.07 ± 0.05	12.01 ± 0.15	1.78 ± 0.36	1.74 ± 0.50	0.764 ± 0.050
139761	K0III	17	0.98	0.16 ± 0.05	11.63 ± 0.14	1.86 ± 0.27	1.82 ± 0.50	0.865 ± 0.054
140117	K1III	11	2.76	0.08 ± 0.03	9.59 ± 0.13	1.74 ± 0.24	1.88 ± 0.50	0.778 ± 0.041
140775	A2V	66	1.41	0.14 ± 0.01	16.14 ± 0.11	1.85 ± 0.28	1.46 ± 0.25	0.299 ± 0.014
140812	F5V	15	0.08	0.06 ± 0.02	2.70 ± 0.05	0.47 ± 0.19	0.55 ± 0.25	0.215 ± 0.005
141003	A0IV	76	0.98	0.38 ± 0.03	145.50 ± 8.04	2.00 ± 0.18	2.46 ± 0.33	0.698 ± 0.046
141187	A0V	37	0.28	0.30 ± 0.01	20.78 ± 0.13	1.59 ± 0.05	1.76 ± 0.25	0.274 ± 0.017
141851	A3V	38	1.41	0.39 ± 0.02	28.84 ± 0.29	1.33 ± 0.13	1.36 ± 0.25	0.427 ± 0.015
142093	G0V	23	0.58	0.11 ± 0.02	3.51 ± 0.03	0.04 ± 0.10	0.21 ± 0.25	0.306 ± 0.006
142908	F0V	78	0.48	0.17 ± 0.02	19.70 ± 0.44	1.02 ± 0.02	0.85 ± 0.25	0.468 ± 0.013
143687	K1III	11	2.57	0.13 ± 0.02	8.00 ± 0.10	1.52 ± 0.26	1.88 ± 0.50	0.749 ± 0.039

Table 2—Continued

HD	Spectral Type	N_{PHOT}	χ^2_ν	A_V (mag)	F_{BOL} (10^8 erg cm^{-2} s^{-1})	$\log L_{FBOL}$ ($L_\odot$)	$\log L_{SP}$ ($L_\odot$)	θ_{EST} (mas)
143894	A0V	53	0.94	0.17 ± 0.01	41.33 ± 0.40	1.58 ± 0.02	1.76 ± 0.25	0.386 ± 0.024
144579	G2V	77	0.60	0.33 ± 0.01	8.25 ± 0.05	-0.27 ± 0.01	0.10 ± 0.25	0.495 ± 0.009
144622	K3IV	4	1.20	1.79 ± 0.19	2.84 ± 0.20	1.75 ± 1.64^a	0.75 ± 0.33	0.949 ± 0.310
144874	A5V	37	0.54	0.13 ± 0.01	16.81 ± 0.16	1.55 ± 0.22	1.18 ± 0.25	0.298 ± 0.009
145457	G8III	9	1.06	0.42 ± 0.03	10.31 ± 0.56	1.71 ± 0.06	1.74 ± 0.50	0.700 ± 0.046
146233	G2V	66	0.58	0.02 ± 0.03	18.40 ± 0.12	0.05 ± 0.04	0.10 ± 0.25	0.728 ± 0.018
146603	G8III	13	0.49	0.21 ± 0.03	12.61 ± 0.17	1.94 ± 0.24	1.74 ± 0.50	0.775 ± 0.048
147025	G5III	19	0.45	0.04 ± 0.02	6.75 ± 0.06	1.70 ± 0.40	1.67 ± 0.50	0.532 ± 0.033
147449	F0V	70	0.52	0.11 ± 0.03	32.25 ± 0.19	0.88 ± 0.09	0.85 ± 0.25	0.601 ± 0.018
147547	A47IV	116	1.15	0.49 ± 0.02	120.80 ± 3.66	2.13 ± 0.03	2.10 ± 0.33	0.954 ± 0.062
148048	F2V	47	0.71	0.06 ± 0.03	26.85 ± 0.20	0.87 ± 0.05	0.50 ± 0.25	0.622 ± 0.018
148317	F5IV	31	1.03	0.58 ± 0.01	8.47 ± 0.07	1.23 ± 0.04	1.55 ± 0.33	0.370 ± 0.017
149630	A0V	42	1.64	0.01 ± 0.03	64.79 ± 0.56	2.24 ± 0.19	1.76 ± 0.25	0.484 ± 0.031
149661	K0V	78	1.10	0.13 ± 0.02	15.84 ± 0.09	-0.32 ± 0.03	-0.34 ± 0.25	0.825 ± 0.018
149681	A7V	18	1.34	0.06 ± 0.02	15.59 ± 0.13	0.94 ± 0.07	1.05 ± 0.25	0.334 ± 0.009
150177	F5V	53	0.98	0.21 ± 0.01	8.11 ± 0.07	0.68 ± 0.13	0.55 ± 0.25	0.392 ± 0.009
151044	F6V	39	0.32	0.18 ± 0.01	8.03 ± 0.07	0.34 ± 0.05	0.49 ± 0.25	0.390 ± 0.009
151627	G5III	10	0.83	0.04 ± 0.03	10.03 ± 0.14	2.13 ± 0.60	1.67 ± 0.50	0.616 ± 0.039
152308	A0V	30	1.56	0.00 ± 0.02	7.44 ± 0.14	1.65 ± 0.36	1.76 ± 0.25	0.164 ± 0.010
152598	F0V	37	0.59	0.03 ± 0.02	18.38 ± 0.17	0.71 ± 0.06	0.85 ± 0.25	0.459 ± 0.012
152614	B8V	65	2.62	0.00 ± 0.01	74.31 ± 0.24	2.08 ± 0.03	2.32 ± 0.25	0.342 ± 0.058
152792	G0V	37	0.91	0.25 ± 0.01	5.49 ± 0.06	0.59 ± 0.09	0.21 ± 0.25	0.417 ± 0.008
152863	G5III	45	0.57	0.20 ± 0.02	13.93 ± 0.10	1.93 ± 0.31	1.67 ± 0.50	0.764 ± 0.048
153226	K1III	34	7.44	0.00 ± 0.02	10.92 ± 0.28	1.11 ± 0.03	1.88 ± 0.50	0.835 ± 0.044
153287	G5III	11	0.39	0.13 ± 0.02	10.54 ± 0.13	1.98 ± 0.36	1.67 ± 0.50	0.674 ± 0.042
154345	G5V	38	0.35	0.20 ± 0.01	6.62 ± 0.05	-0.17 ± 0.04	-0.06 ± 0.25	0.452 ± 0.009
154417	F8V	64	1.35	0.07 ± 0.01	11.34 ± 0.06	0.17 ± 0.01	0.36 ± 0.25	0.506 ± 0.008
154633	G8III	27	0.22	0.16 ± 0.05	13.45 ± 0.88	1.71 ± 0.04	1.74 ± 0.50	0.800 ± 0.055
156826	G8IV	55	1.48	0.19 ± 0.01	10.81 ± 0.09	0.98 ± 0.03	0.80 ± 0.33	0.639 ± 0.018
157214	F8V	86	0.19	0.23 ± 0.03	22.02 ± 0.13	0.15 ± 0.03	0.36 ± 0.25	0.716 ± 0.017
157935	F02IV	23	0.29	0.20 ± 0.01	6.55 ± 0.04	1.54 ± 0.06	1.77 ± 0.33	0.284 ± 0.016
158063	F5III	15	1.23	0.65 ± 0.02	5.03 ± 0.03	2.17 ± 0.11	2.55 ± 0.50	0.288 ± 0.019
158633	G8V	38	0.79	0.07 ± 0.02	8.36 ± 0.06	-0.37 ± 0.03	-0.14 ± 0.25	0.562 ± 0.011
159222	G2V	46	0.79	0.01 ± 0.01	6.58 ± 0.04	0.06 ± 0.05	0.10 ± 0.25	0.443 ± 0.008
159332	F6V	29	1.07	0.07 ± 0.02	15.92 ± 0.17	0.83 ± 0.09	0.49 ± 0.25	0.545 ± 0.014
159410	K3III	5	1.17	0.29 ± 0.09	6.77 ± 0.28	2.15 ± 0.55	2.09 ± 0.50	0.751 ± 0.041
160507	G8III	8	0.89	0.06 ± 0.04	8.05 ± 0.17	1.72 ± 0.31	1.74 ± 0.50	0.603 ± 0.037
161149	F02IV	59	1.30	0.40 ± 0.01	11.78 ± 0.17	1.68 ± 0.05	1.77 ± 0.33	0.380 ± 0.022
161868	A2V	158	1.52	0.05 ± 0.02	91.16 ± 0.39	1.38 ± 0.09	1.46 ± 0.25	0.658 ± 0.030
163641	B9V	46	1.46	0.22 ± 0.01	13.87 ± 0.10	2.28 ± 0.11	2.04 ± 0.25	0.178 ± 0.027
164259	F0V	74	1.06	0.20 ± 0.02	42.74 ± 1.45	0.86 ± 0.02	0.85 ± 0.25	0.689 ± 0.021
164353	B5II	116	0.74	0.44 ± 0.02	240.50 ± 1.13	4.15 ± 1.09	4.31 ± 0.50	0.483 ± 0.150
164595	G2V	22	0.41	0.01 ± 0.02	4.17 ± 0.05	0.04 ± 0.07	0.10 ± 0.25	0.349 ± 0.007
166014	A0IV	68	0.89	0.02 ± 0.03	87.13 ± 2.79	2.49 ± 0.04	2.46 ± 0.33	0.540 ± 0.033
166205	A2V	38	1.65	0.11 ± 0.02	49.42 ± 0.41	1.69 ± 0.09	1.46 ± 0.25	0.513 ± 0.024

Table 2—Continued

HD	Spectral Type	N_{PHOT}	χ^2_ν	A_V (mag)	F_{BOL} (10^8 erg cm^{-2} s^{-1})	$\log L_{FBOL}$ ($L_\odot$)	$\log L_{SP}$ ($L_\odot$)	θ_{EST} (mas)
166435	G2V	23	1.69	0.00 ± 0.02	4.85 ± 0.04	-0.02 ± 0.06	0.10 ± 0.25	0.380 ± 0.007
166620	K2V	76	1.57	0.01 ± 0.01	9.39 ± 0.05	-0.44 ± 0.02	-0.50 ± 0.25	0.703 ± 0.015
167768	G5III	37	0.89	0.02 ± 0.02	13.15 ± 0.10	1.62 ± 0.27	1.67 ± 0.50	0.732 ± 0.046
168009	G0V	32	0.19	0.21 ± 0.02	9.59 ± 0.08	0.19 ± 0.04	0.21 ± 0.25	0.505 ± 0.009
168151	F5V	40	0.40	0.01 ± 0.04	25.75 ± 0.22	0.65 ± 0.04	0.55 ± 0.25	0.652 ± 0.020
168914	A5V	28	0.80	0.26 ± 0.02	26.40 ± 0.27	1.77 ± 0.17	1.18 ± 0.25	0.403 ± 0.012
169702	A0IV	28	1.33	0.26 ± 0.02	32.05 ± 0.27	2.26 ± 0.23	2.46 ± 0.33	0.331 ± 0.020
170920	A3III	33	2.29	0.46 ± 0.02	15.04 ± 0.15	2.16 ± 0.47	2.98 ± 0.50	0.271 ± 0.030
171834	F0V	75	1.20	0.19 ± 0.01	20.47 ± 0.21	0.81 ± 0.02	0.85 ± 0.25	0.477 ± 0.012
173093	F6V	33	0.48	0.00 ± 0.02	7.80 ± 0.07	1.07 ± 0.20	0.49 ± 0.25	0.387 ± 0.009
173417	F0V	28	1.60	0.16 ± 0.02	15.54 ± 0.22	1.12 ± 0.02	0.85 ± 0.25	0.415 ± 0.011
173920	G0III	14	4.36	0.22 ± 0.02	10.07 ± 0.16	2.44 ± 0.09	2.36 ± 0.50	0.552 ± 0.036
174160	F6V	32	0.50	0.02 ± 0.02	8.85 ± 0.07	0.36 ± 0.07	0.49 ± 0.25	0.415 ± 0.010
174368	A0IV	4	1.18	0.43 ± 0.09	1.19 ± 0.02	1.86 ± 1.63^a	2.46 ± 0.33	0.066 ± 0.004
175545	K2III	19	2.54	0.12 ± 0.02	4.40 ± 0.04	1.34 ± 0.35	1.94 ± 0.50	0.581 ± 0.029
175679	G8III	27	0.79	0.09 ± 0.03	12.15 ± 0.11	1.99 ± 0.42	1.74 ± 0.50	0.758 ± 0.048
176303	F5IV	69	0.48	0.33 ± 0.01	27.42 ± 0.10	1.29 ± 0.02	1.55 ± 0.33	0.666 ± 0.031
176437	B9III	89	2.07	0.15 ± 0.02	196.70 ± 1.08	3.37 ± 0.32	3.32 ± 0.50	0.644 ± 0.120
176707	G8III	17	0.52	0.19 ± 0.02	11.56 ± 0.11	1.80 ± 0.24	1.74 ± 0.50	0.736 ± 0.044
176896	G8III	14	0.55	0.16 ± 0.02	14.07 ± 0.17	1.81 ± 0.05	1.74 ± 0.50	0.818 ± 0.049
177196	A5V	50	1.48	0.11 ± 0.01	26.73 ± 0.17	1.11 ± 0.06	1.18 ± 0.25	0.394 ± 0.011
177756	B8V	64	1.37	0.01 ± 0.02	183.80 ± 1.21	1.93 ± 0.10	2.32 ± 0.25	0.538 ± 0.092
178187	A2V	39	1.27	0.35 ± 0.01	18.68 ± 0.18	1.78 ± 0.04	1.46 ± 0.25	0.298 ± 0.014
178539	K2III	8	2.25	0.15 ± 0.03	7.67 ± 0.17	2.78 ± 1.31	1.94 ± 0.50	0.660 ± 0.033
178798	K2III	3	1.60	0.27 ± 0.07	8.96 ± 0.33	2.45 ± 0.13	1.94 ± 0.50	0.826 ± 0.044
180242	G8III	7	0.50	0.00 ± 0.10	12.79 ± 1.35	2.30 ± 0.10	1.74 ± 0.50	0.780 ± 0.062
180777	F0V	57	0.52	0.03 ± 0.01	22.45 ± 0.15	0.72 ± 0.05	0.85 ± 0.25	0.505 ± 0.013
181440	B9V	63	0.55	0.07 ± 0.01	24.61 ± 0.31	2.27 ± 0.08	2.04 ± 0.25	0.237 ± 0.035
181655	G5V	32	0.82	0.03 ± 0.01	8.76 ± 0.06	0.24 ± 0.05	-0.06 ± 0.25	0.520 ± 0.010
182488	G8V	55	0.90	0.19 ± 0.02	9.65 ± 0.07	-0.14 ± 0.03	-0.14 ± 0.25	0.592 ± 0.013
182564	A0V	38	1.55	0.09 ± 0.01	47.80 ± 0.45	1.85 ± 0.02	1.76 ± 0.25	0.415 ± 0.026
182807	F5V	52	0.39	0.22 ± 0.01	10.39 ± 0.08	0.40 ± 0.07	0.55 ± 0.25	0.419 ± 0.009
182900	F02IV	44	0.45	0.37 ± 0.01	17.50 ± 0.20	1.23 ± 0.03	1.77 ± 0.33	0.464 ± 0.027
184385	G5V	18	0.25	0.18 ± 0.02	5.81 ± 0.08	-0.13 ± 0.07	-0.06 ± 0.25	0.418 ± 0.008
184499	F8V	54	0.80	0.19 ± 0.01	6.19 ± 0.05	0.30 ± 0.07	0.36 ± 0.25	0.406 ± 0.007
184606	B57V	83	1.30	0.18 ± 0.01	73.92 ± 0.95	2.91 ± 0.07	2.96 ± 0.25	0.236 ± 0.050
184663	F2V	36	1.89	0.16 ± 0.01	8.50 ± 0.13	0.67 ± 0.02	0.50 ± 0.25	0.348 ± 0.009
184930	B57V	89	0.50	0.17 ± 0.01	132.20 ± 1.61	2.57 ± 0.05	2.96 ± 0.25	0.316 ± 0.067
184960	F6V	58	0.55	0.04 ± 0.01	13.86 ± 0.08	0.45 ± 0.04	0.49 ± 0.25	0.520 ± 0.012
185018	G5III	35	1.07	0.00 ± 0.02	12.66 ± 0.33	2.68 ± 0.18	1.67 ± 0.50	0.731 ± 0.046
185395	F2V	91	0.38	0.01 ± 0.03	40.72 ± 0.23	0.64 ± 0.03	0.50 ± 0.25	0.760 ± 0.021
185423	B5III	26	1.04	0.50 ± 0.02	27.70 ± 0.25	2.54 ± 1.63^a	3.86 ± 0.50	0.137 ± 0.022
185872	B9III	29	1.03	0.06 ± 0.01	26.57 ± 0.27	2.56 ± 0.34	3.32 ± 0.50	0.232 ± 0.042
186547	B9III	20	0.83	0.16 ± 0.02	13.03 ± 0.11	2.40 ± 0.59	3.32 ± 0.50	0.162 ± 0.029
186568	B6IV	56	0.96	0.27 ± 0.01	24.32 ± 0.20	2.76 ± 0.49	3.24 ± 0.33	0.177 ± 0.009

Table 2—Continued

HD	Spectral Type	N_{PHOT}	χ^2_ν	A_V (mag)	F_{BOL} (10^8 erg cm^{-2} s^{-1})	$\log L_{FBOL}$ ($L_\odot$)	$\log L_{SP}$ ($L_\odot$)	θ_{EST} (mas)
186760	F8V	37	0.97	0.12 ± 0.02	9.88 ± 0.09	0.80 ± 0.07	0.36 ± 0.25	0.449 ± 0.008
187013	F6V	130	0.36	0.02 ± 0.02	27.46 ± 0.13	0.57 ± 0.04	0.49 ± 0.25	0.722 ± 0.018
187638	G5III	10	0.56	0.08 ± 0.07	12.15 ± 0.22	2.24 ± 0.38	1.67 ± 0.50	0.708 ± 0.050
187691	F8V	95	0.39	0.06 ± 0.03	25.21 ± 0.82	0.47 ± 0.02	0.36 ± 0.25	0.754 ± 0.018
187923	G2V	47	0.69	0.01 ± 0.02	9.89 ± 0.08	0.37 ± 0.07	0.10 ± 0.25	0.540 ± 0.011
190771	G0V	46	0.55	0.24 ± 0.01	11.15 ± 0.14	0.09 ± 0.01	0.21 ± 0.25	0.543 ± 0.010
192425	A2V	48	0.95	0.23 ± 0.01	31.25 ± 0.26	1.34 ± 0.12	1.46 ± 0.25	0.417 ± 0.019
192640	A5V	60	0.76	0.05 ± 0.01	28.34 ± 0.26	1.17 ± 0.01	1.18 ± 0.25	0.404 ± 0.012
192985	F5V	27	1.52	0.00 ± 0.01	11.10 ± 0.11	0.62 ± 0.01	0.55 ± 0.25	0.428 ± 0.009
193556	G8III	19	0.81	0.02 ± 0.05	11.68 ± 0.13	2.02 ± 0.44	1.74 ± 0.50	0.732 ± 0.047
193621	A0IV	34	0.90	0.08 ± 0.01	6.97 ± 0.07	1.90 ± 0.35	2.46 ± 0.33	0.156 ± 0.009
193664	G0V	40	1.10	0.03 ± 0.02	11.60 ± 0.09	0.05 ± 0.03	0.21 ± 0.25	0.552 ± 0.011
194012	F6V	41	0.35	0.06 ± 0.01	9.42 ± 0.07	0.30 ± 0.06	0.49 ± 0.25	0.429 ± 0.010
194279	B3I	22	2.22	3.63 ± 0.03	43.91 ± 0.54	4.25 ± 1.63^a	4.98 ± 0.50	0.376 ± 0.150
194688	K0III	17	2.29	0.00 ± 0.02	10.72 ± 0.10	2.32 ± 0.57	1.82 ± 0.50	0.762 ± 0.041
194953	G5III	11	0.38	0.11 ± 0.06	11.28 ± 0.19	1.84 ± 0.42	1.67 ± 0.50	0.693 ± 0.048
195019	G2V	27	0.26	0.06 ± 0.02	5.08 ± 0.04	0.35 ± 0.11	0.10 ± 0.25	0.389 ± 0.007
195050	A0V	68	1.32	0.18 ± 0.01	20.08 ± 0.10	1.63 ± 0.03	1.76 ± 0.25	0.269 ± 0.017
195194	G8III	22	0.65	0.08 ± 0.02	6.33 ± 0.08	2.23 ± 0.58	1.74 ± 0.50	0.507 ± 0.031
195564	G2V	42	0.52	0.15 ± 0.02	19.20 ± 0.16	0.55 ± 0.07	0.10 ± 0.25	0.717 ± 0.015
196134	G8III	11	0.60	0.28 ± 0.02	10.32 ± 0.11	1.48 ± 0.18	1.74 ± 0.50	0.703 ± 0.042
196360	G8III	11	1.31	0.09 ± 0.02	7.71 ± 0.09	1.90 ± 0.35	1.74 ± 0.50	0.604 ± 0.037
196850	G2V	33	1.18	0.00 ± 0.01	5.40 ± 0.04	0.09 ± 0.06	0.10 ± 0.25	0.401 ± 0.008
197076	F6V	45	0.76	0.39 ± 0.01	9.78 ± 0.05	0.13 ± 0.01	0.49 ± 0.25	0.434 ± 0.010
198390	F5V	29	0.52	0.02 ± 0.01	10.39 ± 0.10	0.45 ± 0.08	0.55 ± 0.25	0.416 ± 0.009
198478	B1I	15	0.74	1.90 ± 0.05	879.00 ± 11.70	5.12 ± 1.24	5.31 ± 0.50	0.310 ± 0.140
198976	K1III	17	1.71	0.07 ± 0.03	9.84 ± 0.11	1.72 ± 0.30	1.88 ± 0.50	0.822 ± 0.044
199763	K0III	8	0.73	0.11 ± 0.04	8.76 ± 0.16	1.87 ± 0.40	1.82 ± 0.50	0.691 ± 0.039
199960	G0V	57	1.09	0.13 ± 0.01	9.34 ± 0.06	0.31 ± 0.02	0.21 ± 0.25	0.497 ± 0.009
200031	G5III	36	3.33	0.00 ± 0.01	6.17 ± 0.07	2.27 ± 0.11	1.67 ± 0.50	0.510 ± 0.032
200253	G8III	17	1.63	0.15 ± 0.04	13.72 ± 0.17	2.24 ± 0.38	1.74 ± 0.50	0.829 ± 0.054
200577	G8III	20	1.23	0.23 ± 0.04	14.06 ± 0.16	2.25 ± 0.40	1.74 ± 0.50	0.828 ± 0.054
200723	F02IV	26	0.79	0.24 ± 0.02	8.87 ± 0.10	1.45 ± 0.18	1.77 ± 0.33	0.330 ± 0.019
201078	F2II	43	2.01	0.62 ± 0.02	21.33 ± 0.16	3.35 ± 1.17	3.53 ± 0.50	0.508 ± 0.073
202240	A7III	35	2.81	0.37 ± 0.01	13.27 ± 0.09	3.09 ± 0.94	2.81 ± 0.50	0.303 ± 0.023
202314	G5I	34	1.47	0.31 ± 0.04	12.81 ± 0.12	3.35 ± 1.68	4.51 ± 0.50	0.796 ± 0.083
202575	K3V	58	1.61	0.16 ± 0.01	2.74 ± 0.02	-0.65 ± 0.01	-0.58 ± 0.25	0.448 ± 0.010
203245	B57V	31	1.45	0.00 ± 0.01	27.59 ± 0.18	2.37 ± 0.27	2.96 ± 0.25	0.153 ± 0.032
204153	F0V	55	0.79	0.03 ± 0.01	14.90 ± 0.05	0.74 ± 0.01	0.85 ± 0.25	0.407 ± 0.010
204403	B3V	24	1.84	0.30 ± 0.02	107.80 ± 2.02	4.00 ± 0.99	3.53 ± 0.25	0.157 ± 0.033
204642	K1III	13	1.88	0.18 ± 0.02	8.21 ± 0.09	1.39 ± 0.25	1.88 ± 0.50	0.717 ± 0.038
206043	F0V	29	1.02	0.10 ± 0.02	11.92 ± 0.12	0.76 ± 0.10	0.85 ± 0.25	0.380 ± 0.010
206646	K1III	8	2.70	0.11 ± 0.03	6.11 ± 0.07	1.93 ± 0.63	1.88 ± 0.50	0.626 ± 0.033
206660	G8III	16	0.56	0.03 ± 0.02	5.10 ± 0.05	2.02 ± 0.74	1.74 ± 0.50	0.483 ± 0.029
206774	A0V	16	1.12	0.00 ± 0.02	15.96 ± 0.23	1.54 ± 0.03	1.76 ± 0.25	0.240 ± 0.015

Table 2—Continued

HD	Spectral Type	N_{PHOT}	χ_ν^2	A_V (mag)	F_{BOL} (10^8 erg cm^{-2} s^{-1})	$\log L_{FBOL}$ ($L_\odot$)	$\log L_{SP}$ ($L_\odot$)	θ_{EST} (mas)
206860	F8V	43	0.53	0.14 ± 0.02	11.89 ± 0.09	0.10 ± 0.05	0.36 ± 0.25	0.528 ± 0.010
207088	G8III	11	1.11	0.18 ± 0.06	10.41 ± 0.17	1.88 ± 0.36	1.74 ± 0.50	0.690 ± 0.047
207978	F6V	45	0.79	0.01 ± 0.01	16.57 ± 0.13	0.60 ± 0.06	0.49 ± 0.25	0.565 ± 0.013
208667	K1III	4	0.77	0.21 ± 0.10	3.65 ± 0.05	1.59 ± 0.53	1.88 ± 0.50	0.480 ± 0.025
209166	F02IV	22	0.68	0.13 ± 0.02	15.36 ± 0.16	1.37 ± 0.19	1.77 ± 0.33	0.440 ± 0.025
210074	F0V	32	0.46	0.12 ± 0.01	13.51 ± 0.16	1.20 ± 0.13	0.85 ± 0.25	0.392 ± 0.010
210129	B6IV	41	1.91	0.08 ± 0.01	29.68 ± 0.22	2.63 ± 0.47	3.24 ± 0.33	0.187 ± 0.009
210264	G5III	15	1.33	0.00 ± 0.02	4.06 ± 0.02	1.72 ± 0.10	1.67 ± 0.50	0.414 ± 0.026
210373	K3IV	4	1.63	0.02 ± 0.10	3.40 ± 0.04	1.21 ± 0.32	0.75 ± 0.33	0.484 ± 0.024
210460	F8V	45	0.35	0.51 ± 0.01	5.61 ± 0.05	0.73 ± 0.12	0.36 ± 0.25	0.562 ± 0.011
210855	F6V	37	1.76	0.10 ± 0.02	22.10 ± 0.18	0.98 ± 0.06	0.49 ± 0.25	0.654 ± 0.016
211096	A0V	38	1.19	0.00 ± 0.01	18.39 ± 0.23	1.53 ± 0.03	1.76 ± 0.25	0.258 ± 0.016
211211	A0V	30	0.56	0.01 ± 0.02	15.40 ± 0.16	1.55 ± 0.17	1.76 ± 0.25	0.236 ± 0.015
211432	G8III	17	0.85	0.14 ± 0.02	9.88 ± 0.09	1.67 ± 0.29	1.74 ± 0.50	0.693 ± 0.042
211976	F5V	40	0.26	0.00 ± 0.02	8.69 ± 0.07	0.44 ± 0.09	0.55 ± 0.25	0.377 ± 0.009
212593	A0I	54	1.77	0.06 ± 0.01	49.52 ± 0.35	3.81 ± 1.10	4.58 ± 0.50	0.375 ± 0.019
213025	G8III	8	0.40	0.20 ± 0.04	9.91 ± 0.18	1.83 ± 0.33	1.74 ± 0.50	0.684 ± 0.042
213323	A0IV	27	1.01	0.00 ± 0.02	15.91 ± 0.18	1.89 ± 0.27	2.46 ± 0.33	0.231 ± 0.014
213558	A0V	69	0.84	0.01 ± 0.03	92.54 ± 0.64	1.46 ± 0.06	1.76 ± 0.25	0.576 ± 0.038
213619	F0V	29	0.94	0.18 ± 0.01	7.16 ± 0.07	1.23 ± 0.04	0.85 ± 0.25	0.282 ± 0.007
213660	A0IV	31	1.54	0.62 ± 0.01	22.83 ± 0.24	2.42 ± 0.08	2.46 ± 0.33	0.277 ± 0.017
214023	K2III	7	4.07	0.48 ± 0.03	6.42 ± 0.18	2.47 ± 0.21	1.94 ± 0.50	0.699 ± 0.036
214680	B0V	151	1.55	0.27 ± 0.01	303.80 ± 1.20	4.00 ± 0.66	4.76 ± 0.25	0.125 ± 0.022
214734	A0IV	30	1.69	0.33 ± 0.01	29.61 ± 0.23	1.95 ± 0.16	2.46 ± 0.33	0.326 ± 0.020
214923	B8V	70	1.59	0.04 ± 0.03	190.70 ± 1.22	2.39 ± 0.16	2.32 ± 0.25	0.552 ± 0.094
215510	G8III	17	1.35	0.37 ± 0.03	14.24 ± 0.16	1.71 ± 0.31	1.74 ± 0.50	0.809 ± 0.050
215549	K1IV	17	1.45	0.03 ± 0.05	9.53 ± 0.12	0.98 ± 0.14	0.73 ± 0.33	0.738 ± 0.034
216502	K1III	4	0.18	0.10 ± 0.09	4.37 ± 0.05	1.96 ± 0.71	1.88 ± 0.50	0.528 ± 0.028
216538	B5III	16	1.23	0.29 ± 0.02	23.57 ± 0.20	3.05 ± 1.00	3.86 ± 0.50	0.122 ± 0.020
216735	A0IV	71	1.29	0.03 ± 0.01	35.34 ± 0.21	1.92 ± 0.27	2.46 ± 0.33	0.330 ± 0.020
216831	B6IV	27	1.13	0.25 ± 0.02	34.30 ± 0.26	2.85 ± 0.58	3.24 ± 0.33	0.205 ± 0.010
217014	G2IV	128	0.79	0.00 ± 0.01	17.26 ± 0.23	0.11 ± 0.05	1.20 ± 0.33	0.703 ± 0.022
217491	A3III	23	1.55	1.02 ± 0.02	15.93 ± 0.49	3.07 ± 1.06	2.98 ± 0.50	0.272 ± 0.031
217813	G0V	40	0.48	0.14 ± 0.01	6.68 ± 0.07	0.09 ± 0.01	0.21 ± 0.25	0.420 ± 0.008
218235	F5V	43	1.20	0.01 ± 0.01	8.68 ± 0.06	0.70 ± 0.02	0.55 ± 0.25	0.378 ± 0.008
218261	F6V	34	2.45	0.09 ± 0.01	7.75 ± 0.09	0.29 ± 0.08	0.49 ± 0.25	0.387 ± 0.009
218396	A7V	60	1.52	0.14 ± 0.01	10.31 ± 0.08	0.71 ± 0.11	1.05 ± 0.25	0.293 ± 0.008
218470	F2V	52	1.96	0.30 ± 0.01	18.43 ± 0.25	0.83 ± 0.01	0.50 ± 0.25	0.512 ± 0.013
218687	F8V	20	0.43	0.18 ± 0.02	6.90 ± 0.10	0.16 ± 0.08	0.36 ± 0.25	0.412 ± 0.007
219080	F0V	47	0.10	0.04 ± 0.04	39.00 ± 0.39	0.86 ± 0.05	0.85 ± 0.25	0.663 ± 0.024
219446	G8III	5	0.23	0.44 ± 0.07	3.80 ± 0.04	1.91 ± 0.76	1.74 ± 0.50	0.410 ± 0.025
219623	F8V	33	0.75	0.01 ± 0.02	15.75 ± 0.15	0.31 ± 0.04	0.36 ± 0.25	0.595 ± 0.013
221293	G8III	17	0.77	0.16 ± 0.05	14.76 ± 0.18	2.22 ± 0.50	1.74 ± 0.50	0.815 ± 0.053
221354	K0V	38	1.22	0.09 ± 0.01	6.18 ± 0.05	-0.26 ± 0.04	-0.34 ± 0.25	0.504 ± 0.010
222173	B8V	51	1.41	0.01 ± 0.02	84.53 ± 0.62	2.80 ± 0.33	2.32 ± 0.25	0.365 ± 0.062

For our calibration sources, the *a priori* estimate of their angular size θ_{EST} is necessary to account for residual resolution that may be afforded by an interferometer's extraordinarily long baselines. With an expected limb darkened size of $\theta_{EST} \leq 1.00$ mas from the SED fit, calibrators have predicted V^2_{pred} values of $> 92\%$ for a 85-m baseline used at 2.2 μm, and $> 86\%$ for a 110-m baseline. We shall consider this size effectively identical to its uniform disk size, since for most of our potential calibration sources, their effective temperatures are in excess of ~ 5000K, and the difference between the uniform disk and limb darkened sizes is at the few percent level (Davis et al. 2000; Claret & Hauschildt 2003), which is far less than our size estimate error. Ideally, a calibration source would be sufficiently point-like that its measured visibility V^2_{meas} would be indistinguishable from unity, but unfortunately the current system sensitivity does not afford that option. The uncertainty in the calibrator visibility represents one of the fundamental limitations of the system visibility accuracy (van Belle & van Belle 2005). However, our selection of calibrators has been carefully made to be sufficiently small (≤ 1.00 mas) in diameter such that there are no concerns about a varying system calibration due to unaccounted-for calibrator surface morphology, and such that a $\leq 5\%$ uncertainty in angular size will translate to less than a $\leq 1\%$ uncertainty in its predicted visibility V^2_{pred} for PTI.

5. Obtaining Normalized PTI Observations

PTI generates its V^2_{meas} observables through pairwise combination of the starlight collected by two siderostats through a 50/50 beam combiner optic; the combined starlight beams that result are fed into a NICMOS3 detector dewar. The PTI beamtrain from the siderostats to the beam combiner includes pathlength compensation that equalizes the path for each telescope from the star to the beam splitter to ~ 20 nm. Temporally dithering the pathlength compensation within one atmospheric coherence time a distance of one wavelength about

Table 2—Continued

HD	Spectral Type	N_{PHOT}	χ^2_ν	A_V (mag)	F_{BOL} (10^8 erg cm^{-2} s^{-1})	$\log L_{FBOL}$ ($L_\odot$)	$\log L_{SP}$ ($L_\odot$)	θ_{EST} (mas)
222439	B8V	78	1.17	0.05 ± 0.02	100.20 ± 2.46	1.93 ± 0.02	2.32 ± 0.25	0.397 ± 0.068
222603	A7V	76	0.79	0.01 ± 0.02	40.05 ± 0.24	1.08 ± 0.09	1.05 ± 0.25	0.533 ± 0.014
223346	F5IV	37	0.26	0.15 ± 0.02	7.57 ± 0.06	0.86 ± 0.20	1.55 ± 0.33	0.354 ± 0.016
223421	F2V	31	1.95	0.29 ± 0.02	7.51 ± 0.07	1.14 ± 0.15	0.50 ± 0.25	0.375 ± 0.010
224995	A5V	41	0.71	0.12 ± 0.02	8.93 ± 0.08	1.69 ± 0.35	1.18 ± 0.25	0.216 ± 0.006

[a]No Hipparcos distance available; distance estimated from comparison of apparent m_V with absolute M_V expected from the spectra type.
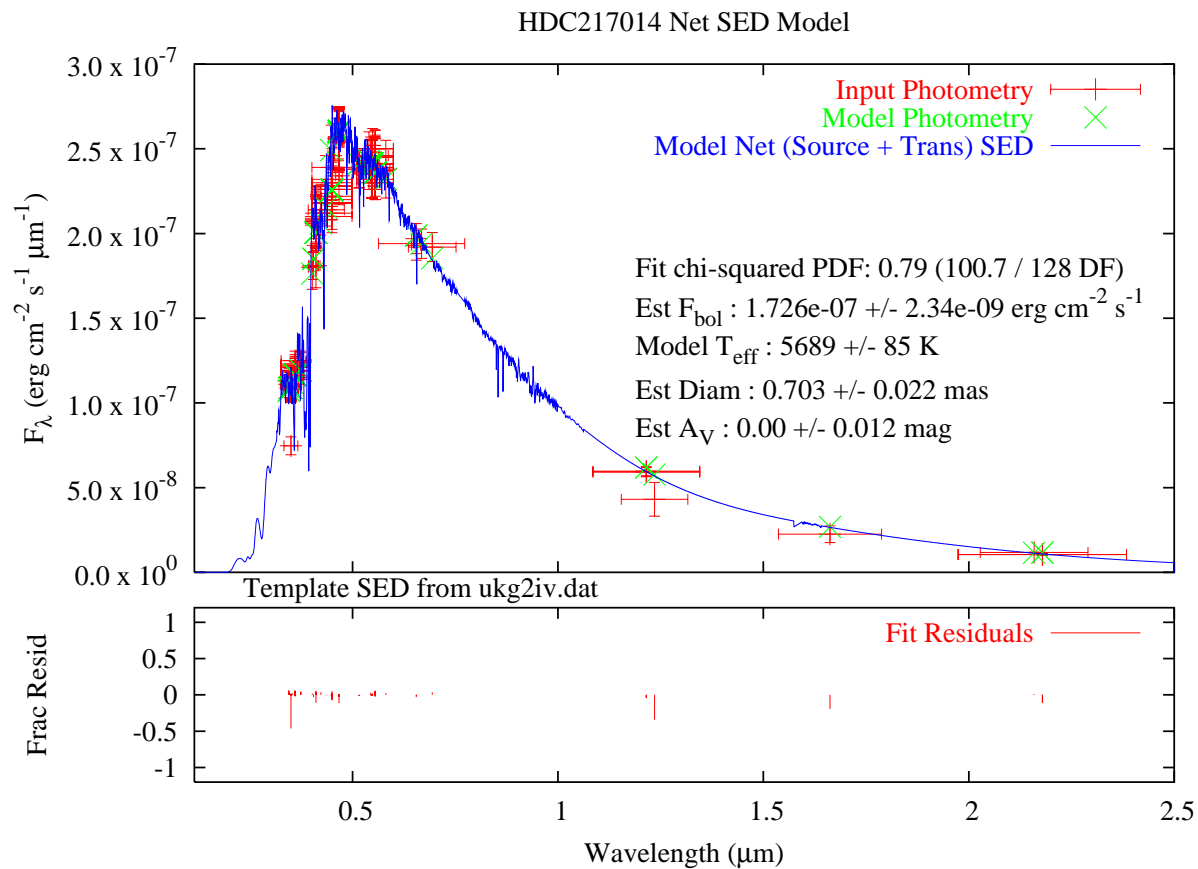
Fig. 1.— Spectral energy distribution fitting for HD 217014, as discussed in §6.1, with a G2 IV spectral template (Pickles 1998) being fit to the wide- and narrow-band photometry available for the star. Vertical bars are errors associated with the photometric data; horizontal bars represent the bandwidth of each photometric data point.

this 'white light' fringe position results in maximum constructive and destructive interference between the two starlight beams. Measurement of this temporally modulated photometric signal leads to a characterization of the V^2_{meas}. Discussion of the PTI fringe detection and tracking particulars is given in significantly greater detail in Colavita et al. (1999).

The V^2_{meas} observables used in any typical PTI study are the synthetic wideband V^2_{meas} values, given by an incoherent signal-to-noise (SNR) weighted average of the individual 5 narrowband channel $V^2_{\mathrm{meas}}(\lambda)$ values in the PTI spectrometer (Colavita 1999). In a similar fashion, incoherent SNR-weighted average bandpasses λ were determined from the raw data. The PTI H and K wavebands are excellent matches to the CIT photometric system (Elias et al. 1982, 1983). Separate calibrations and fits to the narrowband and synthetic wideband V^2_{meas} data sets yield statistically consistent results, with the synthetic wideband data exhibiting superior SNR. Since there is no need in this study for independent narrowband values, we will consequently consider only the synthetic wideband data.

The stars examined in this study were observed by PTI at 1.6 and 2.2 μm on 1,390 observing nights between 1998 Jan 1 and 2005 Dec 31. For most of the nights, PTI's NS 110m baseline (37.1 m E, 103.3 m N, -3.3 m Z) was utilized; the NW 86m baseline (-81.7 m E, -28.2 m N, 3.1 m Z) was used the second most, with the SW 87 m baseline (-44.6 m E, 75.1 m N, -0.2 m Z) being used least. The specific baselines used, in terms of number of nights and number of scans, is given in Table 3 for each star; a summary of the overall observations is given in Table 4. The potential calibration objects were observed multiple times during each of these nights, and each observation, or scan, was approximately 125 s long. For each scan we computed a mean V^2_{meas} value from the scan data, and the error in the V^2_{meas} estimate from the rms internal scatter (Colavita et al. 1999; Colavita 1999).

Table 3. Summary of PTI observations for each potential calibrator, including nights observed and number of calibrated scans, both overall and by baseline.

HD	Raw Nights Observed	All Baselines Calibrated Nights	Calibrated Scans	North-South Calibrated Nights	Calibrated Scans	North-West Calibrated Nights	Calibrated Scans	South-West Calibrated Nights	Calibrated Scans
71	2	2	5	-	-	2	5	-	-
166	67	67	270	53	217	12	49	2	4
167	1	1	2	1	2	-	-	-	-
905	4	4	11	3	7	1	4	-	-
1083	1	1	2	1	2	-	-	-	-
1279	9	9	24	9	24	-	-	-	-
1404	107	104	367	71	243	29	108	4	16
1406	2	2	12	2	12	-	-	-	-
1671	22	22	72	22	72	-	-	-	-
2114	2	2	2	2	2	-	-	-	-
2190	6	6	15	6	15	-	-	-	-
2344	3	3	4	3	4	-	-	-	-
2454	7	7	15	6	14	1	1	-	-
2507	6	6	22	6	22	-	-	-	-
2628	12	11	30	11	30	-	-	-	-
2758	1	1	3	-	-	1	3	-	-
2942	7	7	22	7	22	-	-	-	-
3268	3	3	18	3	18	-	-	-	-
4841	4	4	14	-	-	4	14	-	-
4881	4	3	6	2	3	1	3	-	-
6210	1	1	6	-	-	1	6	-	-
6288	5	4	10	4	10	-	-	-	-
6833	3	3	10	-	-	3	10	-	-
6903	8	8	15	8	15	-	-	-	-
6920	108	105	297	77	204	23	78	5	15
7034	188	186	682	133	491	51	187	2	4
7189	1	1	3	-	-	1	3	-	-
7299	1	1	4	1	4	-	-	-	-
7476	12	12	21	4	4	8	17	-	-
7590	1	1	4	1	4	-	-	-	-
7804	28	28	54	21	40	7	14	-	-
7964	93	90	323	68	257	22	66	-	-
8335	2	2	3	1	2	1	1	-	-
8357	20	20	98	12	63	8	35	-	-
8671	4	3	10	3	10	-	-	-	-
8673	19	19	67	11	32	8	35	-	-
8799	9	9	26	4	6	2	9	3	11
9329	5	5	11	1	1	4	10	-	-
9407	3	3	8	-	-	3	8	-	-
10112	3	3	9	1	3	2	6	-	-
10205	1	1	2	1	2	-	-	-	-
10874	1	1	1	1	1	-	-	-	-
11007	42	42	120	35	98	7	22	-	-
11151	57	56	171	8	15	42	141	6	15

Table 3—Continued

HD	Raw Nights Observed	All Baselines Calibrated Nights	Calibrated Scans	North-South Calibrated Nights	Calibrated Scans	North-West Calibrated Nights	Calibrated Scans	South-West Calibrated Nights	Calibrated Scans
11946	2	2	6	-	-	2	6	-	-
11973	20	19	96	16	89	3	7	-	-
12235	4	4	5	4	5	-	-	-	-
12303	5	5	16	-	-	2	8	3	8
12573	3	3	8	-	-	1	5	2	3
13403	3	3	8	-	-	3	8	-	-
13421	6	6	12	6	12	-	-	-	-
13468	12	11	23	6	10	5	13	-	-
13555	41	40	109	27	67	9	28	4	14
14055	70	69	165	45	94	23	62	1	9
15257	1	1	1	1	1	-	-	-	-
15335	37	37	113	24	66	9	31	4	16
16220	3	3	9	-	-	1	3	2	6
16234	12	7	75	5	42	-	-	2	33
16327	1	1	2	1	2	-	-	-	-
16399	2	2	5	2	5	-	-	-	-
16647	2	2	5	2	5	-	-	-	-
17093	9	9	22	8	19	1	3	-	-
17228	6	6	25	6	25	-	-	-	-
17573	44	44	131	23	76	18	41	3	14
17616	1	1	1	1	1	-	-	-	-
18012	2	2	4	2	4	-	-	-	-
18404	5	5	10	5	10	-	-	-	-
18411	18	17	35	13	26	3	8	1	1
18757	3	2	6	-	-	2	6	-	-
18768	1	1	2	1	2	-	-	-	-
19107	1	1	1	-	-	1	1	-	-
19994	2	2	7	-	-	2	7	-	-
20150	45	45	82	37	68	8	14	-	-
20418	2	2	5	-	-	2	5	-	-
20675	65	63	181	28	69	33	107	2	5
20677	22	22	73	10	36	12	37	-	-
21019	1	1	4	-	-	1	4	-	-
21686	22	21	50	17	40	4	10	-	-
21770	1	1	3	1	3	-	-	-	-
22780	1	1	3	1	3	-	-	-	-
22879	2	2	9	-	-	2	9	-	-
23408	8	8	48	8	48	-	-	-	-
23630	24	24	114	23	107	1	7	-	-
23862	1	1	6	-	-	1	6	-	-
24357	53	50	165	34	120	16	45	-	-
24843	2	2	2	-	-	1	1	1	1
25490	12	12	24	12	24	-	-	-	-
25570	24	24	64	17	43	7	21	-	-

Table 3—Continued

HD	Raw Nights Observed	All Baselines Calibrated Nights	All Baselines Calibrated Scans	North-South Calibrated Nights	North-South Calibrated Scans	North-West Calibrated Nights	North-West Calibrated Scans	South-West Calibrated Nights	South-West Calibrated Scans
25621	2	2	2	2	2	-	-	-	-
25680	45	45	166	33	128	12	38	-	-
25867	45	45	144	34	112	11	32	-	-
25948	3	3	15	-	-	3	15	-	-
25975	1	1	1	1	1	-	-	-	-
26605	1	1	5	1	5	-	-	-	-
26737	-	-	-	-	-	-	-	-	-
26764	3	3	12	-	-	3	12	-	-
27084	5	5	14	2	5	3	9	-	-
27322	3	3	7	-	-	3	7	-	-
27397	52	51	142	35	99	15	40	1	3
27459	25	25	54	13	32	11	21	1	1
27524	3	3	18	1	2	2	16	-	-
27777	1	1	1	1	1	-	-	-	-
27848	1	1	2	1	2	-	-	-	-
27859	1	1	1	1	1	-	-	-	-
27901	24	24	85	20	67	4	18	-	-
27946	6	6	23	6	23	-	-	-	-
28024	113	113	403	86	313	25	82	2	8
28355	16	15	37	11	28	4	9	-	-
28556	13	13	40	6	18	7	22	-	-
28568	-	-	-	-	-	-	-	-	-
28677	9	9	16	7	12	2	4	-	-
28704	6	6	28	4	19	2	9	-	-
28978	2	2	3	2	3	-	-	-	-
29645	35	35	82	24	49	8	26	3	7
29721	1	1	1	1	1	-	-	-	-
30111	11	11	43	7	21	4	22	-	-
30562	1	1	1	-	-	1	1	-	-
30739	31	29	70	23	58	5	9	1	3
30823	8	8	27	5	20	2	5	1	2
31295	32	32	83	28	72	3	9	1	2
31592	2	1	2	-	-	1	2	-	-
31662	2	2	4	-	-	2	4	-	-
32301	18	18	50	12	32	5	17	1	1
32630	14	14	32	11	26	3	6	-	-
32715	2	2	5	-	-	2	5	-	-
33167	25	25	74	10	28	12	41	3	5
33256	2	2	5	-	-	2	5	-	-
33608	4	4	9	-	-	4	9	-	-
34053	1	-	-	-	-	-	-	-	-
34137	2	2	6	-	-	2	6	-	-
34503	1	1	1	-	-	1	1	-	-
34578	3	3	6	3	6	-	-	-	-

Table 3—Continued

HD	Raw Nights Observed	All Baselines Calibrated Nights	All Baselines Calibrated Scans	North-South Calibrated Nights	North-South Calibrated Scans	North-West Calibrated Nights	North-West Calibrated Scans	South-West Calibrated Nights	South-West Calibrated Scans
34658	2	2	6	-	-	2	6	-	-
36512	1	1	2	-	-	1	2	-	-
37147	36	33	84	24	58	9	26	-	-
37329	3	3	5	3	5	-	-	-	-
37394	6	6	15	-	-	5	14	1	1
37594	2	2	5	-	-	2	5	-	-
38558	3	3	13	3	13	-	-	-	-
38858	2	2	4	-	-	2	4	-	-
41074	12	12	38	3	6	8	28	1	4
41117	1	1	2	1	2	-	-	-	-
41330	13	12	25	5	8	6	15	1	2
41636	6	5	11	5	11	-	-	-	-
42807	26	25	145	17	107	8	38	-	-
43042	69	66	197	49	158	17	39	-	-
43043	7	7	23	5	17	2	6	-	-
43318	1	1	2	1	2	-	-	-	-
43386	1	1	2	1	2	-	-	-	-
43587	14	14	43	13	41	1	2	-	-
45067	3	3	3	3	3	-	-	-	-
45542	3	3	10	-	-	3	10	-	-
46300	1	1	1	1	1	-	-	-	-
47703	1	1	2	1	2	-	-	-	-
48682	14	12	37	5	15	7	22	-	-
48805	45	44	134	27	95	15	36	2	3
50019	3	3	4	3	4	-	-	-	-
50692	110	109	325	66	225	40	97	3	3
51000	2	2	8	-	-	2	8	-	-
51530	3	3	26	3	26	-	-	-	-
52711	60	58	186	53	175	5	11	-	-
55575	18	17	47	11	27	6	20	-	-
56537	24	22	52	14	32	8	20	-	-
57006	97	95	249	49	133	45	112	1	4
58461	2	2	2	-	-	2	2	-	-
58551	6	6	28	5	25	1	3	-	-
58715	10	10	20	8	15	2	5	-	-
58855	3	3	8	3	8	-	-	-	-
58946	27	27	80	25	73	2	7	-	-
59984	2	2	11	-	-	2	11	-	-
60111	66	65	161	29	63	35	97	1	1
61110	1	-	-	-	-	-	-	-	-
64493	23	23	51	15	34	7	13	1	4
67006	11	11	23	9	18	2	5	-	-
67228	4	4	7	4	7	-	-	-	-
69478	1	1	1	1	1	-	-	-	-

Table 3—Continued

HD	Raw Nights Observed	All Baselines Calibrated Nights	Calibrated Scans	North-South Calibrated Nights	Calibrated Scans	North-West Calibrated Nights	Calibrated Scans	South-West Calibrated Nights	Calibrated Scans
71030	27	26	81	15	52	10	27	1	2
71148	20	19	52	16	45	3	7	-	-
73262	5	5	8	1	2	4	6	-	-
73665	1	1	1	1	1	-	-	-	-
74198	2	2	12	1	6	1	6	-	-
75137	4	4	7	-	-	4	7	-	-
75332	17	16	48	8	27	7	17	1	4
75596	-	-	-	-	-	-	-	-	-
75732	4	4	11	1	4	2	6	1	1
75927	-	-	-	-	-	-	-	-	-
78366	6	6	18	5	16	-	-	1	2
78715	24	23	61	20	53	3	8	-	-
79373	12	12	43	12	43	-	-	-	-
79439	2	2	3	-	-	2	3	-	-
79452	60	57	203	43	139	14	64	-	-
79969	1	1	7	1	7	-	-	-	-
80715	1	1	1	1	1	-	-	-	-
81192	1	1	2	1	2	-	-	-	-
82106	4	4	12	3	7	1	5	-	-
82443	2	2	2	1	1	-	-	1	1
82621	16	15	36	8	16	7	20	-	-
83287	7	6	16	5	13	1	3	-	-
83362	21	21	77	3	11	12	42	6	24
84737	73	73	185	58	150	14	33	1	2
85795	2	2	7	-	-	2	7	-	-
86728	37	35	93	20	54	13	35	2	4
87696	58	58	171	48	148	8	20	2	3
87737	24	24	113	10	16	10	66	4	31
87883	1	1	3	-	-	1	3	-	-
88737	51	51	151	24	77	26	72	1	2
88972	1	1	2	1	2	-	-	-	-
89125	96	94	234	64	152	27	69	3	13
89389	1	1	3	-	-	1	3	-	-
89744	48	47	130	39	110	7	17	1	3
90277	88	86	235	64	182	19	47	3	6
90508	4	4	7	3	5	1	2	-	-
90839	1	1	2	-	-	1	2	-	-
91262	1	1	3	1	3	-	-	-	-
91752	9	9	38	6	25	1	6	2	7
92825	13	13	40	7	22	4	11	2	7
93702	1	1	3	-	-	1	3	-	-
95128	25	25	70	24	68	1	2	-	-
95241	4	4	13	3	9	1	4	-	-
95934	2	2	5	-	-	2	5	-	-

Table 3—Continued

HD	Raw Nights Observed	All Baselines Calibrated Nights	All Baselines Calibrated Scans	North-South Calibrated Nights	North-South Calibrated Scans	North-West Calibrated Nights	North-West Calibrated Scans	South-West Calibrated Nights	South-West Calibrated Scans
96738	3	3	9	3	9	-	-	-	-
97334	2	2	7	2	7	-	-	-	-
97633	21	20	51	18	48	1	1	1	2
98058	1	1	4	-	-	1	4	-	-
98664	1	1	3	-	-	1	3	-	-
98824	2	2	3	2	3	-	-	-	-
99285	18	18	62	12	41	5	16	1	5
99984	9	9	28	4	6	4	17	1	5
100563	14	14	29	4	8	9	18	1	3
100655	16	16	53	10	36	6	17	-	-
102124	2	2	3	2	3	-	-	-	-
103095	10	10	33	3	8	7	25	-	-
104556	10	9	19	5	12	2	4	2	3
105089	1	1	2	-	-	1	2	-	-
105475	1	1	5	-	-	1	5	-	-
107213	9	9	23	3	7	6	16	-	-
107904	10	10	20	10	20	-	-	-	-
108471	9	9	21	2	3	3	8	4	10
108722	9	9	33	1	3	4	13	4	17
108765	8	8	17	8	17	-	-	-	-
108806	8	8	17	8	17	-	-	-	-
109217	93	92	271	65	181	21	73	6	17
110296	10	10	21	10	21	-	-	-	-
110315	2	2	8	1	5	1	3	-	-
110392	10	10	25	10	25	-	-	-	-
110411	21	20	51	13	36	4	9	3	6
110897	38	37	100	15	34	18	53	4	13
111395	14	14	34	6	16	8	18	-	-
111604	10	10	20	10	20	-	-	-	-
113095	48	47	129	39	107	8	22	-	-
113337	7	6	26	-	-	6	26	-	-
113771	9	9	17	9	17	-	-	-	-
114210	1	-	-	-	-	-	-	-	-
114762	3	3	21	2	18	1	3	-	-
115383	104	101	255	74	183	22	62	5	10
116831	3	2	3	-	-	-	-	2	3
118232	10	9	23	5	14	4	9	-	-
119288	4	4	10	2	3	2	7	-	-
119550	5	5	14	3	7	2	7	-	-
120048	1	1	3	1	3	-	-	-	-
120066	16	15	35	5	12	7	16	3	7
120509	2	2	8	2	8	-	-	-	-
120510	4	3	7	2	3	1	4	-	-
121107	148	145	508	102	375	35	102	8	31

Table 3—Continued

HD	Raw Nights Observed	All Baselines Calibrated Nights	All Baselines Calibrated Scans	North-South Calibrated Nights	North-South Calibrated Scans	North-West Calibrated Nights	North-West Calibrated Scans	South-West Calibrated Nights	South-West Calibrated Scans
121560	20	20	59	13	41	7	18	-	-
122365	1	1	1	1	1	-	-	-	-
122408	15	15	31	6	14	6	11	3	6
122563	13	13	54	9	33	4	21	-	-
122676	2	2	5	-	-	2	5	-	-
123033	1	1	1	1	1	-	-	-	-
124102	1	1	1	1	1	-	-	-	-
124985	1	-	-	-	-	-	-	-	-
125161	7	7	40	4	30	3	10	-	-
125162	17	16	68	7	35	7	22	2	11
125451	1	1	3	-	-	1	3	-	-
126248	1	1	1	-	-	1	1	-	-
126512	1	1	1	1	1	-	-	-	-
127334	52	48	167	29	88	16	67	3	12
128167	230	228	825	154	566	63	218	11	41
128332	2	2	6	-	-	2	6	-	-
129153	1	1	1	1	1	-	-	-	-
130109	5	5	15	1	2	4	13	-	-
130396	1	1	1	1	1	-	-	-	-
130917	1	1	1	1	1	-	-	-	-
130948	111	111	362	70	245	36	98	5	19
132052	5	5	14	-	-	5	14	-	-
132145	1	1	2	1	2	-	-	-	-
132254	76	73	203	41	93	30	105	2	5
132772	2	2	4	2	4	-	-	-	-
133002	2	2	8	-	-	2	8	-	-
133485	12	12	36	12	36	-	-	-	-
134044	3	3	18	1	4	2	14	-	-
134047	1	1	1	-	-	1	1	-	-
134083	227	225	867	148	601	67	234	10	32
134323	47	46	109	31	69	10	27	5	13
135204	2	2	3	-	-	2	3	-	-
135502	4	4	9	4	9	-	-	-	-
136118	6	6	36	-	-	6	36	-	-
136643	13	13	47	13	47	-	-	-	-
137003	1	1	1	1	1	-	-	-	-
137510	59	58	160	43	111	11	36	4	13
138085	1	1	2	1	2	-	-	-	-
138527	1	1	1	1	1	-	-	-	-
138803	1	1	2	1	2	-	-	-	-
139074	30	30	69	18	43	9	20	3	6
139761	9	9	21	9	21	-	-	-	-
140117	2	2	8	-	-	2	8	-	-
140775	4	4	7	3	4	1	3	-	-

Table 3—Continued

HD	Raw Nights Observed	All Baselines Calibrated Nights	All Baselines Calibrated Scans	North-South Calibrated Nights	North-South Calibrated Scans	North-West Calibrated Nights	North-West Calibrated Scans	South-West Calibrated Nights	South-West Calibrated Scans
140812	1	1	1	1	1	-	-	-	-
141003	29	29	125	23	96	3	21	3	8
141187	4	4	16	3	12	1	4	-	-
141851	1	1	3	-	-	1	3	-	-
142093	1	1	2	1	2	-	-	-	-
142908	5	5	13	4	9	1	4	-	-
143687	8	8	35	5	20	3	15	-	-
143894	89	88	291	55	179	30	104	3	8
144579	142	141	392	94	261	41	111	6	20
144622	20	20	71	12	45	6	22	2	4
144874	4	4	12	3	8	1	4	-	-
145457	101	100	334	72	244	25	78	3	12
146233	7	6	15	1	3	4	11	1	1
146603	11	11	30	-	-	11	30	-	-
147025	11	11	49	11	49	-	-	-	-
147449	5	5	13	1	3	4	10	-	-
147547	11	8	24	6	15	-	-	2	9
148048	7	7	17	-	-	7	17	-	-
148317	1	1	2	1	2	-	-	-	-
149630	60	60	171	32	89	26	73	2	9
149661	10	10	24	1	3	9	21	-	-
149681	1	1	2	-	-	1	2	-	-
150177	5	4	11	-	-	3	10	1	1
151044	6	6	20	-	-	6	20	-	-
151627	9	8	20	7	16	1	4	-	-
152308	7	7	12	7	12	-	-	-	-
152598	40	40	93	34	78	4	7	2	8
152614	7	7	19	4	7	3	12	-	-
152792	4	4	14	3	11	1	3	-	-
152863	8	8	19	8	19	-	-	-	-
153226	41	40	101	15	32	23	65	2	4
153287	19	19	53	15	38	4	15	-	-
154345	15	15	45	8	25	7	20	-	-
154417	2	2	5	2	5	-	-	-	-
154633	28	27	97	1	1	26	96	-	-
156826	1	1	1	-	-	1	1	-	-
157214	53	52	140	38	107	13	30	1	3
157935	1	1	4	1	4	-	-	-	-
158063	2	2	5	1	1	1	4	-	-
158633	11	10	30	-	-	10	30	-	-
159222	47	47	151	38	123	9	28	-	-
159332	72	72	193	54	145	16	43	2	5
159410	5	5	16	5	16	-	-	-	-
160507	5	5	13	4	10	1	3	-	-

Table 3—Continued

HD	Raw Nights Observed	All Baselines Calibrated Nights	Calibrated Scans	North-South Calibrated Nights	Calibrated Scans	North-West Calibrated Nights	Calibrated Scans	South-West Calibrated Nights	Calibrated Scans
161149	1	1	14	1	14	-	-	-	-
161868	94	94	228	54	115	37	103	3	10
163641	8	8	21	8	21	-	-	-	-
164259	25	25	35	6	9	15	22	4	4
164353	11	9	17	7	12	2	5	-	-
164595	19	19	68	15	51	4	17	-	-
166014	93	91	264	70	209	17	43	4	12
166205	2	2	8	-	-	2	8	-	-
166435	2	2	4	2	4	-	-	-	-
166620	35	34	105	28	88	5	15	1	2
167768	9	8	11	3	4	5	7	-	-
168009	10	10	29	9	25	1	4	-	-
168151	27	26	122	-	-	26	122	-	-
168914	86	85	230	62	174	19	47	4	9
169702	5	5	15	2	5	3	10	-	-
170920	1	1	2	1	2	-	-	-	-
171834	59	59	144	30	73	27	65	2	6
173093	1	1	2	-	-	1	2	-	-
173417	35	34	94	25	73	7	17	2	4
173920	18	18	39	-	-	18	39	-	-
174160	11	11	37	5	20	2	5	4	12
174368	1	1	23	1	23	-	-	-	-
175545	2	2	3	-	-	2	3	-	-
175679	8	8	15	1	2	7	13	-	-
176303	64	64	170	49	134	11	26	4	10
176437	33	32	233	29	217	3	16	-	-
176707	9	9	17	2	3	7	14	-	-
176896	52	52	139	36	92	15	46	1	1
177196	128	126	404	76	241	46	153	4	10
177756	3	2	3	-	-	2	3	-	-
178187	8	8	15	8	15	-	-	-	-
178539	1	1	2	1	2	-	-	-	-
178798	6	6	13	6	13	-	-	-	-
180242	10	10	22	9	19	1	3	-	-
180777	1	1	2	-	-	1	2	-	-
181440	7	6	20	-	-	6	20	-	-
181655	46	42	120	32	93	8	24	2	3
182488	126	124	412	90	306	31	96	3	10
182564	1	1	3	-	-	1	3	-	-
182807	23	21	69	17	64	4	5	-	-
182900	14	14	27	8	17	6	10	-	-
184385	7	7	23	5	14	2	9	-	-
184499	3	3	12	2	5	1	7	-	-
184606	4	4	11	3	7	1	4	-	-

Table 3—Continued

HD	Raw Nights Observed	All Baselines Calibrated Nights	All Baselines Calibrated Scans	North-South Calibrated Nights	North-South Calibrated Scans	North-West Calibrated Nights	North-West Calibrated Scans	South-West Calibrated Nights	South-West Calibrated Scans
184663	5	5	19	1	2	4	17	-	-
184930	6	6	14	2	5	4	9	-	-
184960	18	17	44	11	27	6	17	-	-
185018	2	2	3	2	3	-	-	-	-
185395	96	95	229	57	124	34	96	4	9
185423	1	1	1	1	1	-	-	-	-
185872	1	-	-	-	-	-	-	-	-
186547	7	7	23	6	19	1	4	-	-
186568	14	14	51	9	37	5	14	-	-
186760	1	1	3	-	-	1	3	-	-
187013	3	3	37	3	37	-	-	-	-
187638	1	1	5	-	-	1	5	-	-
187691	81	81	282	62	210	17	54	2	18
187923	42	40	119	23	62	14	37	3	20
190771	1	1	3	-	-	1	3	-	-
192425	23	23	74	18	61	5	13	-	-
192640	153	150	459	86	261	48	149	16	49
192985	161	158	440	88	248	58	171	12	21
193556	110	110	321	63	184	43	118	4	19
193621	1	1	1	-	-	1	1	-	-
193664	2	2	5	-	-	2	5	-	-
194012	27	27	72	24	63	3	9	-	-
194279	6	6	14	6	14	-	-	-	-
194688	5	5	14	5	14	-	-	-	-
194953	4	3	6	3	6	-	-	-	-
195019	9	9	75	7	69	2	6	-	-
195050	3	3	9	2	5	1	4	-	-
195194	13	13	32	6	10	7	22	-	-
195564	4	4	14	-	-	4	14	-	-
196134	4	4	7	3	5	1	2	-	-
196360	85	85	294	70	243	15	51	-	-
196850	1	1	3	1	3	-	-	-	-
197076	13	13	56	13	56	-	-	-	-
198390	7	7	15	2	4	5	11	-	-
198478	3	3	7	1	3	2	4	-	-
198976	-	-	-	-	-	-	-	-	-
199763	108	104	290	74	210	27	69	3	11
199960	3	3	14	-	-	3	14	-	-
200031	31	31	93	17	47	14	46	-	-
200253	2	2	4	-	-	1	3	1	1
200577	9	9	24	9	24	-	-	-	-
200723	5	5	16	1	3	4	13	-	-
201078	4	4	13	4	13	-	-	-	-
202240	3	3	11	1	4	2	7	-	-

Table 3—Continued

HD	Raw Nights Observed	All Baselines Calibrated Nights	Calibrated Scans	North-South Calibrated Nights	Calibrated Scans	North-West Calibrated Nights	Calibrated Scans	South-West Calibrated Nights	Calibrated Scans
202314	4	4	8	4	8	-	-	-	-
202575	1	1	1	1	1	-	-	-	-
203245	1	1	1	1	1	-	-	-	-
204153	59	59	181	38	120	20	58	1	3
204403	2	2	5	2	5	-	-	-	-
204642	1	1	6	1	6	-	-	-	-
206043	6	6	19	4	12	1	3	1	4
206646	51	51	144	29	81	20	56	2	7
206660	3	3	8	-	-	3	8	-	-
206774	1	1	2	1	2	-	-	-	-
206860	13	13	45	10	35	3	10	-	-
207088	101	101	321	63	201	36	118	2	2
207978	10	10	46	8	40	2	6	-	-
208667	4	4	13	4	13	-	-	-	-
209166	3	2	9	-	-	2	9	-	-
210074	28	28	89	17	59	10	26	1	4
210129	5	5	18	1	10	4	8	-	-
210264	4	4	12	4	12	-	-	-	-
210373	3	3	9	3	9	-	-	-	-
210460	5	5	15	5	15	-	-	-	-
210855	22	22	124	-	-	22	124	-	-
211096	11	11	33	5	16	6	17	-	-
211211	1	1	3	1	3	-	-	-	-
211432	42	42	106	29	76	13	30	-	-
211976	16	16	50	9	24	7	26	-	-
212593	21	21	43	15	28	6	15	-	-
213025	1	1	2	1	2	-	-	-	-
213323	1	1	3	1	3	-	-	-	-
213558	43	43	96	29	60	11	29	3	7
213619	2	2	4	2	4	-	-	-	-
213660	1	1	2	1	2	-	-	-	-
214023	2	2	5	2	5	-	-	-	-
214680	2	2	4	2	4	-	-	-	-
214734	2	2	6	-	-	2	6	-	-
214923	55	54	192	43	155	11	37	-	-
215510	30	30	161	25	131	5	30	-	-
215549	13	11	19	3	5	5	10	3	4
216502	1	1	1	1	1	-	-	-	-
216538	2	1	4	1	4	-	-	-	-
216735	9	9	19	4	7	5	12	-	-
216831	2	2	4	1	1	-	-	1	3
217491	1	1	2	1	2	-	-	-	-
217813	3	3	6	2	2	1	4	-	-
218235	30	30	84	26	71	2	8	2	5

6. Statistical Tests for the Observational Data

6.1. 51 Peg: The PTI 'Gold Standard' Calibrator

51 Peg (HD 217014, HP 113357, HR 8729) is well-known throughout the astronomical community as the first solar-like star for which an extrasolar planet has been detected (Mayor & Queloz 1995; Marcy et al. 1997). When the sinusoidal radial velocity signature was detected in 1995, the $\sin i$ ambiguity in the mass term led some to suspect that perhaps what was being observed was a binary star system in a face-on orientation, rather than a star-planet pairing.

Interferometric observations have the potential to detect such binary star systems through spatially resolving and directly detecting the individual components. As such, when PTI operations began in 1996, a vigorous campaign of 51 Peg observations was begun to attempt to detect any putative stellar companion of the primary star. Despite some ambiguous initial indications associated with a new instrument learning curve, in the end a rigorous evaluation of the PTI data excluded the presence of a companion brighter than $\Delta K < 4.27$ (corresponding to a brightness ratio $r(K) > 0.020$) at the 99% confidence level, corresponding to an upper mass limit on the 51 Peg secondary of 0.22 $M_\odot$ (Boden et al. 1998b). Given the unusually detailed evaluation of the 18 nights available (at that time) of PTI data on 51 Peg, it now constitutes a 'gold standard' calibration source, as far as being an object whose nature as a system possessing a single star has been established to the limits of PTI's detection ability. For this particular investigation, we may leverage that detailed investigation of 51 Peg to use it as a reference calibration object, to which other potential calibrators may be compared.

6.2. Known Bad Calibrators: PTI Binaries

In contrast to 51 Peg, we may also select well-studied PTI sources as known bad calibrators - namely, the binary stars that PTI has observed over the years. The full roster of published PTI binaries, along with 51 Peg, are summarized in Table 5. Also included on this list is an unpublished binary star, HD178449, which with a primary-secondary brightness ratio of $\Delta K \sim 3.5-3.8$ represents the 'worst case' binary for our various methods to attempt to detect; as will be discussed in more detail on §7, this level of ΔK is consistent with the median value of $V^2_{\mathrm{meas}} \sim 0.93-0.95$ in Equation 8.

These known binary stars are of great utility to the evaluation of our unknown potential calibrator objects. By subjecting these known binary stars to our statistical tests for

Table 3—Continued

HD	Raw Nights Observed	All Baselines		North-South		North-West		South-West	
		Calibrated Nights	Calibrated Scans	Calibrated Nights	Calibrated Scans	Calibrated Nights	Calibrated Scans	Calibrated Nights	Calibrated Scans
218261	11	11	35	10	33	1	2	-	-
218396	8	8	29	6	16	2	13	-	-
218470	22	22	57	10	16	12	41	-	-
218687	10	10	30	9	28	1	2	-	-
219080	47	46	123	33	75	13	48	-	-
219446	10	9	26	9	26	-	-	-	-
219623	31	31	102	-	-	31	102	-	-
221293	2	2	7	2	7	-	-	-	-
221354	2	2	6	-	-	2	6	-	-
222173	106	103	301	71	201	31	96	1	4
222439	8	8	16	8	16	-	-	-	-
222603	3	3	3	3	3	-	-	-	-
223346	3	3	6	3	6	-	-	-	-
223421	4	4	14	-	-	4	14	-	-
224995	2	2	3	2	3	-	-	-	-

Table 4.   Summary of observations.

Baselines	Number of Stars	Proportion[a]		
		NS	NW	SW
NS only	148	1.00	-	-
NW only	88	-	1.00	-
SW only	1	-	-	1.00
NS, NW	135	0.63	0.37	-
NS, SW	5	0.66	-	0.34
NW, SW	7	-	0.52	0.48
NS, NW, SW	105	0.60	0.32	0.08
None (uncalibrated)	10	-	-	-

[a]Distribution, on average, of the observations for each of the 3 PTI baselines.

appropriateness of a calibration star, we may test the sensitivity of those tests to binaries of varying brightness ratio and separation.

6.3. Moment Values for 51 Peg

For detailed statistical testing of the visibility data on each of our potential calibrator stars found in Table 2, we sought to compare the ensemble of 51 Peg V^2_{norm} points with the various sets associated each potential calibrator star first by means of a Mahalanobis distance comparison, and second through a Principal Component Analysis. The variable of interest is an individual normalized PTI observation, $V^2_{\mathrm{norm},i}$, with associated error term $\sigma_{V^2,i}$. For each star we have a number of observations of V^2_{norm} that form a frequency distribution. Our hypothesis is that the frequency distribution associated with calibrator stars differs from non-calibrator stars such as binary stars. The challenge is to characterize the frequency distribution. A very old technique is that of using Pearson curves which are characterized by the first four moments of a distribution. A function of the raw moments of the frequency distribution of V^2_{norm} for each star forms the input for our comparison with the first four moments of 51 Peg V^2_{norm} data.

The observations were weighted by $w_i^* = 1/(\sigma_{V^2,i})^2$. If $W = \sum_i w_i$ for specific k star, and $w_i = w_i^*/W$, then the weighted mean, m_1, of $V^2_{\mathrm{norm},i}$ is $m_{1k} = \sum_i w_i V^2_{\mathrm{norm},i}$. The weighted second, third and fourth moments for this star are

$$m_{jk} = \left[\sum_i w_i (V^2_{\mathrm{norm},i} - m_1)^j \right]^{1/j} \tag{4}$$

for $j = 2, 3, 4$. For m_{3k} we retained the sign associated with the third moment. The rescaled moments have a natural interpretation; for example, m_{2k}, is the standard deviation of the V^2_{norm} values for star k.

These moments $m_{1k}, m_{2k}, m_{3k}, m_{4k}$ form the basis for the calculation of the Mahalanobis distance and the Principal Component Analysis distance from 51 Peg, our 'gold standard'. The four moment values for 51 Peg were calculated to be,

$$m_{1,51\ \mathrm{Peg}} = 1.006659$$
$$m_{2,51\ \mathrm{Peg}} = 0.041568$$
$$m_{3,51\ \mathrm{Peg}} = 0.032527$$
$$m_{4,51\ \mathrm{Peg}} = 0.0919526$$

The moments can be used to calculate $a_3 = skewness$ and $a_4 = kurtosis$ statistics. For

a Gaussian distribution the values are $a_3 = 0$ and $a_4 = 3$. For the $V^2_{\rm norm}$ values from 51 Peg these values are,

$$a_3 = \quad m_{3k}/m_{2k}{}^{3/2} \quad = 1.32$$
$$a_4 = \quad m_{4k}/m_{2k}{}^{2} \quad = 12.1$$

Thus these data suggest that the 51 Peg $V^2_{\rm norm}$ data are skewed to the right and leptokurtic.

The skewness of the 51 Peg data is a result of there being a few, but notable, outlying data points with $V^2_{\rm norm} \gg 1$, as seen in Figure 2. These data points are all associated with periods of poor system visibility when the system visibility was low, typically $V^2_{\rm sys} < 0.60$, which is usually a result of poor seeing; of the 340 data points in the 51 Peg dataset, 20 were in the low system visibility category. Up until this point in the analysis, all of the data from 51 Peg contributed to the statistical analysis, in order to examine all nights in a homogenous manner, regardless of atmospheric conditions. However, if we use that parameter as a guide and exclude data points with $V^2_{\rm sys} < 0.60$ from that analysis, we find $a_3 = -0.048$ with $a_4 = 6.13$ — a negligible amount of skewness.

The leptokurtic nature of the 51 Peg $V^2_{\rm norm}$ data is seen with both the full ensemble and the $V^2_{\rm sys} > 0.60$ subset — in terms of shape, a leptokurtic distribution has a more acute peak around the mean and longer tails. A histogram of the full 51 Peg $V^2_{\rm norm}$ dataset is seen in Figure 3, in bins of $\Delta V^2 = 0.05$. Two fits were compared to this binned data: the first was single Gaussian, which resulted in a mean of $\overline{V}^2 = 1.004$ and a width of 0.030 on an amplitude of 90.9, and a reduced χ^2 per degree of freedom of $\chi^2/{\rm DOF}=5.44$; the second was two Gaussians, with an identical mean but widths of 0.024 and 0.098 on amplitdues of 82.8 and 12.5, respectively, with $\chi^2/{\rm DOF}=1.32$. The second fit suggests that two sources of noise are present in the data. Restricting these fits to the $V^2_{\rm sys} > 0.60$ subset, we find that the single Gaussian fit has a width of 0.029 with a $\chi^2/{\rm DOF}=5.02$, and the two-Gaussian fit has widths of 0.080 and 0.023 with $\chi^2/{\rm DOF}=1.22$; no notable change for either fit resulted in the amplitudes or $\overline{V}^2$ values.

These latter fits suggest that for those times when the interferometer is performing best (resulting in better $V^2_{\rm sys}$ values) the wider 'pedestal' Gaussian of the two-Gaussian fit reduces in width. Since the instrument is operated in a fairly uniform manner and reports lowered $V^2_{\rm sys}$ values generally during periods of particularly poor atmospheric seeing, our suspicion is that the error pedestal is associated with those occasional periods of poor seeing. Such observations do not get properly normalized due to limitations of the calibration process for coping with those occasional rapid fluctuations in seeing, but are identifiable in the data set in part due to their low $V^2_{\rm sys}$ values. Further examination of the 51 Peg dataset can exclude other measurement outliers (and the spread on $V^2_{\rm norm}$ will then approach the $\sim 1.5\%$ value
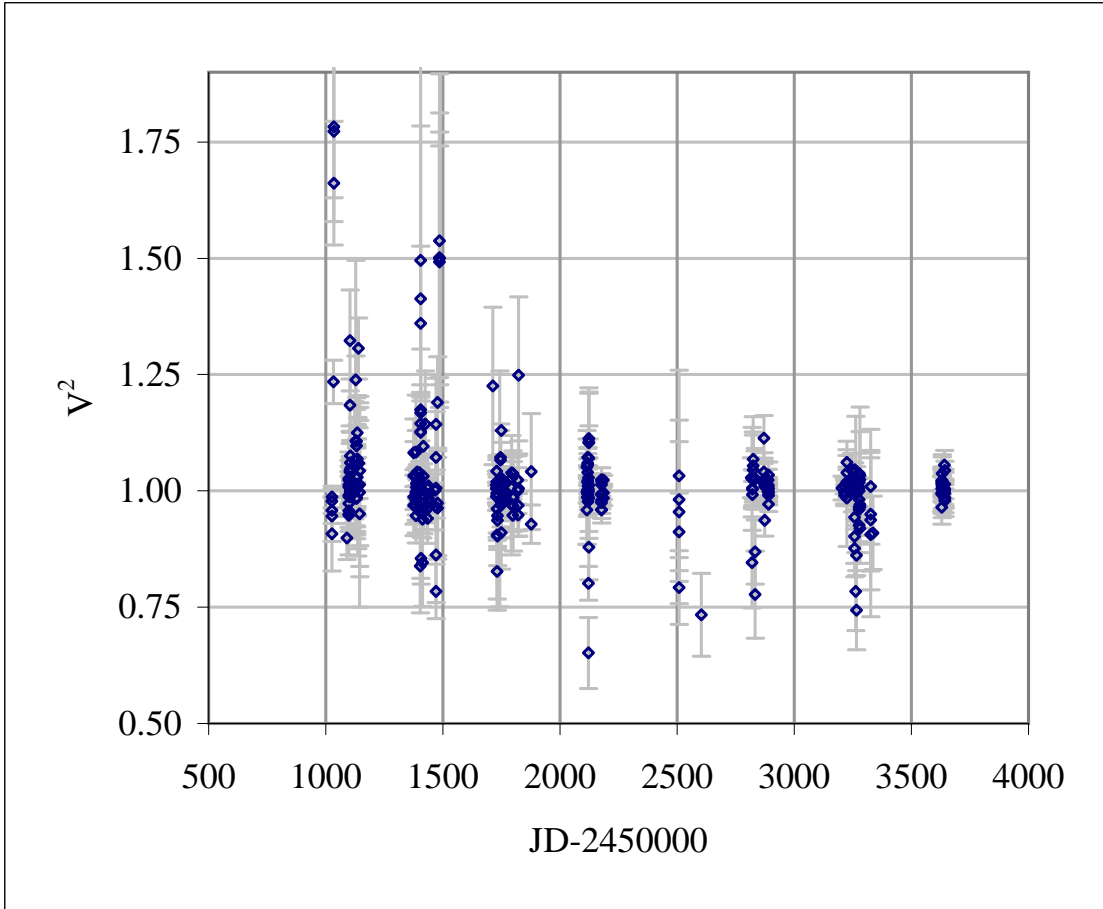
Fig. 2.— Normalized visibility measurements (V^2_{norm}) for 51 Peg, as discussed in §6.3.

seen in (Boden et al. 1998b)) but this is time-consuming and potentially quite subjective. As such, we will maintain the integrity of the normalized visibilities being examined for all sources and not cut for V_{sys}^2 in the following sections.

6.4. Mahalanobis and Principal Component Analysis Distances

The Mahalanobis distance (MD) is a multivariate generalization of one-dimensional Euclidean distance (Bartkowiak & Jakimiec 1989; Ronen et al. 1999). Given N stars characterized by M variables (coordinates) m_{jk}, the sample distance of a particular star, k, from the centroid of the distances is,

$$MD_k = \sum_{j=1}^{M} \left(\frac{m_{jk} - \overline{m_j}}{s_j} \right)^2 \tag{5}$$

where $\overline{m_j}$ is the mean for the jth variable, and s_j is its standard deviation. Alternatively, the MD of one star from a specific star k^*, in this case 51 Peg say, is given by,

$$MD_k = \sum_{j=1}^{M} \left(\frac{m_{jk} - m_{jk^*}}{s_j} \right)^2 \tag{6}$$

where m_{jk^*} are the coordinates for star k^*. The Mahalanobis distances from 51 Peg for these stars and their ranks are listed in Table 7, and a histogram of the Mahalanobis distances is found in Figure 4.

Principal Components Analysis (PCA) is a statistical method for partitioning total variability in a sample into linear combinations that are orthogonal to each other (Ronen et al. 1999). The first principal component is generated to maximize the variation of that linear combination; the second principal component is chosen orthogonal to the first and with maximum variation conditional on the orthogonality. For these data the four moments, $m_{1k}, m_{2k}, m_{3k}, m_{4k}$, for each star k again form the basis for the calculations.

The PCA is carried out on the correlation matrix so at this stage we do not need to adjust for the variances. The principal component for 51 Peg for the basis for the distance calculation of each star from 51 Peg. Specifically, let p_{jk} be the principal components for star k and p_{jk^*} the principal component for reference star k^*. Then the distance star k is from the reference star is,

$$PD_k = \sum_{j=1}^{M} \left(\frac{p_{jk} - p_{jk^*}}{sp_j} \right)^2 \tag{7}$$
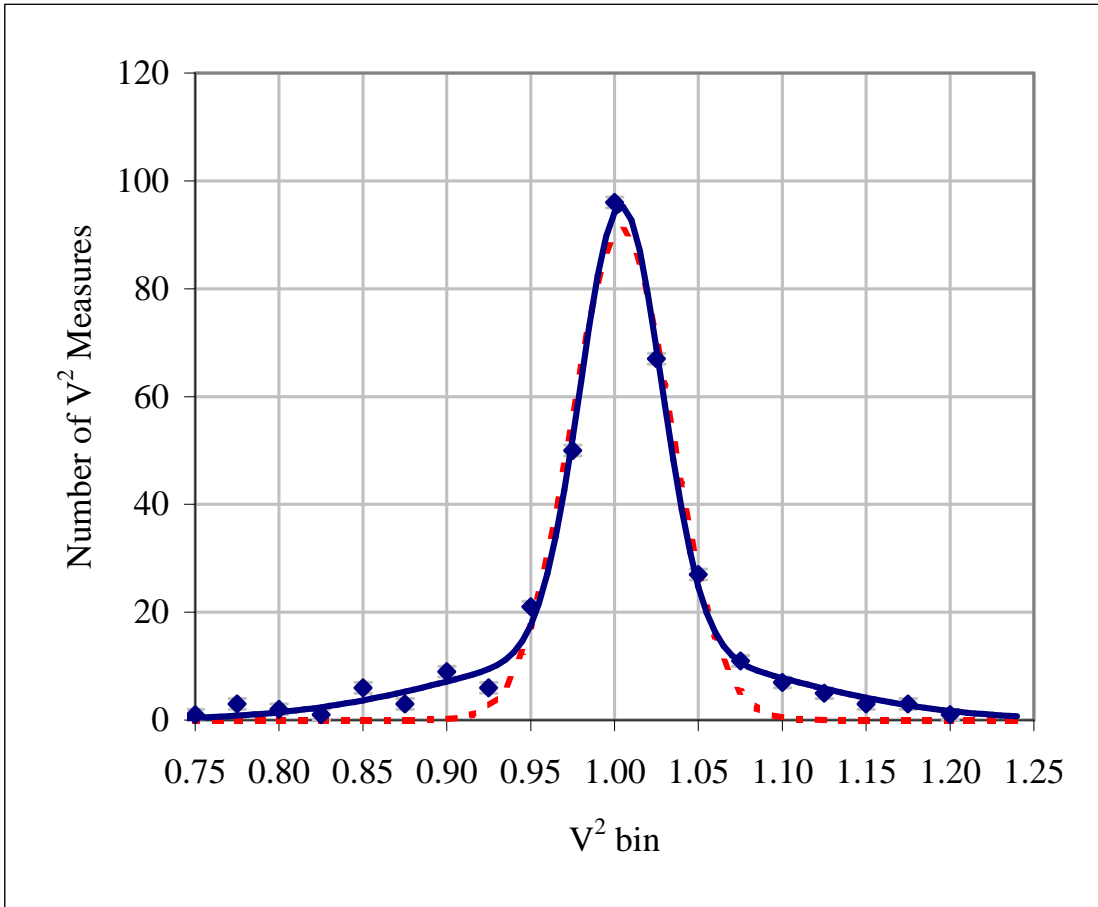
Fig. 3.— Histogram of the 51 Peg normalized visibility measurements (V^2_{norm}) as discussed in §6.3, in bins of $\Delta V^2 = 0.05$. The dotted line is a single Gaussian fit, with amplitude of 90.9 and width 0.0297, and the solid line is a two-Gaussian fit with amplitude/width of 82.8/0.0242 and 12.5/0.098, respectively. The χ^2 per degree of freedom for the former is 5.44, with χ^2/DOF for the latter being 1.32.

where sp_j is the standard deviation for the jth principal component. The PCA distances and their ranks are given in Table 7, and a histogram of the PCA distances is found in Figure 5.

The choice between Mahalanobis distance and the PCA-based distance will be based on convenience. The Mahalanobis distance has the advantage that it is more immediately linked to the four moments of the distribution. There is a very close correlation between the Mahalanobis distance and the PCA-based distance as seen in Figure 6. The PCA based approach has the advantage that the contribution of each of the principal components can be calculated - e.g., for the data considered here the first principal component accounts for 53 % of the total variability.

We find that the first of the known PTI binaries to appear among the ranked potential calibrators of Table 6 is HD 178449 - not unsurprising given its large ΔK value. The large brightness ratio makes the object appear more like a calibrator than the other binary stars, and at distances of $MD_{\mathrm{HD178449}} = 1.20$, $PD_{\mathrm{HD178449}} = 1.83$. Consideration of the HD 178449 Maha and PCA ranks and an examination of Figures 4 and 5 provides insight into the distributions for both Maha and PCA distances. Given that the sources were pre-selected to *likely* be suitable as calibration sources, it is reasonable to expect that distributions should peak at values corresponding to suitable calibrators. If we select all stars that fall towards the smaller values of those distribution, we can have some confidence that we have statistically selected the stars that have been demonstrated in this dataset to be suitable for use as calibrators. As such, we established our cutoff at $MD, PD < 1.0$. The resulting calibrator list is available online at the MSC web site[4].

It is important to note that the 'rejection' of a star as a suitable calibrator from this analysis does not necessarily indicate it is a heretofore unresolved binary - merely that, within this particular dataset, the data indicate it is unsuitable for use as a calibrator. This *could* be due to some previously undetected binarity, but could also be merely due to poor quality of data for that particular object in the dataset. A key indicator of this possibility is the fact that the stars in Table 6 that are listed as 'acceptable' have, on average, a larger expected angular size (0.449 mas) than those in the 'reject' category (0.301 mas). The smaller stars are, on average, more distant, and hence, are also on average dimmer - resulting in lower signal-to-noise in the PTI system. Such objects are more susceptible to poor seeing and/or weather conditions, and are ultimately more likely to be rejected due to poor data quality that is unrelated to actual system binarity. For the purposes of this investigation, rejection of such sources is acceptable in exchange for attempting to eliminate false positives for acceptable calibrators.

---

[4]http://msc.caltech.edu
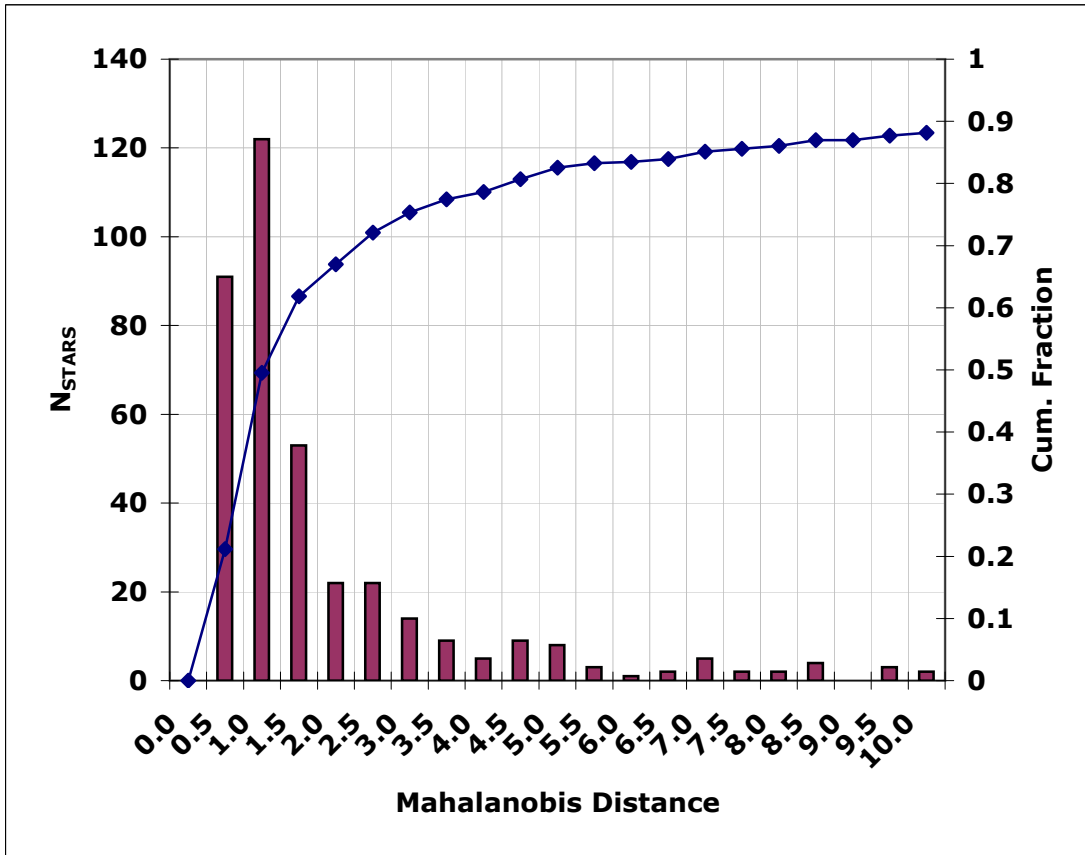
Fig. 4.— Histogram of Mahalanobis distances from HD217014 for potential calibrator stars.
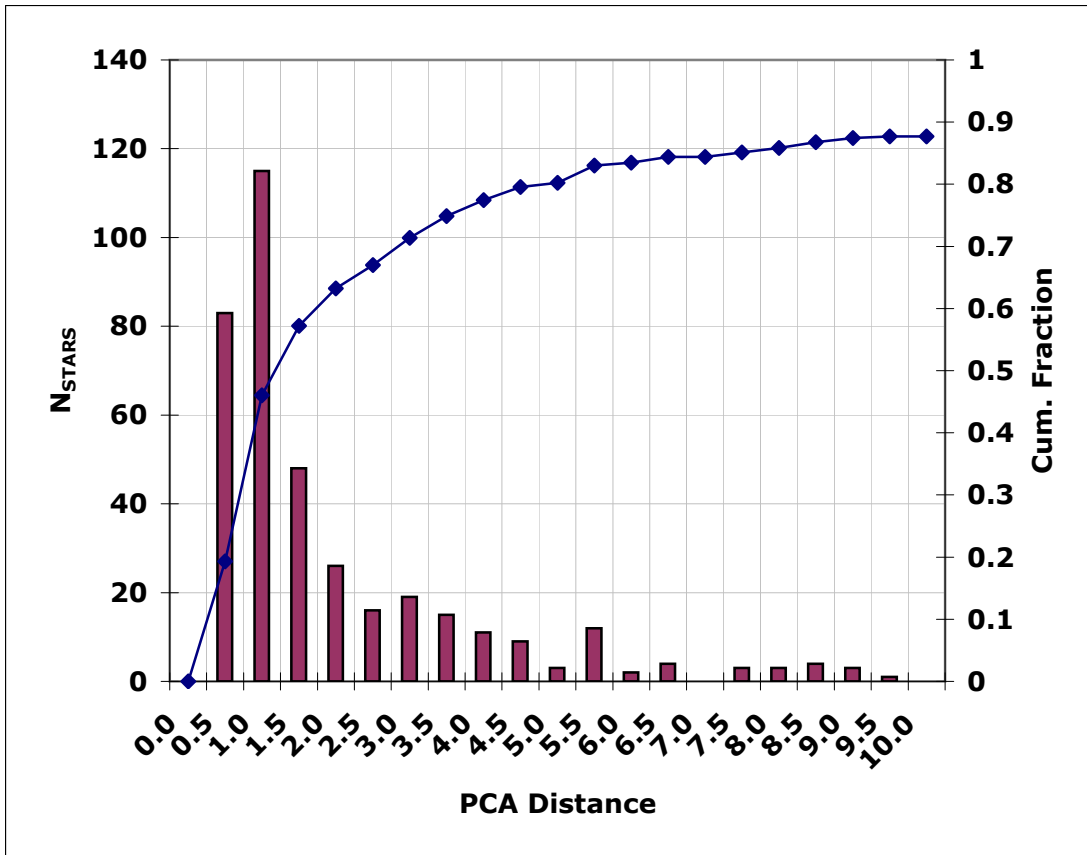
Fig. 5.— Histogram of Principal Component Analysis distances from HD217014 for potential calibrator stars.
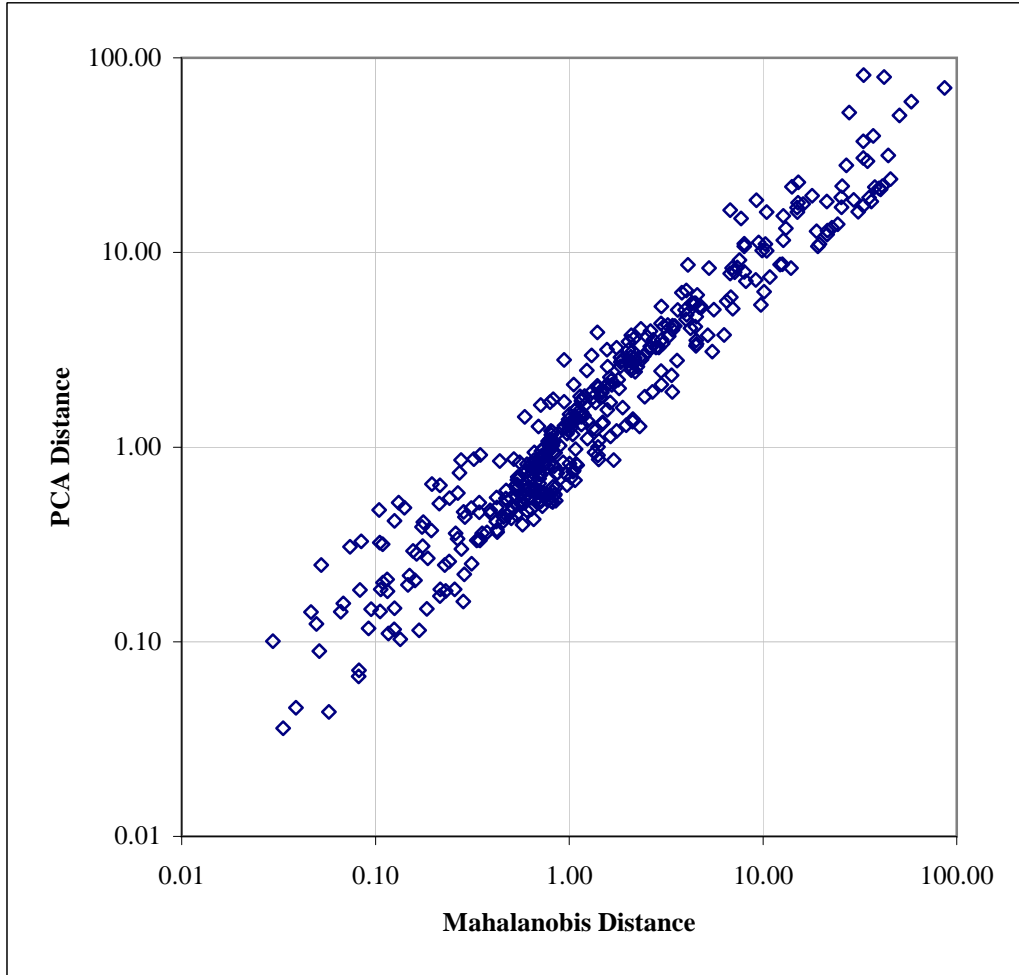
Fig. 6.— Principal Component Analysis versus Mahalanobis distances from HD217014 for potential calibrator stars.
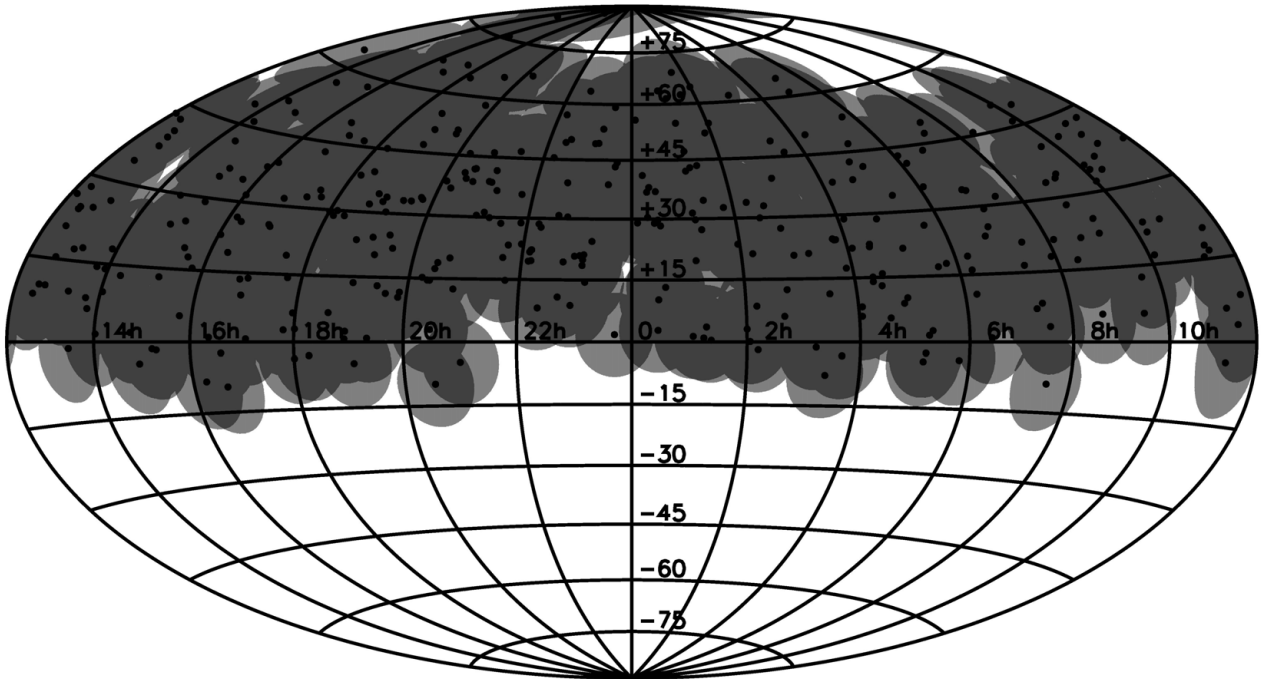
Fig. 7.— Equatorial sky coverage map of statistically vetted calibrators displayed in an equal area Aitoff projection. Light grey circles represent 10° radii cones projected onto the sky, representing regions of appropriate calibrator proximity to astrophysical targets; darker grey regions represent areas with two or more calibrators within 10°. For PTI's nominal sky accessibility of $5^o < \delta < 55^o$, these calibrators represent $\gtrsim 96\%$ sky coverage.

Table 5.   Summary of spectroscopic binary stars spatially resolved by PTI.

Star	HD	a (mas)	ΔK	Reference
64 Psc	4676	6.50	0.11	Boden et al. (1999b)
	6118	5.56	0.40	Konacki & Lane (2004)
TZ Tri	13480	2.10	1.75	Koresko et al. (1998)[a]
Atlas	23850	12.94	1.86	Pan et al. (2004)
	27483	1.26	0.00	Konacki & Lane (2004)
omi Leo	83808	4.46	1.49	Hummel et al. (2001)
12 Boo	123999	3.39	0.61	Boden et al. (2000, 2005)
	178449	n/a	$\sim 3.5 - 3.8$	Unpublished
	195987	15.38	1.06	Torres et al. (2002)
iota Peg	210027	10.33	1.61	Boden et al. (1999a)
BY Dra	234677	4.40	0.57	Boden & Lane (2001)
51 Peg	217014	n/a	> 4.27	Boden et al. (1998b)

[a]See discussion in §6.2.

Table 6.   Mahalanobis distance rank and principal components analysis rank of the potential calibrator stars.

HD	Mahalanobis Rank	Mahalanobis Distance	PCA Rank	PCA Distance	Geometric Non-detection[a]	Binary Reference
Suitable as calibrators (MD and $PD < 1.0$):						
71	94	0.51	82	0.49	0.036	
1404	63	0.28	74	0.47	-	
1671	134	0.66	190	0.94	-	
2344	30	0.13	64	0.42	0.010	
2454	172	0.79	203	1.04	0.000	
2628	135	0.66	173	0.83	-	
2942	66	0.31	79	0.49	0.000	
4841	35	0.15	34	0.22	0.002	
6210	195	0.84	112	0.57	0.188	
6288	15	0.08	26	0.18	0.002	
6833	69	0.33	49	0.33	0.007	
6920	185	0.82	217	1.20	-	
7189	171	0.78	98	0.54	0.188	
7299	141	0.69	87	0.52	0.197	
7476	199	0.86	130	0.62	-	
7590	154	0.72	118	0.59	0.197	
7804	80	0.42	105	0.55	-	
7964	224	1.07	249	1.55	-	
8671	67	0.31	38	0.25	0.010	
9407	123	0.62	107	0.55	0.007	
11007	78	0.39	71	0.46	-	
11151	183	0.81	210	1.10	-	
11946	180	0.80	218	1.21	0.036	
11973	181	0.81	213	1.16	-	
12235	210	0.97	135	0.64	0.002	
12573	186	0.82	91	0.52	0.007	
13421	146	0.70	142	0.69	0.000	
13468	93	0.50	66	0.43	-	
14055	192	0.83	205	1.06	-	
15335	96	0.53	132	0.63	-	Heintz (1994) - Yes? Fischer & Valenti (2005) - No
16220	226	1.07	139	0.67	0.007	
16647	158	0.73	83	0.50	0.040	
17093	179	0.80	195	0.97	0.000	
17573	12	0.07	44	0.31	-	
18012	235	1.15	259	1.73	0.040	
18404	49	0.22	23	0.17	0.001	
18757	60	0.28	181	0.86	0.036	
20150	65	0.29	68	0.44	-	
21019	116	0.61	168	0.82	0.188	
21770	222	1.05	158	0.76	0.197	
22879	214	1.00	246	1.47	0.036	
23408	44	0.19	40	0.27	0.000	

Table 6—Continued

HD	Mahalanobis Rank	Mahalanobis Distance	PCA Rank	PCA Distance	Geometric Non-detection[a]	Binary Reference
23630	11	0.07	21	0.16	-	
23862	193	0.84	163	0.80	0.188	
25490	58	0.27	116	0.58	-	
25570	10	0.07	16	0.14	-	
25680	196	0.84	189	0.94	-	
26605	122	0.62	129	0.62	0.197	
26764	237	1.16	230	1.30	0.007	
27397	212	0.99	220	1.23	-	
27946	75	0.36	54	0.36	0.000	
28355	104	0.55	141	0.68	-	
28556	81	0.42	58	0.38	-	
30111	211	0.98	229	1.30	-	
30739	87	0.47	100	0.54	-	
31295	113	0.59	106	0.55	-	
32301	217	1.02	235	1.34	-	
32630	16	0.08	48	0.33	-	
33608	23	0.11	46	0.32	0.002	
34137	111	0.58	101	0.55	0.036	
34578	132	0.66	159	0.78	0.010	
34658	55	0.26	27	0.19	0.036	
37147	209	0.97	216	1.17	-	
37394	24	0.11	31	0.20	-	
38858	128	0.65	154	0.74	0.036	
41636	117	0.61	75	0.47	0.001	
42807	38	0.16	41	0.28	-	
45067	48	0.21	134	0.64	0.010	
48682	166	0.77	192	0.94	-	
50692	105	0.55	175	0.84	-	
51000	190	0.83	119	0.59	0.036	
55575	204	0.93	223	1.25	-	
57006	198	0.86	214	1.16	-	
58855	173	0.79	169	0.82	0.010	
59984	106	0.56	147	0.70	0.036	
60111	157	0.72	186	0.90	-	
67228	18	0.10	18	0.15	0.002	
71030	62	0.28	22	0.16	-	
73262	194	0.84	110	0.57	-	
74198	85	0.46	63	0.42	0.037	
78366	167	0.77	99	0.54	-	
79373	9	0.06	3	0.04	-	
79439	184	0.81	204	1.06	0.036	
79452	176	0.80	209	1.09	-	
83287	140	0.68	160	0.78	0.000	
83362	7	0.05	7	0.09	-	
85795	219	1.03	224	1.26	0.036	

Table 6—Continued

HD	Mahalanobis Rank	Mahalanobis Distance	PCA Rank	PCA Distance	Geometric Non-detection[a]	Binary Reference
86728	174	0.79	197	0.98	-	
87696	2	0.03	8	0.10	-	
87737	39	0.17	11	0.11	-	
87883	45	0.19	57	0.37	0.188	
88737	52	0.23	25	0.18	-	
90277	72	0.34	72	0.46	-	
90508	142	0.69	149	0.72	0.001	Hale (1994) - M3V companion
92825	129	0.65	144	0.70	-	
95128	74	0.35	188	0.91	-	
95241	162	0.74	177	0.85	0.001	
95934	107	0.57	84	0.51	0.036	
98058	202	0.89	201	1.02	0.188	
98664	197	0.85	97	0.53	0.188	
99285	225	1.07	238	1.37	-	
99984	13	0.08	5	0.07	-	
100563	228	1.08	243	1.43	-	
100655	25	0.11	33	0.21	-	
104556	207	0.95	227	1.29	-	
105475	86	0.46	67	0.44	0.188	
107213	124	0.63	167	0.81	-	
107904	213	0.99	239	1.39	-	
108471	27	0.12	10	0.11	-	
108722	115	0.60	123	0.60	-	
108806	144	0.70	226	1.28	0.000	
109217	82	0.42	81	0.49	-	
110296	41	0.18	45	0.31	-	
110315	206	0.94	258	1.71	0.037	
110392	37	0.16	32	0.21	-	
110411	8	0.05	36	0.25	-	
111395	61	0.28	43	0.30	-	
111604	121	0.62	127	0.61	-	
113095	89	0.48	69	0.44	-	
113337	177	0.80	208	1.09	0.000	
113771	155	0.72	194	0.95	-	
114762	170	0.78	206	1.07	0.007	
116831	153	0.71	148	0.72	0.037	
119288	227	1.08	196	0.98	0.002	
120066	50	0.22	28	0.19	-	
121560	103	0.54	146	0.70	-	
122408	53	0.24	39	0.26	-	
122563	17	0.09	13	0.12	-	
125162	119	0.61	128	0.62	-	
128332	59	0.27	153	0.74	0.036	
130109	97	0.53	70	0.45	-	
130948	3	0.03	2	0.04	-	

Table 6—Continued

HD	Mahalanobis Rank	Mahalanobis Distance	PCA Rank	PCA Distance	Geometric Non-detection[a]	Binary Reference
132052	40	0.17	59	0.39	0.001	
133002	95	0.52	184	0.87	0.036	
134044	231	1.10	241	1.41	0.007	
134083	77	0.39	76	0.47	-	Nordström et al. (2004) - Yes?
134323	34	0.15	30	0.20	-	
135502	149	0.70	117	0.58	0.002	
137510	70	0.34	51	0.33	-	
139074	29	0.13	20	0.15	-	
141003	130	0.65	161	0.78	-	
142908	126	0.64	104	0.55	0.000	
143687	148	0.70	138	0.65	-	
144579	218	1.02	143	0.70	-	
145457	131	0.66	65	0.43	-	
146233	20	0.11	47	0.32	-	
146603	164	0.74	113	0.58	-	
147449	208	0.96	150	0.73	-	
147547	189	0.83	131	0.62	-	
149661	159	0.73	198	0.98	-	
152614	220	1.04	215	1.16	-	
152792	238	1.16	247	1.51	0.001	
152863	168	0.77	111	0.57	0.000	
153226	91	0.49	73	0.46	-	
153287	191	0.83	260	1.76	-	
154417	147	0.70	108	0.55	0.040	
154633	236	1.16	244	1.43	-	
157214	114	0.59	242	1.43	-	
158633	56	0.26	53	0.36	-	
159222	57	0.27	52	0.34	-	
159332	79	0.42	62	0.41	-	
160507	150	0.71	92	0.52	0.000	
161149	42	0.18	61	0.41	0.197	
163641	175	0.79	257	1.70	0.000	
164353	26	0.12	24	0.18	0.000	
164595	178	0.80	200	1.01	-	
166435	229	1.09	171	0.82	0.040	
167768	51	0.23	37	0.25	-	
168009	36	0.16	42	0.29	0.000	
168151	32	0.13	9	0.10	-	
168914	4	0.04	4	0.05	-	
169702	127	0.64	124	0.61	0.000	
173417	98	0.54	126	0.61	-	
173920	109	0.57	115	0.58	-	
174160	156	0.72	95	0.53	-	
174368	136	0.67	125	0.61	0.197	
175545	90	0.48	93	0.53	0.036	

Table 6—Continued

HD	Mahalanobis Rank	Mahalanobis Distance	PCA Rank	PCA Distance	Geometric Non-detection[a]	Binary Reference
175679	112	0.59	88	0.52	-	
176303	28	0.13	12	0.12	-	
176437	108	0.57	60	0.40	-	
176707	101	0.54	85	0.51	-	
180242	120	0.61	145	0.70	0.000	
182564	232	1.10	166	0.81	0.188	
182900	188	0.82	193	0.95	-	
184499	233	1.12	248	1.52	0.007	
184930	201	0.87	152	0.74	-	
184960	21	0.11	17	0.14	-	
185395	5	0.05	15	0.14	-	
186760	125	0.64	78	0.48	0.188	
187638	221	1.05	155	0.75	0.188	
192425	151	0.71	253	1.65	-	
192640	133	0.66	180	0.86	-	
193556	64	0.29	35	0.22	-	
193664	169	0.77	162	0.79	0.036	
194012	73	0.35	50	0.33	-	
194688	152	0.71	96	0.53	0.001	
194953	118	0.61	157	0.75	0.010	
195019	76	0.38	55	0.36	0.000	
195194	163	0.74	165	0.81	-	
196134	83	0.42	56	0.37	0.001	
196360	160	0.74	185	0.88	-	
196850	200	0.86	151	0.73	0.197	
198390	145	0.70	120	0.59	-	
199763	102	0.54	140	0.68	-	
199960	68	0.32	183	0.87	0.007	
200031	239	1.17	261	1.77	-	
200577	19	0.10	77	0.48	-	
202314	215	1.00	172	0.82	0.002	
204153	92	0.50	103	0.55	-	
204642	240	1.19	245	1.45	0.197	
206043	100	0.54	136	0.64	-	
206646	47	0.21	86	0.51	-	
206860	137	0.67	156	0.75	-	
207088	230	1.09	251	1.57	-	
208667	31	0.13	89	0.52	0.002	
210074	143	0.69	176	0.84	-	
210129	84	0.44	178	0.85	0.000	
210264	33	0.14	80	0.49	0.002	
210373	54	0.24	102	0.55	0.010	
210460	6	0.05	14	0.12	0.001	
211096	22	0.11	29	0.19	-	
211432	14	0.08	6	0.07	-	

Table 6—Continued

HD	Mahalanobis Rank	Mahalanobis Distance	PCA Rank	PCA Distance	Geometric Non-detection[a]	Binary Reference
212593	187	0.82	202	1.02	-	
213558	216	1.01	231	1.31	-	
214023	46	0.20	137	0.65	0.040	
214734	165	0.75	170	0.82	0.036	
215510	99	0.54	109	0.56	-	
215549	139	0.68	164	0.80	-	
216735	110	0.58	133	0.64	-	
217014	1	0.00	1	0.00	N/A	
217813	203	0.93	174	0.83	0.007	
218235	43	0.18	19	0.15	-	
218687	161	0.74	114	0.58	0.000	
219623	71	0.34	90	0.52	-	
221293	182	0.81	94	0.53	0.040	
221354	138	0.67	121	0.60	0.036	
222173	88	0.47	122	0.60	-	
Probably suitable as calibrators (MD and $PD < 3.0$):						
166	316	2.69	270	1.92	-	
1406	269	1.57	250	1.55	0.040	
7034	245	1.25	237	1.36	-	
8335	257	1.41	199	1.00	0.037	
8673	272	1.62	283	2.29	-	
10112	254	1.40	276	2.07	0.007	
13403	242	1.21	254	1.66	0.007	
13555	251	1.36	256	1.70	-	
18411	261	1.46	263	1.80	-	
19994	308	2.37	300	2.81	0.036	Hale (1994) - M3V companion
20418	280	1.79	282	2.22	0.036	
25948	303	2.19	285	2.44	0.007	
27459	223	1.06	278	2.09	-	
29645	255	1.41	274	2.01	-	
30823	298	2.13	240	1.39	-	
33256	266	1.49	234	1.34	0.036	
41074	273	1.62	255	1.69	-	
41330	309	2.43	306	2.94	-	
43587	271	1.58	290	2.60	-	
48805	283	1.84	304	2.89	-	
50019	247	1.31	271	1.93	0.010	
52711	323	2.99	280	2.10	-	
56537	260	1.45	262	1.80	-	
67006	322	2.98	286	2.46	0.000	
78715	294	2.09	289	2.58	-	
82106	286	1.89	252	1.60	0.001	
84737	244	1.24	211	1.10	-	
89389	243	1.23	287	2.48	0.188	
89744	284	1.85	294	2.73	-	

Table 6—Continued

HD	Mahalanobis Rank	Mahalanobis Distance	PCA Rank	PCA Distance	Geometric Non-detection[a]	Binary Reference
93702	282	1.84	292	2.60	0.188	
96738	248	1.33	222	1.24	0.010	
102124	262	1.47	268	1.91	0.040	
108765	292	2.08	295	2.76	0.000	
115383	205	0.94	299	2.81	-	
121107	304	2.24	291	2.60	-	
122676	299	2.14	301	2.86	0.036	
125161	301	2.15	293	2.70	-	
125451	256	1.41	187	0.91	0.188	
132254	270	1.57	279	2.09	-	Nordström et al. (2004) - Yes?
136643	234	1.14	266	1.82	-	
140117	265	1.49	233	1.33	0.036	
148048	288	1.99	296	2.78	-	
150177	258	1.42	182	0.86	-	
151044	277	1.70	179	0.86	0.000	
151627	275	1.64	281	2.20	0.000	
152598	285	1.86	298	2.79	-	
159410	293	2.09	288	2.48	0.001	
161868	310	2.45	265	1.81	-	
166620	267	1.53	275	2.03	-	
176896	305	2.29	303	2.87	-	
177196	274	1.63	212	1.14	-	
177756	250	1.35	191	0.94	0.036	
178449	241	1.20	267	1.83	N/A	PTI (Uupublished)
182807	279	1.76	219	1.21	-	
184385	263	1.47	272	1.97	0.000	
184606	297	2.13	236	1.35	0.001	
185018	246	1.30	307	2.95	0.040	
187013	259	1.42	207	1.08	0.010	
194279	306	2.31	225	1.28	0.000	
200723	291	2.08	305	2.91	-	
201078	276	1.66	277	2.09	0.002	
202240	287	1.97	228	1.30	0.007	
209166	252	1.38	221	1.23	0.036	
211976	264	1.48	232	1.32	-	
214923	249	1.33	264	1.80	-	
218261	302	2.18	302	2.87	-	
219446	281	1.81	273	2.00	-	
Unsuitable as calibrators (MD or $PD > 3.0$):						
905	334	3.50	339	4.19	0.001	
1279	398	18.91	388	12.86	-	
2190	315	2.64	314	3.25	0.000	
2507	347	4.49	357	5.48	0.000	
2758	391	14.08	414	21.73	0.188	
3268	406	25.33	409	19.17	0.010	

Table 6—Continued

HD	Mahalanobis Rank	Mahalanobis Distance	PCA Rank	PCA Distance	Geometric Non-detection[a]	Binary Reference
4676	413	32.89	421	30.58	N/A	Boden et al. (1999b)
4881	379	9.89	379	10.22	0.007	
6118	405	24.30	392	13.97	N/A	Konacki & Lane (2004)
6903	416	33.02	430	81.44	0.000	
8357	390	13.96	370	8.30	-	Nordström et al. (2004)
8799	385	12.23	375	8.65	-	Tokovinin & Smekhov (2002)
9329	289	2.02	322	3.49	-	
9939	378	9.76	354	5.38	N/A	
13480	359	5.57	348	5.09	N/A	Koresko et al. (1998)
16234	394	15.14	403	17.97	-	Mason (1997)
16399	351	4.55	320	3.39	0.040	
17228	353	4.68	351	5.25	0.000	
20675	344	4.29	355	5.47	-	
20677	361	6.49	358	5.61	-	
21686	337	3.81	361	6.22	-	
23850	380	10.14	362	6.28	N/A	Pan et al. (2004)
24357	426	44.39	422	31.56	-	
25867	319	2.89	317	3.26	-	
27084	318	2.80	315	3.25	0.000	
27483	383	10.46	378	10.18	N/A	Konacki & Lane (2004)
27524	397	17.95	410	19.56	0.007	
27901	399	19.22	381	10.77	-	
28024	348	4.51	319	3.31	-	
28677	335	3.61	297	2.78	0.000	
28704	339	4.00	343	4.54	0.000	
28978	362	6.78	367	7.79	0.040	
31662	278	1.75	313	3.24	0.036	
32715	320	2.90	316	3.26	0.036	
33167	368	7.37	373	8.37	-	
37594	396	16.14	402	17.72	0.036	
38558	268	1.57	312	3.16	0.010	
43042	325	3.00	324	3.56	-	
43043	341	4.03	345	4.78	0.000	
45542	382	10.43	395	16.12	0.007	Mason (1997)
51530	428	50.62	425	50.61	0.010	
58551	386	12.59	376	8.70	0.000	
58715	346	4.48	337	4.15	0.000	
58946	313	2.61	318	3.29	0.000	
60803	423	40.40	411	21.14	N/A	
64493	336	3.63	346	5.07	-	
71148	358	5.48	308	3.09	-	
75137	422	39.65	412	21.36	0.002	
75332	354	4.74	353	5.31	-	
75732	349	4.52	344	4.67	-	
79969	395	15.22	417	22.94	0.197	

Table 6—Continued

HD	Mahalanobis Rank	Mahalanobis Distance	PCA Rank	PCA Distance	Geometric Non-detection[a]	Binary Reference
82621	419	36.17	405	18.29	-	
83808	407	25.48	400	17.06	N/A	Hummel et al. (2001)
89125	317	2.72	325	3.57	-	
91752	290	2.02	311	3.16	-	
97334	360	6.31	331	3.76	0.040	
97633	253	1.40	332	3.88	-	
98824	321	2.98	342	4.32	0.040	
103095	296	2.13	310	3.11	-	
110897	327	3.09	338	4.18	-	
118232	330	3.37	284	2.34	-	
119550	388	12.73	386	11.55	0.000	
120048	340	4.02	363	6.38	0.197	
120509	345	4.41	356	5.48	0.040	
120510	409	26.89	419	28.05	0.007	
123999	417	34.62	420	29.47	N/A	Boden et al. (2000, 2005)
127334	311	2.53	327	3.68	-	
128167	363	6.78	398	16.49	-	
132772	373	8.01	380	10.74	0.040	
133485	365	6.94	371	8.32	-	
136118	331	3.41	269	1.92	0.000	
139761	343	4.22	336	4.09	-	
140775	410	27.84	426	52.44	0.001	
141187	329	3.26	328	3.72	0.001	
143894	300	2.14	326	3.60	-	
144622	371	8.00	384	11.10	-	
144874	384	10.86	366	7.47	0.001	
147025	420	36.99	424	39.69	-	
149630	338	3.97	347	5.07	-	Baize (1989)
152308	401	21.37	404	18.28	0.000	
154345	364	6.83	359	5.89	-	
157935	375	9.18	365	7.23	0.197	
158063	374	8.16	364	7.12	0.037	
164259	425	42.11	429	79.71	-	
166014	295	2.09	329	3.75	-	
166205	367	7.14	368	7.91	0.036	
171834	387	12.71	394	15.43	-	
178187	370	7.70	393	14.97	0.000	
178798	312	2.55	309	3.10	0.000	
181440	333	3.42	334	4.01	0.000	
181655	418	35.34	408	19.14	-	
182488	369	7.55	377	9.14	-	
184663	392	15.00	399	16.97	-	
186547	332	3.42	340	4.21	0.000	
186568	350	4.53	323	3.53	-	
187691	307	2.34	335	4.05	-	

7. Estimation of the Undetected Binary Rate

One primary concern with the selection of potential calibration sources is choosing objects that are previously undetected binaries. For this reason, it is standard operating procedure to observe no less than 2 calibration sources in conjunction with astrophysical targets, allowing some means of cross-calibration between the potential calibrators. Although we cannot know for certain which of our previously unobserved calibration sources might have a heretofore undetected companion, we may attempt to characterize the likelihood with which such an undetected companion would escape detection once such a binary star system were to be placed on the observing queue.

We generated a synthetic, random sample of 4096 binary stars, starting with selecting an object with a random spectral type consistent with our potential calibrator list, which is within the range of B8 to K1. Luminosity class for these objects was statically assigned to be either III or V, to test the sensitivity of binary detection to primary star luminosity class. Absolute V, K magnitudes, radii and masses for these primary stars were then drawn from the standard MK type values found in Bessell & Brett (1988) and Cox (2000); apparent magnitude was randomly assigned a value between $m_K = 3.5$ to 5.0, which is consistent with the apparent magnitudes of PTI calibrators. Secondary stars were then randomly generated for each of these primaries: spectral type was selected to be equal to or later than the primary star, down to a class of M9[5], and for giant star primaries, luminosity class of the secondary objects was randomly assigned either III or V. Absolute V, K magnitudes, radii and masses for these secondary stars were then estimated also using the same references. Orbital separation a was then randomly assigned to be between 2 and 50 Roche diameters; distance of the binary star pair was established from the distance modulus, with an apparent angular separation resulting from the distance and true separation of the primary and secondary. Periods were established from the physical separation and the masses. Orbital parameters, such as eccentricity e, inclination i, and longitude of the ascending node Ω were randomly assigned. Angular sizes of each component were estimated using the $V - K$ technique described in van Belle (1999); given the $m_K = 3.5 - 5.0$ prior, the primaries were all well within the PTI calibrator selection criterion of $\theta < 1.0$ mas. Additionally, this sample well represents a potential sample of overlooked binary stars, with $a < 0.1$ arcsec, regardless of luminosity class.

Our overall goal was to test this subsample for PTI's ability to detect deviations from

---

[5]Implicit in this condition is a 'flat' mass ratio $q = M_1/M_2$ for binary stars, a topic which is discussed extensively in Duquennoy & Mayor (1991) and more recently in Goldberg et al. (2003), which appears to be reasonable for this experiment.

Table 6—Continued

HD	Mahalanobis Rank	Mahalanobis Distance	PCA Rank	PCA Distance	Geometric Non-detection[a]	Binary Reference
187923	393	15.07	396	16.13	-	
192985	357	5.27	372	8.32	-	
195050	414	32.94	423	37.19	0.007	
195564	355	4.81	350	5.22	0.002	
195987	412	31.05	397	16.19	N/A	Torres et al. (2002)
197076	381	10.28	383	11.05	-	
198478	328	3.23	341	4.24	0.007	
204403	366	6.98	349	5.14	0.040	
206660	400	19.58	382	11.05	0.007	
210027	402	21.46	387	12.39	N/A	Boden et al. (1999a)
210855	408	25.63	415	21.88	-	
211006	356	5.20	330	3.76	N/A	
213619	324	2.99	352	5.29	0.040	
214680	352	4.57	360	6.06	0.040	
216538	427	45.47	418	23.78	0.197	
216831	372	8.00	369	7.95	0.037	
218396	314	2.63	333	3.95	0.000	
218470	389	13.13	390	13.28	-	
219080	342	4.10	374	8.62	-	
222439	429	58.27	427	59.45	0.000	
222603	376	9.26	406	18.55	0.010	
223346	326	3.04	321	3.41	0.010	
223421	411	29.36	407	18.63	0.002	
224995	430	86.67	428	70.04	0.040	
234677	424	41.32	416	21.90	N/A	Boden & Lane (2001)

[a]Probability of a binary system non-detection due to lack of total nights on the sky, as discussed in §7.

what was expected to be normal calibrator object behavior. The expected squared visibility in a narrow passband for a binary system is given by

$$V^2(\lambda) = \frac{V_1^2 + V_2^2 r^2 + 2V_1 V_2 r \cos[(2\pi/\lambda)\mathbf{B} \cdot \mathbf{s}]}{(1+r)^2} \tag{8}$$

where V_1 and V_2 are the visibility moduli for the two stars alone as given by Equation 3, r is the apparent brightness ratio between the primary and secondary, B is the projected baseline vector at the system sky position, and s is the primary-secondary angular separation vector on the plane of the sky (Hummel et al. 1995; Boden et al. 1999a). V_1 and V_2 were estimated from the angular sizes estimates. A conservative detection limit would be a $3 - \sigma$ threshold of $\Delta V^2 > 0.06$, roughly three times PTI's limiting V^2 precision of $\sim 0.015 - 0.020$, where ΔV^2 is the difference between the expected single star V^2 as described in Equation 3 and the binary star V^2 from Equation 8. Objects with binary V^2 excursions less than PTI's limiting V^2 precision would effectively be single stars as far as PTI is concerned, and were excluded from consideration.

Figuring prominently into this characterization of PTI's ability to detect these synthetic binary stars is the geometric orientation of the target systems relative to the instrument's baseline in use, contained in the $\mathbf{B} \cdot \mathbf{s}$ term of Equation 8. If PTI's baseline in use is orthogonal to the primary-secondary separation vector, the departure from point-source source visibility will potentially be undetectable, depending upon the brightness ratio. Since the relative geometry between binary system and projected baseline varies with orbital phase, these 4096 systems were then examined over the course of 20 random epochs between the years covered by this study, 1998-2005, using PTI configurations consistent with the available baselines. As the number of nights increases, the likelihood that a binary system would remain undetected is given in Table 7.

Two categories of binary stars were problematic for PTI: First, stars with detectable V^2 excursions ($\Delta V^2_{max} \geq 0.06$) but in poor geometric orientation, due to orbital phase or apparent sky separation relative to baseline used, are found to escape initial detection by the array. However, after a few (~ 5) nights of observing, virtually all of these objects exhibited a detectable excursion and would be detected as binaries. Second, and more problematic, are the stars with V^2 excursions below the $3 - \sigma$ threshold of obvious detectability, but above PTI's limiting V^2 precision of $\sim 0.015 - 0.020$. These objects would remain always unconfirmed as binaries, yet their varying V^2 response could affect system calibration at the 2-4% level.

For example, in a single night of observing with the NS baseline has approximately $\sim 30\%$ of the binary systems with a main sequence primary are undetected. However, this proportion drops rapidly to $\sim 5.5\%$ after only 5 nights of observing, and to $\sim 5\%$ after 20

Table 7.   Percentage of undetected binaries from the synthetic binary star subsample, by number of nights observed per baseline and baselines used, as discussed in §7. Average value for the brightness ratio is given for those binary systems expected to be detected and undetected by PTI.

Baseline(s)	Primary lum. class	1 (%)	2 (%)	3 (%)	Nights Observed 4 (%)	5 (%)	6 (%)	20 (%)	Undetected Brightness Ratio	Detected Brt. Ratio
NS,NW,SW	V	30.0 ± 0.4	13.6 ± 0.4	8.9 ± 0.2	7.2 ± 0.1	6.4 ± 0.1	5.9 ± 0.0	5.0 ± 0.2	0.00967 ± 0.00035	0.312 ± 0.004
NS,NW,SW	III	34.6 ± 0.7	21.2 ± 0.7	16.6 ± 0.6	14.8 ± 0.7	13.9 ± 0.6	13.3 ± 0.7	12.0 ± 0.6	0.00543 ± 0.00004	0.289 ± 0.003
NS	V	29.6 ± 0.5	13.3 ± 0.5	8.6 ± 0.4	6.8 ± 0.2	6.0 ± 0.2	5.6 ± 0.3	4.7 ± 0.3	0.01012 ± 0.00114	0.311 ± 0.004
NS	III	34.6 ± 0.7	21.5 ± 0.3	16.6 ± 0.3	14.7 ± 0.2	13.7 ± 0.2	13.1 ± 0.3	11.9 ± 0.3	0.00545 ± 0.00012	0.296 ± 0.008

nights of observing, as it does for using the three PTI baselines in sequence. For binary systems with giant primaries, the limiting proportion of undetected binaries is higher, at $\sim 12\%$ after 20 nights. This larger value is consistent with a greater number of binary systems with a large brightness ratio, specifically those systems with a main sequence secondary star. This non-zero proportion of undetected binary systems is compelling motivation to employ multiple calibrators for any study with PTI, or any other interferometer. As we shall see in §6, we have many stars that show PTI V^2 data that are consistent with the point-response of a single, rather than binary, star system. The lingering uncertainty of undetected binarity for minimally observed stars can be drawn from the percentages given in Table 7.

8. Discussion

Some of the objects categorized as 'acceptable' calibrators due to their PTI V^2 are still found to have references indicating possible binary nature or other astrophysical effects which may cause them to be less-than suitable as calibrators; these objects are discussed below in §8.1. Interferometer observations of hierarchical systems have the potential to accidentally observe the wrong star and so appear to have a variation in angular size. Variations in metallicity will mean a potential calibrator won't fit SED templates well for predicting size. Stars with extreme rotational velocity will potentially exhibit angular size variations depending upon interferometer baseline utilized, and potentially "thrown off" material (as seen with the Be star phenomena) will also affect visibility measurements if the disk is detected. Additionally, evidence in the literature was uncovered for rejected calibrator candidates and is discussed in §8.2.

8.1. Objects thought to be acceptable calibrators

HD 905 is listed as a periodic variable star (Koen & Eyer 2002).

HD 1279 shows P Cygni type profiles in UV spectra taken with IUE (Snow et al. 1994).

HD 2758 is listed as a binary in the Tycho-2 catalog (Fabricius et al. 2002) with a companion at position angle 69.6 degrees and separation of $0\rlap{.}''44$.

HD 3268 is listed in Cayrel de Strobel et al. (1997) as metal poor with [Fe/H] = -0.23.

HD 15335 is listed in Heintz (1994) as an $0\rlap{.}''020$ astrometric binary, detected via photographic plates obtained with the 61 cm Sproul refractor, although the comments cite it as "astrom.,probable", and no secondary component magnitude is listed. Follow-up work by

Fischer & Valenti (2005) report a null result not only on detecting a stellar companion, but also down to planetary mass.

Both HD 19994 and HD 90508 are indicated to be binary stars in Hale (1994). HD 19994 is notable in that it has a Jupiter-mass planet (Mayor et al. 2004), and the F8V star's stellar companion is an M3V dwarf a few arcseconds away, which makes it undetectable by PTI from a brightness ratio standpoint. Similarly, HD 90508 is a F9V star with a M3V companion.

HD 24357 is listed in Cayrel de Strobel et al. (1997) as metal rich with [Fe/H] = 0.30.

HD 27524 is listed in Cayrel de Strobel et al. (1997) as metal poor with [Fe/H] = -0.46.

HD 28024 is listed in the Washington Double Star Catalog as a visual double with $104\rlap{.}{''}3$ separation and a delta magnitude of 8.23 (Worley & Douglass 1996). It has a GCVS period of 0.148 days (Samus et al. 2004) and in addition, it is cited as a delta Scuti variable (Rodriguez et al. 2000). It also has high rotational velocity (see below).

HD 28677 is listed in the GCVS as a possible variable star, however, no period or variability type is identified and this designation may be in doubt (Samus et al. 2004). We also note that this star is listed in a catalogue of binaries detected using lunar occultation and has a separation from its companion of 16.2 ± 5.2 mas, at a position angle of 205.9 degrees, with a delta magnitude of 0.0 ± 1.62 magnitudes at 547 nm (Mason 1995). There is no evidence for binarity in the PTI data, despite the 9 nights of available calibrated PTI data (7 on the NS baseline, 2 on the NW baseline).

HD 28704 is listed in the Washington Double Star Catalog as being a hierarchical quadruple system with separations from the primary ranging from $76\rlap{.}{''}4$ to $113\rlap{.}{''}7$ and delta magnitudes with respect to the primary ranging from 0.71 to 7.3 (Worley & Douglass 1996).

HD 31662 is listed in the Washington Double Star Catalog as being a visual double with separation $5\rlap{.}{''}4$ and a delta magnitude of 5.47 (Worley & Douglass 1996). There is no evidence for binarity in the PTI data.

HD 33167 has a large range of metallicities in the literature, from [Fe/H] = 0.09 (Cayrel de Strobel et al. 1997) to [Fe/H] = -0.36 to -0.37 (Ibukiyama & Arimoto (2002) and Marsakov & Shevelev (1995), respectively).

HD 38558 is noted by Adelman (2001) to have variability of 0.01 magnitudes in the Hipparcos data.

HD 43042 is listed in the Washington Double Star Catalog as being a hierarchical quadruple system with separations from the primary ranging from $32\rlap{.}{''}0$ to $91\rlap{.}{''}2$ and delta

magnitudes with respect to the primary ranging from 4.8 to 6.0 (Worley & Douglass 1996).

HD 51530 is listed in the Washington Double Star Catalog as being a hierarchical triple system with separations from the primary of 0''.5 and 28''.2 and a delta magnitude of the larger separated component of 6.0 magnitudes (Worley & Douglass 1996). There is no evidence for binarity in the PTI data.

HD 58551 is noted to be extremely metal poor, with [Fe/H] = -0.6 (Bartkevicius 1984; Cayrel de Strobel et al. 1997).

HD 58715 is noted as a double in the Hipparcos Input Catalogue with unknown separation and magnitude difference (Turon et al. 1993). It is listed as an eruptive Gamma Cas variable by (Samus et al. 2004) and has high rotational velocity (see below).

HD 58946 is listed as a hierarchical quadruple system spread over 5 arcminutes. The closest companion to the primary is separated by 3''.4 with a delta magnitude of 8.4 (Turon et al. 1993). Worley & Douglass (1996) goes on to list the A component in the system as a spectroscopic binary. However, Galland et al. (2005) use the system as a constant RV source to demonstrate the stability of their ELODIE instrument in searching for brown dwarfs and extrasolar planets. Samus et al. (2004) lists it in the GCVS with unknown variability type. And finally Adelman (2001) shows it to have 0.01 magnitudes of variability, as measured by Hipparcos.

HD 71148 is listed in the GCVS (Samus et al. 2004) as a previously misidentified variable star. It is metal poor with [Fe/H] = -0.15 (Ibukiyama & Arimoto 2002).

HD 75332 has been studied extensively in radial velocity surveys searching for extrasolar planets, however, no evidence for any are found to date (Fischer & Valenti 2005).

HD 75732 is a visual double with a separation of 85''.0 and a delta magnitude of 7.2. It has been found to have planets (Fischer & Valenti 2005), which are well below the sensitivity threshold of PTI to detect.

HD 89125 is a visual double with a separation of 7''.4 (Turon et al. 1993). Additionally, it is seen to have low-metallicity ranging from [Fe/H] = -0.19 to -0.39 (Cayrel de Strobel et al. 1997; Marsakov & Shevelev 1988).

HD 97334 is a hierarchical quadruple system with separations from the primary ranging from 88''.2 to 128''.4 and magnitude differences from 1.5 to 6.0 (Worley & Douglass 1996).

HD 97633 is flagged as a variable star by Samus et al. (2004) with the variable type and period unidentified. Further, it is extremely metal-rich with [Fe/H] = 0.40 (Cayrel de Strobel et al. 1997).

HD 103095 is flagged as a suspected varaible star by Samus et al. (2004) with the variable type and period unidentified. It has also been studied by Latham et al. (2002) for binarity and was found to have radial velocity measurements which varied at the 2-3 km s^{-1} level, with no indication of binarity or an orbital solution.

HD 119550 has also been studied by Latham et al. (2002) for binarity and was found to have radial velocity measurements which varied at the 1 km s^{-1} level, with no indication of binarity or an orbital solution.

HD 128167 is flagged as a suspected variable star by Samus et al. (2004) with the variable type, based on a reference, potentially a sigma bootes variable with an unidentified period. It is identified in the Washington Double Star catalog as a member of a hierarchical triple system with separations from the primary of 248$''$0 and 237$''$0 and 5.34 and 6.80 magnitudes respectively (Worley & Douglass 1996). Finally, it displays a wide range of low metallicities, from [Fe/H] = -0.18 to -0.60 (Cayrel de Strobel et al. 1997).

Both HD 132254 and HD 134083 are flagged by Nordström et al. (2004) as spectroscopic binaries, although no other supporting evidence in the literature could be found for this conclusion for either star. Indeed, in Galland et al. (2005), HD 134083 is cited as having a constant radial velocity at the $\sim$ 50 m/s level, which would preclude any binary detectable by PTI. HD 132254 was well-behaved enough for Kharchenko et al. (2004) to list the object as a candidate RV standard.

HD 136118 has been studied extensively with radial velocity techniques and is know to have a planet (Santos et al. 2003; Santos, Israelian & Mayor 2004), which are well-below the sensitivity threshold of PTI to detect.

HD 141187 is studied in a catalog of astrometric binaries, identified using Hipparcos and Tycho data, to have nonlinear proper motion (Makarov & Kaplan 2005). It is also seen to have high rotational velocity (see below).

HD 154345 is listed in Samus et al. (2004) as a suspected variable star in the GCVS, however no period of variability type is listed.

HD 166205 is flagged in Mason et al. (1999) as a suspected binary based on ground-based and Hipparcos data, however the binarity was not able to be confirmed, so it is listed in their Table 7 as a "problem star". Finally, it is flagged in Adelman (2001) as a variable star in the Hipparcos survey with 0.01 magnitudes of variability.

HD 171834 is flagged as a binary with 0$''$1 arcsecond separation and no notation of the secondary's magnitude in Worley & Douglass (1996). It is also seen to have a low metallicity compared to solar of [Fe/H] = -0.42 (Cayrel de Strobel et al. 1997).

HD 182488 has been studied extensively using the radial velocity technique and is found to have no detectable planet or stellar companions Fischer & Valenti (2005).

HD 186568 is a member of a hierarchical triple with separations of 15″.4 and 33″.9 and magnitude differences of 7.75 and 5.44 respectively (Worley & Douglass 1996).

HD 187691 is a member of a hierarchical quintuple system with separations from the primary ranging from 20″.5 to 89″.7 and magnitude differences of 7.69 to 8.59 Worley & Douglass (1996). It was used by Mazeh, Latham & Stefanik (1996) as an RV standard in the study of orbits of three spectroscopic binary systems. Fischer & Valenti (2005) have studied it extensively in their radial velocity searches for planets and find no evidence for a companion. And finally, it is flagged in the GCVS as a rotating variable star with no period listed (Samus et al. 2004).

HD 187923 is a member of a visual double system with a separation from the secondary of 93″.9 and a magnitude difference of 5.57 (Worley & Douglass 1996). It has been studied extensively using radial velocity techniques and is found to have no companions Fischer & Valenti (2005). It is flagged in the GCVS as variable, but no variability type or period is identified (Samus et al. 2004).

HD 195564 is a member of a hierarchical triple system with separations of 4″.6 and 100″.2 and magnitude differences of 5.5 and 4.2 respectively (Worley & Douglass 1996). It has been studied extensively using radial velocity techniques and is found to have no companions Fischer & Valenti (2005).

HD 197076 is a member of a hierarchical triple system with separations of 98″.8 and 125″.0 and magnitude differences of 5.45 and 6.95 respectively (Worley & Douglass 1996). It has been studied extensively using radial velocity techniques and is found to have no companions Fischer & Valenti (2005).

HD 198478 is a member of a visual double system with a separation of 20″.5 and a magnitude difference of 5.32 (Worley & Douglass 1996). It is flagged in the GCVS as being a pulsating variable star (Samus et al. 2004) and has an identified period of 0.20472 days (Koen & Eyer 2002).

HD 210855 is a member of hierarchical triple system with separations of 79″.6 and 56″.0 and magnitude differences of 5.26 and 8.46 respectively (Worley & Douglass 1996).

HD 214680 is a member of a visual double system with a separation of 60″.4 and a magnitude difference of 5.14 (Worley & Douglass 1996). Further, it is flagged in the GCVS as a beta Cephei variable star (Samus et al. 2004).

HD 218396 is flagged in the GCVS as a rotating ellipsoidal variable (Samus et al. 2004) and as a probable lambda Bootis variable by Gerbaldi, Faraggiana & Lai (2003).

HD 219080 is flagged as a new periodic variable star by Koen & Eyer (2002).

HD 222439 is a member of a hierarchical triple system with separations of 46″.6 and 103″.2 and magnitude differences of 7.16 for both companions (Worley & Douglass 1996). Further, it is flagged in the GCVS as a variable star of unknown type (Samus et al. 2004).

In addition, the following stars have rotational velocities (v sin i) between 100 and 200 km/s: HD 7804, HD 18411, HD 20150, HD 26605, HD 27397, HD 27946, HD 28677, HD 30739, HD 32301, HD 32630, HD 37147, HD 50019, HD 56537, HD 60111, HD 67006, HD 79439, HD 83287, HD 85795, HD 87696, HD 92825, HD 102124, HD 107904, HD 108765, HD 110411, HD 111604, HD 116831, HD 122408, HD 125161, HD 125162, HD 132052, HD 141003, HD 143894, HD 147547, HD 152614, HD 161868, HD 166014, HD 166205, HD 168914, HD 169702, HD 177196, HD 177756, HD 192425, HD 204153, HD 206043, HD 210129, HD 213558, HD 214734, HD 214923, HD 216735, HD 222439. The following stars have rotational velocities higher than 200 km/s: HD 11946, HD 17573, HD 20418, HD 21686, HD 23630, HD 23862, HD 28024, HD 30823, HD 58715, HD 73262, HD 93702, HD 98058, HD 130109. These data were taken mainly from Vizier catalogs associated with the following papers: Glebocki, Gnacinski & Stawikowski (2000), Royer et al. (2002) and de Medeiros et al. (2002). Rapidly rotating stars have an additional uncertainty in their predicted angular size due to rotational distortion, which is on the order of $\sim 10 - 15\%$ (van Belle et al. 2006). However, if this was a significant factor, the statistical vetting of §6 would have rejected these objects as valid calibrators.

8.2. Objects rejected as acceptable calibrators

HD 8357 is flagged by Nordström et al. (2004) as a spectroscopic binary, with a mass ratio of $q = 0.841 \pm 0.009$.

HD 8799 was found to be listed as a visual (but not physical) binary of unspecified separation in Tokovinin & Smekhov (2002).

HD 13480 is flagged by Nordström et al. (2004) as a spectroscopic binary, with a mass ratio of $q = 1.062 \pm 0.010$.

HD 16234 is flagged by Nordström et al. (2004) as a spectroscopic binary, with a mass ratio of $q = 1.039 \pm 0.041$.

HD 18012 was examined by Lu et al. (1987) using speckle interferometry at the 4m Mayall telescope, without any detection of a secondary companion.

HD 27483 is flagged by Nordström et al. (2004) as a spectroscopic binary, with a mass ratio of $q = 0.937 \pm 0.011$.

HD 27901 was examined by Mason et al. (1993) using speckle interferometry, without any detection of a secondary companion.

HD 37594 is found to have a range of spectral classifications from A5mF2 (Bertaud & Floquet 1967) to F0Vp (Abt & Morrell 1995) as found by Skiff (2005) indicating that the model fits to these data may be problematic.

HD 43587 is noted by Nidever et al. (2002) as having a radial velocity RMS > 0.1 km/s, and Makarov & Kaplan (2005) cite the object as a possible astrometric binary from Hipparcos proper motion discrepancies, with the factor Q_0 as discussed in that study, related to the lower bound of a possible secondary companion's mass, having a value of $\log Q_0$=-1.6 yr^{-1}.

HD 75137 is listed by Turon et al. (1993) to have a companion separated by $12\rlap{.}''4$ with a magnitude difference of 7.5. Worley & Douglass (1996) state that the primary in the system is a spectroscopic binary with an orbital period of 8.2 days. It also has high rotational velocity (see below).

HD 79969 is noted by Horch et al. (2004), using speckle interferometry, to have a secondary companion. The orbital axis is $0\rlap{.}''66 \pm 0\rlap{.}''007$ with a period of 34.2 years Henry & McCarthy (1993).

HD 118232 is flagged as a suspected variable star by Samus et al. (2004) with the variable type and period unidentified. A visual inspection of the PTI visibility data for the 9 nights this object was observed shows 7 that are qualitatively identical to the associated calibrators, and 2 that are marginally offset $\Delta V^2 \approx 0.05$ from those calibrators.

HD 120510 is flagged by Nordström et al. (2004) as a spectroscopic binary, with a mass ratio of $q = 1.000 \pm 0.009$.

HD 122676 is noted by Nidever et al. (2002) as having a radial velocity RMS > 0.1 km/s.

HD 123999 is flagged by Nordström et al. (2004) as a spectroscopic binary, with a mass ratio of $q = 0.963 \pm 0.010$.

HD 141187 is noted by Makarov & Kaplan (2005) as a possible astrometric binary from

Hipparcos proper motion discrepancies, with $\log Q_0$=-1.1 yr^{-1}.

HD 149630 is noted by Makarov & Kaplan (2005) as a possible astrometric binary from Hipparcos proper motion discrepancies, with $\log Q_0$=-1.0 yr^{-1}.

HD 152308 is noted in Hoffleit & Jaschek (1991) as having "suspected variable radial velocity". It appears in the GCVS catalog as a rotating variable star Samus et al. (2004) and has an identified period of 0.9366 days Renson & Catalano (2001).

HD 157935 has a radial velocity of -51.9 km s^{-1} quoted in Duflot et al. (1995) (no error given, but a radial velocity quality of 'B' on a scale of 'A' to 'E', where 'A' is best), but a value of -54.7 ± 1.6 km s^{-1} listed in Nordström et al. (2004) - possibly an indication of a variable radial velocity.

HD 181655 is noted by Nidever et al. (2002) as having a stable radial velocity with RMS < 100 m/s.

HD 195050 is noted by Makarov & Kaplan (2005) as a possible astrometric binary from Hipparcos proper motion discrepancies, with $\log Q_0$=-1.1 yr^{-1}. It is also seen to have high rotational velocity (see below).

HD 120048, HD 120509, HD 136643, HD 158063, HD 186547, and HD 234677 are all listed in the radial velocity study of Famaey et al. (2005) as having "no evidence for radial-velocity variations".

HD 216538 is flagged by Samus et al. (2004) as a long-period pulsating B star.

HD 216831 is a member of a visual double system with a separation of 49$\farcs$6 and a magnitude difference of 3.76 Worley & Douglass (1996). Further, it was examined by McAlister et al. (1987) using speckle interferometry at the 3.6m CFHT, without any detection of a secondary companion. Finally, it has anomalously high metallicity compared to solar of [Fe/H] = 0.40 (Cayrel de Strobel et al. 1997).

HD 223346 is flagged to have anomalously low metallicity compared to solar of [Fe/H] = -0.42 (Ibukiyama & Arimoto 2002).

HD 223421 is flagged to have anomalously low metallicity compared to solar ranging from [Fe/H] = -0.20 to -0.35 (see for example Ibukiyama & Arimoto (2002) and Cayrel de Strobel et al. (1997)). It is flagged as a probable spectroscopic binary in a catalog of overluminous F-type stars, though identification was problematic (Griffin & Suchkov 2003).

In addition, the following stars have rotational velocities (v sin i) between 100 and 200 km/s: HD 20677, HD 23850, HD 27322, HD 27901, HD 45542, HD 75137, HD 82621,

HD 141187, HD 141851, HD 144874, HD 178449, HD 195050, HD 204403. The following stars have rotational velocities higher than 200 km/s: HD 149630 and HD 184606. These data were taken mainly from Vizier catalogs associated with the following papers: Glebocki, Gnacinski & Stawikowski (2000), Royer et al. (2002) and de Medeiros et al. (2002).

9. Conclusion

We have examined 8 years of PTI visibility data for candidate single, point-like stellar calibrator sources. To vet the appropriate sources, we subjected the data to a rigorous statistical evaluation, comparing the sources to a well-understood and intensively studied standard PTI calibrator, HD217014. Of the candidates that satisfied the *a priori* selection criteria, approximately 350 were found to be 'well-behaved' in an empirical, statistical sense, with ~ 140 being rejected. These vetted calibrator objects represent $\gtrsim 96\%$ sky coverage for PTI in the declination range $5^o < \delta < 55^o$ and form a set of well-characterized calibrator anchors for future PTI observations, archival studies, and observations at other interferometric facilities.

REFERENCES

Abt, H. A. & Morrell, N. I. 1995, ApJS, 99, 135

Adelman, S. J. 2001, å, 367, 297

Alcaino, G. 1965, Lowell Observatory Bulletin, 6, 167

Allen, D. A. 1973, MNRAS, 161, 145

Anthony-Twarog, B. J., & Twarog, B. A. 1994, AJ, 107, 1577

Appenzeller, I. 1966, Zeitschrift fur Astrophysics, 64, 269

Ardeberg, A., Sarg, K., & Wramdemark, S. 1973, A&AS, 9, 163

Arellano Ferro, A., Parrao, L., Schuster, W., Gonzalez-Bedolla, S., Peniche, R., & Pena,
    J. H. 1990, A&AS, 83, 225

Argue, A. N. 1963, MNRAS, 125, 557

Argue, A. N. 1966, MNRAS, 133, 475

Arp, H. C. 1958, AJ, 63, 118

Baize, P. 1989, A&AS, 81, 415

Bakos, G. A. 1968, AJ, 73, 187

Barry, D. C. 1969, PASP, 81, 339

Bartkevicius, A. 1984, Vilnius Astronomijos Observatorijos Biuletenis, 68, 3

Bartkowiak, A., & Jakimiec, M. 1989, Acta Astronomica, 39, 85

Beichman, C. A., Neugebauer, G., Habing, H. J., Clegg, P. E., & Chester, T. J. 1988,
    Infrared astronomical satellite (IRAS) catalogs and atlases. Volume 1: Explanatory
    supplement, 1

Bertaud, C. & Floquet, M. 1967, J. Obs., 50, 425

Bessell, M. S., & Brett, J. M. 1988, PASP, 100, 1134

Blaauw, A., West, R. M., Bartaya, R. A., & Tolbert, C. R. 1976, A&AS, 23, 393

Blanco, C., Marilli, E., & Catalano, S. 1979, A&AS, 36, 297

Boden, A. F., & Lane, B. F. 2001, ApJ, 547, 1071

Boden, A. F., Colavita, M. M., van Belle, G. T., & Shao, M. 1998, Proc. SPIE, 3350, 872

Boden, A.F, et al., 1998, ApJ, 504, L39

Boden, A. F., et al. 1999, ApJ, 515, 356

Boden, A. F., et al. 1999, ApJ, 527, 360

Boden, A. F., Creech-Eakman, M. J., & Queloz, D. 2000, ApJ, 536, 880

Boden, A. F., Torres, G., & Hummel, C. A. 2005, ApJ, 627, 464

Bok, B. J., Bok, P. F., & Miller, E. W. 1972, AJ, 77, 733

Bond, H. E. 1970, ApJS, 22, 117

Bond, H. E. 1980, ApJS, 44, 517

Bordé, P., Coudé du Foresto, V., Chagnon, G., & Perrin, G. 2002, A&A, 393, 183

Bouigue, R., Boulon, J., & Pedoussaut, A. 1961, Annales de l'Observatoire Astron. et Meteo. de Toulouse, 28, 33

Bouigue, R., Boulon, J., & Pedoussaut, A. 1963, Annales de l'Observatoire Astron. et Meteo. de Toulouse, 29, 17

Bouigue, R. 1959, Annales de l'Observatoire Astron. et Meteo. de Toulouse, 27, 47

Breger, M. 1968, AJ, 73, 84

Breger, M. 1974, ApJ, 188, 53

Bronkalla, W., & Notni, P. 1961, Astronomische Nachrichten, 286, 179

Burnichon, M. L., & Garnier, R. 1976, A&AS, 24, 89

Cameron, R. C. 1966, Georgetown Observatory Monogram, 21,

Cardelli, J. A., Clayton, G. C., & Mathis, J. S. 1989, ApJ, 345, 245

Carney, B. W., & Aaronson, M. 1979, AJ, 84, 867

Carney, B. W. 1978, AJ, 83, 1087

Carney, B. W. 1979, ApJ, 233, 211

Carney, B. W. 1983, AJ, 88, 610

Cayrel de Strobel, G., et al. 1997, A&AS, 144, 299.

Celis S., L. 1975, A&AS, 22, 9

Claret, A., & Hauschildt, P. H. 2003, A&A, 412, 241

Colavita, M.M., et al., 1999, ApJ, 510, 505

Colavita, M.M., 1999, PASP, 111, 111

Coleman, L. A. 1982, AJ, 87, 369

Cousins, A. W. J., & Stoy, R. H. 1962, Royal Greenwich Observatory Bulletin, 64, 103

Cousins, A. W. J. 1962, Monthly Notes of the Astronomical Society of South Africa, 21, 20

Cousins, A. W. J. 1962, Monthly Notes of the Astronomical Society of South Africa, 21, 61

Cousins, A. W. J. 1963, Monthly Notes of the Astronomical Society of South Africa, 22, 12

Cousins, A. W. J. 1963, Monthly Notes of the Astronomical Society of South Africa, 22, 58

Cousins, A. W. J. 1963, Monthly Notes of the Astronomical Society of South Africa, 22, 130

Cousins, A. W. J. 1964, Monthly Notes of the Astronomical Society of South Africa, 23, 10

Cousins, A. W. J. 1964, Monthly Notes of the Astronomical Society of South Africa, 23, 175

Cousins, A. W. J. 1965, Monthly Notes of the Astronomical Society of South Africa, 24, 120

Cousins, A. W. J. 1973, Monthly Notes of the Astronomical Society of South Africa, 32, 117

Cousins, A. W. J. 1984, South African Astronomical Observatory Circular, 8, 59

Cousins, A. W. J. 1987, South African Astronomical Observatory Circular, 11, 93

Cowley, A. P., Hiltner, W. A., & Witt, A. N. 1967, AJ, 72, 1334

Cox, A. N. 2000, Allen's astrophysical quantities, 4th ed. Publisher: New York: AIP Press; Springer, 2000. Editedy by Arthur N. Cox. ISBN: 0387987460,

Crawford, D. L., & Barnes, J. V. 1969, AJ, 74, 818

Crawford, D. L., & Barnes, J. V. 1970, AJ, 75, 978

Crawford, D. L., & Barnes, J. V. 1974, AJ, 79, 687

Crawford, D. L., & Perry, C. L. 1966, AJ, 71, 206

Crawford, D. L., & Perry, C. L. 1976, AJ, 81, 419

Crawford, D. L., Barnes, J. V., Faure, B. Q., & Golson, J. C. 1967, AJ, 71, 709

Crawford, D. L., Barnes, J. V., & Golson, J. C. 1971, AJ, 76, 1058

Crawford, D. L., Barnes, J. V., Gibson, J., Golson, J. C., Perry, C. L., & Crawford, M. L. 1972, A&AS, 5, 109

Crawford, D. L., Barnes, J. V., Golson, J. C., & Hube, D. P. 1973, AJ, 78, 738

Crawford, D. L. 1963, ApJ, 137, 523

Crawford, D. L. 1975, AJ, 80, 955

Cutri, R. M., et al. 2003, VizieR Online Data Catalog, 2246,

Danziger, I. J., & Dickens, R. J. 1967, ApJ, 149, 55

Danziger, I. J., & Faber, S. M. 1972, A&A, 18, 428

Davis, J., Tango, W. J., & Booth, A. J. 2000, MNRAS, 318, 387

de Medeiros, J. R., Udry, S., Burki, G. & Mayor, M. 2002, å, 395, 97

de Vaucouleurs, G. 1959, Planet. Space Sci., 2, 26

Deutschman, W. A., Davis, R. J., & Schild, R. E. 1976, ApJS, 30, 97

Dickens, R. J., Kraft, R. P., & Krzeminski, W. 1968, AJ, 73, 6

Duflot, M., Figon, P., & Meyssonnier, N. 1995, A&AS, 114, 269

Duquennoy, A., & Mayor, M. 1991, A&A, 248, 485

Dyck, H. M., Benson, J. A., van Belle, G. T., & Ridgway, S. T. 1996, AJ, 111, 1705

Echevarria, J., Roth, M., & Warman, J. 1979, Revista Mexicana de Astronomia y Astrofisica, 4, 287

Eggen, O. J. 1963, AJ, 68, 483

Eggen, O. J. 1965, AJ, 70, 19

Eggen, O. J. 1966, Royal Greenwich Observatory Bulletin, 120, 333

Eggen, O. J. 1971, PASP, 83, 741

Eggen, O. J. 1972, ApJ, 175, 787

Eggen, O. J. 1973, PASP, 85, 542

Elias, J., Frogel, J., Matthews, K., Neugebauer, G., 1982, AJ, 87, 1029

Elias, J., Frogel, J., Hyland, A., Jones, T., 1983, AJ, 88, 1027

Elliott, J. E. 1974, AJ, 79, 1082

Epps, E. A. 1972, Royal Greenwich Observatory Bulletin, 176, 127

Erro, B. I. 1969, Boletin del Instituto de Tonantzintla, 5, 89

Evans, D. S. 1966, Royal Greenwich Observatory Bulletin, 110, 185

Fabregat, J., & Reglero, V. 1990, A&AS, 82, 531

Fabricius, C. et al. 2002, å, 384, 180.

Famaey, B., Jorissen, A., Luri, X., Mayor, M., Udry, S., Dejonghe, H., & Turon, C. 2005, A&A, 430, 165

Fernie, J. D., Hagen, J. P. J., Hagen, G. L., & McClure, L. 1971, PASP, 83, 79

Fernie, J. D. 1969, JRASC, 63, 133

Fernie, J. D. 1976, PASP, 88, 116

Fernie, J. D. 1983, ApJS, 52, 7

Fischer, D. A., & Valenti, J. 2005, ApJ, 622, 1102

Fitch, W. S. 1955, ApJ, 121, 690

Franco, G. A. P. 1989, A&AS, 80, 127

Galland, F., Lagrange, A.-M., Udry, S., Chelli, A., Pepe, F., Queloz, D., Beuzit, J.-L., & Mayor, M. 2005, A&A, 443, 337

Galland, F. et al. 2005, å, 443, 337

Garmany, C. D., & Ianna, P. A. 1977, A&AS, 28, 295

Gascoigne, S. C. B. 1962, MNRAS, 124, 201

Gehrels, T., & Owings, D. 1962, ApJ, 135, 906

Gerbaldi, M., Faraggiana, R. & Lai, O. 2003, å, 412, 447

Gezari, D.Y., Pitts, P.S., Schmitz, M., 1996, Catalog of Infrared Observations, edition 3.5

Giclas, H. L., Burnham, R., & Thomas, N. G. 1971, Flagstaff, Arizona: Lowell Observatory, 1971,

Giclas, H. L. 1954, AJ, 59, 128

Glass, I. S. 1974, Monthly Notes of the Astronomical Society of South Africa, 33, 53

Glass, I. S. 1975, MNRAS, 171, 19P

Glebocki, R., Gnacinski, P. & Stawikowski, A. 2000, Acta Astron., 50, 509

Goldberg, D., Mazeh, T., & Latham, D. W. 2003, ApJ, 591, 397

Grant, G. 1959, ApJ, 129, 62

Gray, R. O., & Olsen, E. H. 1991, A&AS, 87, 541

Griffin, R. F. & Suchkov, A. A. 2003, ApJS, 147, 103

Gronbech, B., & Olsen, E. H. 1976, A&AS, 25, 213

Gronbech, B., Olsen, E. H., & Stromgren, B. 1976, A&AS, 26, 155

Guetter, H. H., & Hewitt, A. V. 1984, PASP, 96, 441

Guetter, H. H. 1980, PASP, 92, 215

Gutierrez-Moreno, A., & et al. 1966, Publications of the Department of Astronomy University of Chile, 1, 1

Häggkvist, L., & Oja, T. 1966, Arkiv for Astronomi, 4, 137

Häggkvist, L., & Oja, T. 1969, Arkiv for Astronomi, 5, 125

Häggkvist, L., & Oja, T. 1969, Arkiv for Astronomi, 5, 303

Häggkvist, L. 1966, Arkiv for Astronomi, 4, 165

Haggkvist, T., & Oja, T. 1970, Private Communication,

Haggkvist, L., & Oja, T. 1973, A&AS, 12, 381

Hale, A. 1994, AJ, 107, 306

Hardie, R. H., Seyfert, C. K., & Gulledge, I. S. 1960, ApJ, 132, 361

Hardie, R. 1958, ApJ, 127, 620

Harmanec, P., Horn, J., Koubsky, P., Zdarsky, F., Kriz, S., & Pavlovski, K. 1980, Bulletin of the Astronomical Institutes of Czechoslovakia, 31, 144

Harris, D. L., & Upgren, A. R. 1964, ApJ, 140, 151

Harris, D. L. 1955, ApJ, 121, 554

Harris, D. L. 1956, ApJ, 123, 371

Hartkopf, W. I., Mason, B. D., & McAlister, H. A. 1996, AJ, 111, 370

Hartkopf, W. I., Mason, B. D., & Worley, C. E. 2001, AJ, 122, 3472

Hauck, B., & Mermilliod, M. 1998, A&AS, 129, 431

Haug, U., & Walter, K. 1970, A&AS, 1, 29

Haug, U. 1970, A&AS, 1, 35

Haupt, H. F., & Schroll, A. 1974, A&AS, 15, 311

Heck, A., & Manfroid, J. 1975, A&AS, 22, 323

Heck, A., & Manfroid, J. 1980, A&AS, 42, 311

Heintz, W. D. 1994, AJ, 108, 2338

Henden, A. A. 1980, MNRAS, 192, 621

Henry, T.J. & McCarthy, D.W. Jr. 1993, AJ, 106,773

Hilditch, R. W., Hill, G., & Barnes, J. V. 1976, MmRAS, 82, 95

Hill, G., & Barnes, J. V. 1982, Publications of the Dominion Astrophysical Observatory Victoria, 16, 71

Hiltner, W. A., & Johnson, H. L. 1956, ApJ, 124, 367

Hiltner, W. A. 1956, ApJS, 2, 389

Hoag, A. A., Johnson, H. L., Iriarte, B., Mitchell, R. I., Hallam, K. L., & Sharpless, S. 1961, Publications of the U.S. Naval Observatory Second Series, 17, 343

Hoffleit, D., & Jaschek, C. —. 1991, New Haven, Conn.: Yale University Observatory, —c1991, 5th rev.ed., edited by Hoffleit, Dorrit; Jaschek, Carlos —v(coll.)

Hogg, A. R. 1958, Mount Stromlo Observatory Mimeographs, 2, 1

Horch, E. P., Meyer, R. D., & van Altena, W. F. 2004, AJ, 127, 1727

Hummel, C. A., Armstrong, J. T., Buscher, D. F., Mozurkewich, D., Quirrenbach, A., & Vivekanand, M. 1995, AJ, 110, 376

Hummel, C. A., Carquillat, J.-M., Ginestet, N., Griffin, R. F., Boden, A. F., Hajian, A. R., Mozurkewich, D., & Nordgren, T. E. 2001, AJ, 121, 1623

Ibukiyama, A. & Arimoto, N. 2002, å, 394, 927

Iriarte, B., Johnson, H. L., Mitchell, R. I., & Wisniewski, W. K. 1965, S&T, 30, 21

Iriarte, B. 1969, Boletin de los Observatorios Tonantzintla y Tacubaya, 5, 89

Iriarte, B. 1970, Boletin de los Observatorios Tonantzintla y Tacubaya, 5, 317

Irwin, J. B. 1961, ApJS, 6, 253

Jennens, P. A., & Helfer, H. L. 1975, MNRAS, 172, 667

Jerzykiewicz, M., & Serkowski, K. 1966, PASP, 78, 546

Jerzykiewicz, M. 1971, Acta Astronomica, 21, 501

Johansen, K. T., & Gyldenkerne, K. 1970, A&AS, 1, 165

Johnson, H. L., & Harris, D. L. 1954, ApJ, 120, 196

Johnson, H. L., & Knuckles, C. F. 1955, ApJ, 122, 209

Johnson, H. L., & Knuckles, C. F. 1957, ApJ, 126, 113

Johnson, H. L., & Mitchell, R. I. 1958, ApJ, 128, 31

Johnson, H. L., & Morgan, W. W. 1953, ApJ, 117, 313

Johnson, H. L., Iriarte, B., Mitchell, R. I., & Wisniewskj, W. Z. 1966, Communications of the Lunar and Planetary Laboratory, 4, 99

Johnson, H. L., MacArthur, J. W., & Mitchell, R. I. 1968, ApJ, 152, 465

Johnson, H. L. 1952, ApJ, 116, 640

Johnson, H. L. 1953, ApJ, 117, 361

Johnson, H. L. 1955, Annales d'Astrophysique, 18, 292

Johnson, H. L. 1964, Boletin de los Observatorios Tonantzintla y Tacubaya, 3, 305

Johnson, H. L. 1965, ApJ, 141, 923

Johnson, H. L. 1965, Communications of the Lunar and Planetary Laboratory, 3, 73

Johnson, H. L., 1968, in Stars and Stellar Systems, 7, Nebulae and Interstellar Matter, ed.
    B.M. Middlehurst & L.H. Aller (Chicago: Univ. of Chicago Press), chap. 5

Joner, M. D., Taylor, B. J., Powell, J. M., & Johnson, S. B. 1995, PASP, 107, 27

Jones, D. H. P. 1969, Acta Astronomica, 19, 53

Jordi, C., Figueras, F., Torra, J., & Asiain, R. 1996, A&AS, 115, 401

Kharchenko, N. V., Piskunov, A. E., & Scholz, R.-D. 2004, Astronomische Nachrichten, 325,
    439

Kilkenny, D., & Malcolm, G. 1984, MNRAS, 209, 169

Kilkenny, D., & Menzies, J. W. 1986, MNRAS, 222, 373

Kilkenny, D. 1987, MNRAS, 228, 713

Knude, J. K. 1977, A&AS, 30, 297

Knude, J. 1981, A&AS, 44, 225

Koch, R. H. 1960, AJ, 65, 127

Koen, C. & Eyer, L. 2002, MNRAS, 331, 45

Konacki, M., & Lane, B. F. 2004, ApJ, 610, 443

Koresko, C. D., et al. 1998, ApJ, 509, L45

Kornilov, V. G., Volkov, I. M., Zakharov, A. I., Kozyreva, L. N., Kornilova, L. N., & et al.
    1991, Trudy Gosudarstvennogo Astronomicheskogo Instituta, 63, 4

Kozok, J. R. 1985, A&AS, 61, 387

Kubiak, M. 1973, Acta Astronomica, 23, 23

Kubinec, W. R. 1973, Publications of the Warner & Swasey Observatory, 1, 1

Lake, R. 1962, Monthly Notes of the Astronomical Society of South Africa, 21, 56

Lake, R. 1962, Monthly Notes of the Astronomical Society of South Africa, 21, 191

Lake, R. 1964, Monthly Notes of the Astronomical Society of South Africa, 23, 14

Lake, R. 1964, Monthly Notes of the Astronomical Society of South Africa, 23, 136

Lake, R. 1965, Monthly Notes of the Astronomical Society of South Africa, 24, 41

Landolt, A. U. 1967, AJ, 72, 1012

Latham, D. W., et al. 2002, AJ, 124, 1144

Lee, T. A. 1968, ApJ, 152, 913

Lindgren, H., & Bern, K. 1980, A&AS, 42, 335

Ljunggren, B., & Oja, T. 1961, Uppsala Astronomical Observatory Annals, 4, 1

Ljunggren, B., & Oja, T. 1965, Arkiv for Astronomi, 3, 439

Ljunggren, B. 1966, Arkiv for Astronomi, 3, 535

Loden, K., Lindblad, P. O., Schober, J., & Urban, A. 1980, A&AS, 41, 85

Lu, P. K., Demarque, P., van Altena, W., McAlister, H., & Hartkopf, W. 1987, AJ, 94, 1318

Lucke, P. B. 1974, ApJS, 28, 73

Lutz, T. E., & Lutz, J. H. 1977, AJ, 82, 431

Lutz, T. E. 1971, PASP, 83, 488

Makarov, V. V., & Kaplan, G. H. 2005, AJ, 129, 2420

Makarov, V. V. & Kaplan, G. H. 2005, AJ, 129, 2420

Malmquist K.G., & Ljunggren B. And Oja T. 1960, Uppsala Astronomical Observatory Annals, 4, 1

Manfroid, J., & Sterken, C. 1987, A&AS, 71, 539

Marcy, G. W., Butler, R. P., Williams, E., Bildsten, L., Graham, J. R., Ghez, A. M., & Jernigan, J. G. 1997, ApJ, 481, 926

Markkanen, T. 1977, Observatory and Astrophysics Laboratory University of Helsinki Report, 1,

Marlborough, J. M. 1964, AJ, 69, 215

Marsakov, V. A. & Shevelev, Y. G. 1988, BICDS, 35, 129

Marsakov, V. A. & Shevelev, Y. G. 1995, BICDS, 47, 13

Mason, B. D., McAlister, H. A., Hartkopf, W. I., & Bagnuolo, W. G. 1993, AJ, 105, 220

Mason, B. D. 1995, PASP, 107, 299

Mason, B. D. 1997, AJ, 114, 808

Mason, B. D., et al. 1999, AJ, 117, 1890

Mayor, M., & Queloz, D. 1995, Nature, 378, 355

Mayor, M., Udry, S., Naef, D., Pepe, F., Queloz, D., Santos, N. C., & Burnet, M. 2004, A&A, 415, 391

Mazeh, T., Latham, D. W. & Stefanik, R. P. 1996, ApJ, 466, 415

McAlister, H. A., Hartkopf, W. I., Hutter, D. J., Shara, M. M., & Franz, O. G. 1987, AJ, 93, 183

McClure, R. D. 1970, AJ, 75, 41

McClure, R. D. 1976, AJ, 81, 182

McMillan, R. S., Breger, M., Ferland, G. J., & Loumos, G. L. 1976, PASP, 88, 495

McNamara, B. J. 1976, PASP, 88, 144

Mechler, G. E. 1976, AJ, 81, 107

Mendoza, E. E., & Gonzalez, S. F. 1974, Revista Mexicana de Astronomia y Astrofisica, 1, 67

Mendoza, E. E., Gomez, V. T., & Gonzalez, S. 1978, AJ, 83, 606

Mendoza, E. E., Rolland, A., & Rodriguez, E. 1990, A&AS, 84, 29

Mendoza V., E. E. 1958, ApJ, 128, 207

Mendoza, E. E. 1967, Boletin de los Observatorios Tonantzintla y Tacubaya, 4, 106

Mendoza, E. E. 1967, Boletin de los Observatorios Tonantzintla y Tacubaya, 4, 149

Mendoza, E. E. 1969, Boletin de los Observatorios Tonantzintla y Tacubaya, 5, 57

Mendoza, E. E. 1970, Boletin de los Observatorios Tonantzintla y Tacubaya, 5, 269

Mermilliod, J.-C. 1986, Catalogue of Eggen's UBV data. (1986),

Mermilliod, J.-C., Mermilliod, M., & Hauck, B. 1997, A&AS, 124, 349

Miczaika, G. R. 1954, AJ, 59, 233

Millis, R. L. 1969, Lowell Observatory Bulletin, 7, 113

Moffett, T. J., & Barnes, T. G. 1979, PASP, 91, 180

Moffett, T. J., & Barnes, T. G. 1980, ApJS, 44, 427

Moreno, H. 1971, A&A, 12, 442

Mozurkewich, D., et al., 1991, AJ, 101, 2207

Mumford, G. S. 1956, AJ, 61, 213

Nakagiri, M., & Yamashita, Y. 1979, Annals of the Tokyo Astronomical Observatory, 17, 221

Naur, P. 1955, ApJ, 122, 182

Neckel, H. 1974, A&AS, 18, 169

Nekrasova, S. V., & Nikonov, V. B. 1965, Izvestiya Ordena Trudovogo Krasnogo Znameni Krymskoj Astrofizicheskoj Observatorii, 34, 69

Nicolet, B. 1978, A&AS, 34, 1

Niconov, V. B., Nekrasova, S. V., Polosuina, N. S., Rachkouvsky, N. D., & Chuvajev, W. K. 1957, Izvestiya Ordena Trudovogo Krasnogo Znameni Krymskoj Astrofizicheskoj Observatorii, 17, 42

Nidever, D. L., Marcy, G. W., Butler, R. P., Fischer, D. A., & Vogt, S. S. 2002, ApJS, 141, 503

Nikrasova, V., Nikonov, V. B., Polosukhina, N. S., & Rybka, E. 1962, Izvestiya Ordena Trudovogo Krasnogo Znameni Krymskoj Astrofizicheskoj Observatorii, 27, 228

Nordström, B., et al. 2004, A&A, 418, 989

Norris, J., Bessell, M. S., & Pickles, A. J. 1985, ApJS, 58, 463

Oblak, E. 1978, A&AS, 34, 453

Oblak, E. 1990, A&AS, 83, 467

Oja, T. 1963, Arkiv for Astronomi, 3, 273

Oja, T. 1983, A&AS, 52, 131

Oja, T. 1984, A&AS, 57, 357

Oja, T. 1985, A&AS, 59, 461

Oja, T. 1985, A&AS, 61, 331

Oja, T. 1986, A&AS, 65, 405

Oke, J. B. 1964, ApJ, 140, 689

Olsen, E. H. 1977, A&AS, 29, 313

Olsen, E. H. 1982, A&AS, 48, 165

Olsen, E. H. 1983, A&AS, 54, 55

Olsen, E. H. 1993, A&AS, 102, 89

Olsen, E. H. 1994, A&AS, 104, 429

Olsen, E. H. 1994, A&AS, 106, 257

Olson, E. C. 1974, AJ, 79, 1424

Oosterhoff, P. T. 1960, Bull. Astron. Inst. Netherlands, 15, 199

Pan, X., Shao, M., & Kulkarni, S. R. 2004, Nature, 427, 326

Parsons, S. B., & Montemayor, T. J. 1982, ApJS, 49, 175

Pena, J. H., Peniche, R., Mujica, R., Ibanoglu, C., Ertan, A. Y., Tumer, O., Tunca, Z., & Evren, S. 1993, Revista Mexicana de Astronomia y Astrofisica, 25, 129

Penprase, B. E. 1992, ApJS, 83, 273

Penston, M. J. 1973, MNRAS, 164, 133

Perry, C. L. 1969, AJ, 74, 139

Perry, C. L. 1969, AJ, 74, 705

Perryman, M. A. C., et al. 1997, A&A, 323, L49

Pfleiderer, J., Dachs, J., & Haug, U. 1966, Zeitschrift fur Astrophysics, 64, 116

Philip, A. G. D., & Philip, K. 1973, ApJ, 179, 855

Pickles, A. J. 1998, PASP, 110, 863

Piirola, V. 1976, Observatory and Astrophysics Laboratory University of Helsinki Report, 1,

Pourbaix, D. et al. 2004, å, 424, 272

Przybylski, A., & Kennedy, P. M. 1965, MNRAS, 131, 95

Reglero, V., & Fabregat, J. 1991, A&AS, 90, 25

Reglero, V., Gimenez, A., de Castro, E., & Fernandez-Figueroa, M. J. 1987, A&AS, 71, 421

Renson, P. & Catalano, F. A. 2001, å, 378, 113

Richichi, A., & Percheron, I. 2005, A&A, 434, 1201

Rodriguez, E., Lopez-Gonzalez, M. J., Lopez de Coca, P. 2000, A&AS, 144, 469

Roman, N. G. 1955, ApJS, 2, 195

Ronen, S., Aragon-Salamanca, A., & Lahav, O. 1999, MNRAS, 303, 284

Royer, F. et al. 2002, å, 393, 897

Rufener, F. 1976, A&AS, 26, 275

Rybka, E. 1969, Acta Astronomica, 19, 229

Söderhjelm, S. 1999, A&A, 341, 121

Samus, N. N. et al. 2004, Combined Catalog of Variable Stars (GCVS4.2 2004 Ed.), Inst. of Astronomy of Russian Academy of Sciences

Sandage, A. 1964, ApJ, 139, 442

Santos, N. C., et al. 2003, å, 398, 363

Santos, N. C., Israelian, G. & Mayor, M. 2004, å, 415, 1153

Schild, R. E. 1973, AJ, 78, 37

Schuster, W. J., & Nissen, P. E. 1986, Informational Bulletin on Variable Stars, 2943, 1

Schuster, W. J., & Nissen, P. E. 1988, A&AS, 73, 225

Schuster, W. J., Parrao, L., & Contreras Martinez, M. E. 1993, A&AS, 97, 951

Serkowski, K. 1961, Lowell Observatory Bulletin, 5, 157

Shao, C. Y. 1964, AJ, 69, 858

Sharpless, S. 1952, ApJ, 116, 251

Sharpless, S. 1962, ApJ, 136, 767

Shobbrook, R. R., Herbison-Evans, D., Johnston, I. D., & Lomb, N. R. 1969, MNRAS, 145, 131

Sjögren, U. 1964, Arkiv for Astronomi, 3, 339

Skiff, B. A. 2005, General Catalogue of Stellar Spectral Classifications, Lowell Observatory

Slettebak, A., Bahner, K., & Stock, J. 1961, ApJ, 134, 195

Snow, T. P., Lamers, H. J. G. L. M., Lindholm, D. M. & Odelle, A. P. 1994, ApJS, 95, 163

Sowell, J. R., & Wilson, J. W. 1993, PASP, 105, 36

Stetson, P. B. 1991, AJ, 102, 589

Stobie, R. S. 1970, MNRAS, 148, 1

Stokes, N. R. 1972, MNRAS, 159, 165

Stokes, N. R. 1972, MNRAS, 160, 155

Stoy, R. H. 1963, Monthly Notes of the Astronomical Society of South Africa, 22, 157

Sturch, C. R., & Helfer, H. L. 1972, AJ, 77, 726

Sturch, C. 1972, PASP, 84, 666

Szabados L. 1977, Mitteilungen der Sternwarte der Ungarischen Akademie der Wissenschaften Budapest, 70, 1

Szabados, L. 1981, Commmunications of the Konkoly Observatory Hungary, 77, 1

Taylor, B. J., & Joner, M. D. 1992, PASP, 104, 911

Tifft, W. G. 1963, MNRAS, 125, 199

Tokovinin, A. A., & Smekhov, M. G. 2002, A&A, 382, 118

Tokovinin, A. et al. 2006, å, 450, 681

Tolbert, C. R. 1964, ApJ, 139, 1105

Torres, G., Boden, A. F., Latham, D. W., Pan, M., & Stefanik, R. P. 2002, AJ, 124, 1716

Turon, C. et al. 1993, BICDS, 43, 5

van Belle, G. T. 1999, PASP, 111, 1515

van Belle, G.T., Lane, B.F., Thompson, R.R., The PTI Collaboration, 1999, AJ, 117, 521

van Belle, G. T., & van Belle, G. 2005, PASP, 117, 1263

van Belle, G. T., et al. 2006, ApJ, 637, 494

van den Bergh, S. 1967, AJ, 72, 70

Veeder, G. J. 1974, AJ, 79, 1056

Walker, R. L. 1971, PASP, 83, 177

Wallerstein, G., & Helfer, H. L. 1961, ApJ, 133, 562

Wallerstein, G., Greenstein, J. L., Parker, R., Helfer, H. L., & Aller, L. H. 1963, ApJ, 137, 280

Warren, W. H., & Hesser, J. E. 1977, ApJS, 34, 115

Warren, W. H. 1973, AJ, 78, 192

Wesselink, T., van Paradijs, J., Staller, R. F. A., Meurs, E. J. A., & Kester, D. 1980, Informational Bulletin on Variable Stars, 1800, 1

Westerlund, B. E. 1963, MNRAS, 127, 83

Westin, T. N. G. 1982, A&AS, 49, 561

Wickramasinghe, D. T., & Warren, P. R. 1976, MNRAS, 177, 59P

Williams, J. A. 1966, AJ, 71, 615

Wolf, S. C., & Morrison, N. D. 1975, PASP, 87, 231

Wolff, S. C., & Wolff, R. J. 1971, AJ, 76, 422

Worley, C. E. & Douglass, G. G. 1996, A&AS, 125, 523

Wramdemark, S. 1973, A&AS, 11, 365

Zdanavicius, K., et al. 1972, Vilnius Astronomijos Observatorijos Biuletenis, 34, 3

Zhang, E.-H. 1983, AJ, 88, 825

Zissell, R. 1972, AJ, 77, 610